JOHANN WOLFGANG GOETHE
UNIVERSITÄT
FRANKFURT AM MAIN

Paul-Ehrlich-Institut
Bundesinstitut für Impfstoffe und biomedizinische Arzneimittel
Federal Institute for Vaccines and Biomedicines

DISSERTATION

To obtain the academic degree
Doctor in Science

Comparative characterization of Hepatitis B virus genotypes on mitochondrial dynamics and their relevance for host-associated signaling pathways

Submitted to the

Department of Biochemistry, Chemistry and Pharmacy
Johann Wolfgang-Goethe-Universität
Frankfurt am Main - Germany

Presented by
Anja Isabel Schollmeier
Born in Bad Soden/Taunus

Frankfurt am Main (2024)
(D30)

vom Fachbereich Biochemie, Chemie, Pharmazie (14) der
Johann Wolfgang-Goethe-Universität als Dissertation angenommen.

Dekan: Prof. Dr. Clemens Glaubitz
Johann-Wolfgang-Goethe University
Max-von-Laue-Straße 9
60438 Frankfurt am Main

Gutachter: Prof. Dr. Martin Pos
Johann-Wolfgang-Goethe University
Institute of Biochemistry
Max-von-Laue-Straße 9
60438 Frankfurt am Main, Germany

Prof. Dr. Eberhard Hildt
Paul-Ehrlich-Institute
Department 2, Virology
Paul-Ehrlich-Straße 51-59
63225 Langen, Germany

Datum der Disputation: 16. Juli 2024

„*The greatest enemy of knowledge is not ignorance,*

it is the illusion of knowledge.”

- Stephen Hawking

Table of Contents

List of Abbreviations IV

List of Figures VII

List of Tables IX

1. Introduction 1

1.1. Discovery and history of infectious hepatitis 1

1.2. Hepatitis B virus infections 2

1.2.1. Viral hepatitis 2

1.2.2. Taxonomic Classification 2

1.2.3. Epidemiology and Transmission 3

1.2.4. Genetic Variability of Hepatitis B virus 4

1.2.5. Pathogenesis and treatment 7

1.3. Molecular virology 13

1.3.1. Structure and morphology of virions and subviral particles 13

1.3.2. Viral nucleic acid and genome organization 14

1.3.3. Viral proteins 16

1.4. Viral life cycle 20

1.4.1. Attachment and Entry 21

1.4.2. Nuclear import and viral replication 21

1.4.3. Encapsidation and egress 22

1.5. Mitochondria in virus infection 24

1.5.1. Mitochondria biogenesis and function 24

1.5.2. Mitochondria in hepatic infections 27

2. Context and specification of this study 30

3. Materials and Methods 31

3.1. Materials 31

3.1.1. Cell lines – Eukaryotic 31

3.1.2. Cell lines – Prokaryotic 31

3.1.3. Plasmids 31

3.1.4. Oligonucleotides 33
3.1.5. Enzymes 35
3.1.6. Reagents for cell culture 35
3.1.7. Antibodies and fluorescence dyes 36
3.1.8. Reagents 37
3.1.9. Commercial Kits 38
3.1.10. Inhibitors 38
3.1.11. Chemicals 39
3.1.12. Buffers and media 40
3.1.13. Devices 42
3.1.14. Consumables 43
3.1.15. Software 44
3.2. Methods 45
3.2.1. Cell-biological methods 45
3.2.2. Molecular biological methods 46
3.2.3. Protein-biochemical methods 50
3.2.4. Immunological methods 53
3.2.5. Microscopy and image acquisition 54
3.2.6. Quantification and statistical analysis 55
4. Results 57
4.1. Characterization and validation of the experimental design 57
4.1.1. HBx protein expression and cellular distribution are not affected by a reporter tag 57
4.1.2. The cellular compartmentalization of the HBx protein depends on the protein level 58
4.2. Cellular characterization between genetic variants of HBx reveals significant differences in quantity, localization and host kinome profile 59
4.2.1. HBx protein amount and cellular distribution vary among distinct genotypes 59
4.2.2. Kinome profile analysis reveals a significant, HBx genotypes-dependent impact on host signaling pathways 60

4.3. HBx induces profound changes in mitochondrial morphology and abundance in a genotype-dependent manner 64
4.3.1. HBx trigger the mitochondrial network structure towards fission genotype dependently....64
4.3.2. HBx reduces the mitochondrial mass depending on the HBV genotype....66
4.3.3. HBx effects mitochondrial dynamics genotype-dependent in HepG2 cells....68
4.4. HBx alters mitochondrial function and homeostasis in a genotype-dependent manner through association with VDAC3....69
4.4.1. Genetic variants of HBx interact with VDAC3 to varying degrees 69
4.4.2. Genotype-dependent interaction between HBx and the VDAC diminish the $\Delta\Psi_m$-level and cytochrome c oxidase activity 70
4.5. HBx-mediated perturbation of mitochondrial integrity induces oxidative stress and pro-inflammatory responses....73
4.5.1. HBx genotypes influence the intracellular ROS level 73
4.5.2. HBx-induced ROS levels trigger cytoprotective gene-expression and inflammatory processes....74
4.6. Genetic variants of HBx highly influence the removal of dysfunctional mitochondria by mitophagy....76
4.6.1. HBx induces mitophagy in a genotype-dependent manner....76
4.6.2. Mitochondrial degradation is mediated by the host lysosomal system 77
4.7. HBx variants recruits the Pink1/Parkin signaling pathway to induce mitophagy....79
5. Discussion....82
6. Summary....89
7. Zusammenfassung....91
8. References....96
9. Acknowledgements 114
10. Declaration of own contribution....115
11. Declaration of an oath 116
12. Publications....117
13. Curriculum vitae 119

List of Abbreviations

%	Percent
(v/v)	Volume per volume
(w/v)	Weight per volume
°C	Degree Celsius
µl	Microliter
aa	Amino acid
ACLF	Acute-on-chronic liver failure
ALT	Alanine aminotransferase
AuAg	Australian Antigen
ATF4	Activating Transcription Factor 4
BSA	Bovines Serum Albumin
cccDNA	Covalently closed circular DNA
CCCP	Carbonyl cyanide m-chlorophenyl hydrazine
CHB	Chronic hepatitis B
CLSM	Confocal laser scanning microscope
Cp	Crossing point
CTCF	Corrected total cell fluorescence
C-terminal	Carboxy terminal
Cyt c	Cytochrome c
d/h p.i.	Days/Hours post infection
DDB1	DNA damage-specific DNA-binding protein 1
DMEM	Dulbecco's modified Eagle's medium
DMSO	Dimethyl sulfoxide
DNA	Deoxyribonucleic acid
DR	Direct repeats
Drp1	GTPase dynamin-related protein
dslDNA	Double stranded linear DNA
e.g.	Exempli gratia (for example)
EGFR	Epidermal growth factor receptor
ER	Endoplasmic reticulum
ESCRT	Endo-lysosomal sorting complex required for transport
et al.	et alia
ε	encapsidation signal

FAO	fatty acid oxidation
FIS1	Mitochondrial fission 1 protein
G	Gramm
GFP	Green fluorescence protein
Gt	Genotype
H	Hour(s)
HA-tag	Hemagglutinin-tag
HBcAg	Hepatitis B virus core antigen
HBeAg	Hepatitis e antigen
HBsAg	Hepatitis B virus surface antigen
HBV	Hepatitis B virus
HBx	Multifunctional X-protein
HCC	Hepatocellular carcinoma
HSPG	Heparan sulfate proteoglycans
IF	Immunofluorescence
IL	Interleukin
IMM	Inner mitochondrial membrane
JAK	Janus kinase
kb	Kilobases
kDa	Kilodalton
KEGG	Kyoto Encyclopedia of Genes and Genomes
KOBAS	KEGG Orthology Based Annotation System
LC3	Light chain 3 protein
LHBs	Large hepatitis B virus surface proteins
LIR	LC3-interaction region
LSEC	Liver sinusoidal endothelial cells
MFF	Mitochondrial fission factor
MFN1/2	Mitofusin
MHBs	Middle hepatitis B virus surface proteins
min	Minute(s)
ml	Milliliter(s)
mM	Millimolar
mRNA	Messenger RNA
mtROS	mitochondrial-related radical oxygen stress
MVB	Multi vesicular bodies
NF-κB	Nuclear factor-κB
ng	Nanogram(s)

NLRP3	NLR family pyrin domain containing 3
nM	Nanomolar
NPC	Nuclear pore complex
nt	Nucleotide
NTCP	Sodium taurocholate co-transporting receptor
NUCs	Nucleos(t)ide analogues
OBI	Occult hepatitis B infection
OMM	Outer mitochondrial membrane
OXPHOS	Oxidative phosphorylations
PAGE	Polyacrylamide gel electrophoresis
pgRNA	Pregenomic RNA
PINK1	PTEN-induced putative kinase 1
qPCR	Quantitative polymerase chain reaction
rcDNA	Relaxed circular DNA
RIG	Retinoic acid-inducible gene I
RLU	Relative light units
RNA	Ribonucleic acid
ROS	Radical oxidative stress
RRID	Research Resource Identifiers
S	Surface region
SARS-CoV-2	Severe acute respiratory syndrome coronavirus
SDS	Sodium dodecyl sulphate
SEM	Standard error of the mean
SFK	Scr-family kinase
sgDNA	Subgenomic DNA
SHBs	Small hepatitis B virus surface proteins
SVP	Subviral particles
TCA	Tricarboxylic acid cycle
tMOC	Thresholded Mander’s overlap coefficient
TP	Terminal protein domain (Polymerase)
Ub	Ubiquitin
VDAC	Voltage-dependent anion channels
WB	Western blot
WHO	World Health Organization
$\Delta\Psi_m$	Mitochondrial membrane potential

List of Figures

Figure 1: Global prevalence of HBV infections 3
Figure 2: Geographical distribution of HBV genotypes worldwide 5
Figure 3: Natural history of chronic hepatitis B infection 9
Figure 4: Schematic representation of HBV particles 14
Figure 5: HBV genome organization 15
Figure 6: Functional domains of HBx protein 18
Figure 7: Schematic overview of HBx-mediated liver transformation processes 19
Figure 8: Liver microanatomy and viral life cycle during HBV infection 23
Figure 9: Mitochondrial network dynamics 26
Figure 10: Schematic overview of HBx-mediated mitochondrial dysfunction 29
Figure 11: Detection and localization of HBx are independent from the reporter tag 57
Figure 12: Intracellular compartmentalization of HBx varies among different timepoints after transfection 58
Figure 13: Cellular distribution and protein amount of HBx varies among different HBV genotypes in transiently transfected Huh7 cells 59
Figure 14: HBx-genotype A impairs mitochondrial associated signaling pathways 61
Figure 15: HBx protein of different genotypes display distinct regulatory effects in the kinome profile 62
Figure 16: HBx genotype A and G heavily induce global mitochondrial fragmentation 65
Figure 17: The mitochondrial protein amount, but not the mRNA level is modulated by HBx in a genotype-dependent manner 67
Figure 18: HBx induce mitochondrial fragmentation in HepG2 cells 68
Figure 19: HBx colocalizes with the VDAC3 in a genotype-dependent manner 69
Figure 20: Genetic variants of HBx have a distinct impact on the mitochondrial membrane potential 70
Figure 21: The cytochrome c activity is altered by HBx, dependent on the genotype 72
Figure 22: The intracellular ROS level is modulated depending on the genotype 73
Figure 23: Induction of AP-1 or NF-κB-dependent gene-expression and inflammatory response varies among the genetic variants of HBx 74
Figure 24: Mitophagy is mediated depending on the genetic variants of HBx 76
Figure 25: Genotype-specific, HBx-induced mitophagy is associated with host proteins of the endo-lysosomal system 77
Figure 26: HBx leads to a genotype-dependent induction of intracellular Pink1 and Parkin levels 79
Figure 27: HBx lead to and genotype-dependent accumulation of Parkin 80

Figure 28: Schematic representation of the genotype-dependent impact on HBx-mediated changes in mitochondria morphology and function, discovered in this study 90

List of Tables

Table 1: Clinical characteristics among hepatitis B genotypes. 11
Table 2: Eukaryotic cell lines used. 31
Table 3: Prokaryotic cell line used. 31
Table 4: Plasmids used. 31
Table 5: Light cycler oligonucleotides used. 33
Table 6: Oligonucleotides used for cloning. 34
Table 7: Oligonucleotides used for sequencing. 34
Table 8: Enzymes and related buffers used. 35
Table 9: Reagents used for cell culture. 35
Table 10: Primary antibodies used. 36
Table 11: Secondary antibodies used. 36
Table 12: Fluorescence reagents used. 37
Table 13: Reagents used. 37
Table 14: Commercial Kits used. 38
Table 15: Inhibitors used. 38
Table 16: Chemicals used. 39
Table 17: Buffers and media used. 40
Table 18: Electrophorese and blotting systems used. 42
Table 19: Microscopes used. 42
Table 20: Flow cytometer used. 42
Table 21: Further devices used. 42
Table 22: Consumables used. 43
Table 23: Software used. 44
Table 24: Amplification program for HBx HA cloning. 47
Table 25: Amplification program for HBx eGFP cloning. 48
Table 26: RT-qPCR program for genomic transcripts. 49

1. Introduction

1.1. Discovery and history of infectious hepatitis

Throughout the world, viral hepatitis is associated with significant mortality and morbidity, afflicting millions of individuals [1]. The history of viral hepatitis began already in ancient times by describing an “epidemic jaundice”, followed 1865, when R. Virchow characterized the disease with symptoms of hepatic injury and inflammatory processes [2, 3]. During the following century, several hepatitis epidemics were reported, however, the causative agent remained long time unknown [4]. In 1960, the geneticist and hematologist Baruch S. Blumberg described the discovery of the Australian Antigen (AuAg), which was identified a few years later, as the hepatitis B virus surface antigen (HBsAg) and the foremost specific infection marker of viral hepatitis [5]. With this background, the discovery of the AuAg is considered as the most important milestone in the history of viral hepatitis and represents the initial force in the development of viral diagnostics and vaccines. For this work, Blumberg was awarded for the Nobel Prize for Physiology and Medicine, together with D. C. Gadjusek [6, 7]. Later in 1970, David S. Dane investigated purified AuAg by electron microscopy and identified a 42 nm size particle with a clear inner core structure. The particle was classified as hepatitis B virus (HBV), or so-called “Dane particle” [8].

Just a few years later, diluted and inactivated AuAg-positive serum was acknowledged as hepatitis B-specific vaccine and represents the first generation of hepatic vaccines [9]. The identification of the HBsAg sequence however, enables the recombinant production of HBsAg as a vaccine and represented a new “era” in the development of a viral hepatitis-specific vaccine. A yeast-derived, HBsAg-based HBV vaccine was implemented as an effective and safe standard vaccine and has been recommended since 1992 by the World Health Organization (WHO) as a worldwide universal childhood vaccination [1]. Although HBV vaccine development advanced rapidly, the global prevalence of HBV infections has declined only slightly to date [10]. The reason for this constraint remains the limited number of effective antiviral therapies, the lack of a complete viral clearance after infection, but also limited vaccine coverage and medical care in low-income regions. [6].

Recently, the sodium taurocholate co-transporting receptor (NTCP) has been identified as key HBV entry factor and provides a major success by establishing robust in vitro models to study fundamental insights of the viral live cycle and interactions with the biochemical processes of the host [11, 12]. However, despite the discovery of the hepatitis B virus and the rapidly advising improvements over the past 50 years, many aspects are still unknown or have been neglected in the past. Especially, the dimension of the genetic variability of HBV and associated pathogenesis provides a huge gap in this area [6].

1.2. Hepatitis B virus infections

1.2.1. Viral hepatitis

Hepatitis is characterized by acute or chronic inflammation of the liver and is considered as major global health problem with significant morbidity and mortality rates, worldwide. Despite drugs, alcohol, and certain diseases, the leading etiology for hepatitis is represented by hepatotropic viruses and comprises hepatitis A, B, C, D, and E viruses [13]. Although hepatotropic viruses differ fundamentally in their biological characteristics, they are responsible for an estimated 325 million individuals with chronic viral hepatitis and cause approximately 1.6 million deaths annually. In particular, the hepatitis B virus is the most relevant viral trigger of chronic hepatitis and the most notorious factor for liver-related deaths worldwide [14]. The clinical presentation of virus-induced hepatitis varies from asymptomatic or temporally flu-like illness to acute liver disease including fulminant hepatitis or chronic liver failure. Chronic liver disease processes are ultimately associated with liver fibrosis and the risk of hepatocellular carcinoma development [15].

Nowadays, viral hepatitis becomes rather simple and efficiently detected by monitoring technologies based on serological biomarkers screening and viral nucleic acid amplification tests and enables an appropriate treatment response [15, 16]. Also, the development of vaccines for some of these viruses greatly contributes to the containment of virus-induced hepatitis. In this regard, the WHO forces the goal to eliminate viral hepatitis as a global health problem by 2030. However, HBV infections remain still inadequately evaluated and under-treated, particularly in low-income countries, so the annual global deaths by HBV are unlikely to decrease significantly, if the status quo remains unchanged [17, 18].

1.2.2. Taxonomic Classification

The human hepatitis B virus is classified as the prototype member of the *Hepadnaviridae* family, with unique features and sequence homology compared to other known viruses. Based on the International Committee on Taxonomy of Viruses (ICTV), HBV was classified apart from other families of DNA viruses [19]. The *Hepadnaviridae* family (hepatotropic DNA viruses) is characterized by unique sequential and structural properties, together with a narrow species and tissue specificity. The human HBV and other related *Hepadnaviridae*, who infect mammals (gibbons, woodchuck, ground squirrel etc.) share the same genus, called *orthohepadnaviruses*. The genera of *avihepadnaviruses* infect birds (ducks, storks, herons etc.). Interestingly, even the *avihepadnaviruses* share only a nucleic acid homology of 40%, compared to the human genus [20, 21].

1.2.3. Epidemiology and Transmission

Despite the existence of an effective vaccine, until now infections with HBV are still one of the major global health problems and the leading agents for cirrhosis and liver cancer worldwide. The course of disease encompasses acute flares, fulminant hepatic failure, as well as chronic liver burden including extrahepatic manifestations. The WHO estimates worldwide around 296 million chronically infected individuals and accounted in 2019 more than 800.000 deaths caused by long-term sequelae. Notably, the global burden of chronic HBV infections is unevenly distributed in an inverse proportion of the income level [18, 22]. In particular, varying access to vaccines in combination with underdiagnoses and treatment availabilities are immensely in low-income countries and thus reasonable for a varying global prevalence and endemicity. The highest endemicity (prevalence > 8%) prominently concentrated in the Western Pacific Region and South Africa region, as well as some parts of South and North America. East, South Europe, Russia, South-, East Asia and Central-, South America indicate a prevalence between 2 – 7%. In the USA, West-Europe and Australia is the endemicity rather low (< 2%) (fig. 1) [23–25].

Importantly, it has to be considered, that the estimates of global prevalence comprise some limitations, on the one hand, based on the various use of methodologies due to different modeling assumptions and data availabilities. On the other hand, international migration changes the overall perspectives on the global burden and shifts the disparate distribution. Overall, socioeconomic parameters such as living conditions, healthcare and cultural aspects are highly associated with viral endemicity, but rather complex in their validation [18, 26, 27].

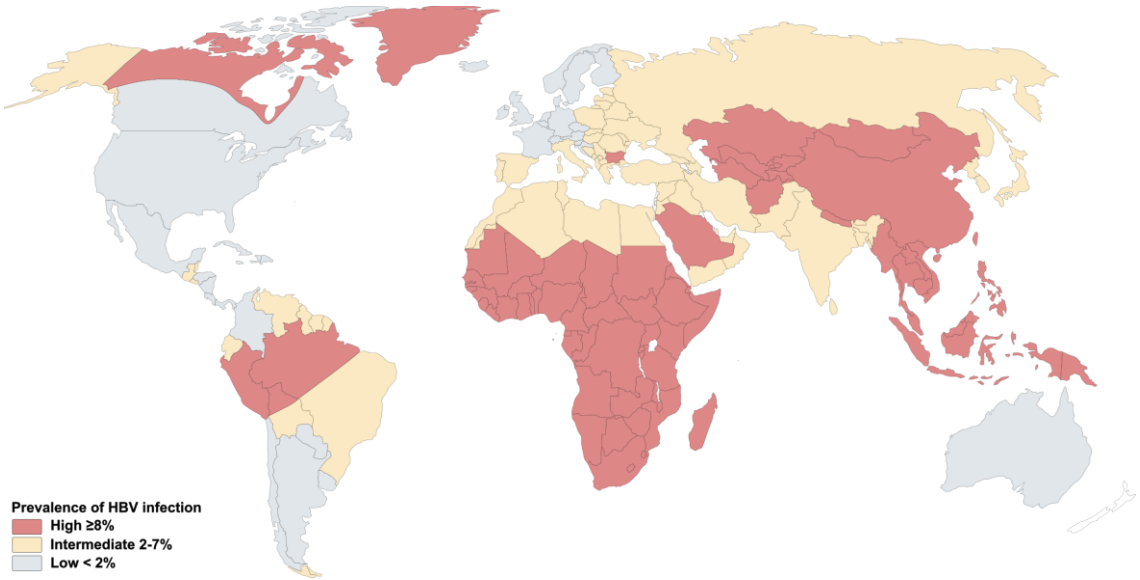

Figure 1: Global prevalence of HBV infections. The highest prevalence with over 8% is represented in Western Pacific Region, South-Africa, and some parts in South and North America (red areas), East-, South-Europe, Russia, South-, East-Asia and Central-, South-America indicate an intermediate prevalence between 2 – 7% (yellow areas). A low prevalence under 2% (grey) occurs in USA, West-Europe and Australia. (Underlying literature is reported by Pedersini et al. [28])

In addition, the demographic distribution of HBV burden is also associated with different modes of transmission that are predominant in the respective population. Since the infection reveals high viral titers in the blood, the main transmission occurs by contact with blood of infected individuals, beyond HBV is also present in body fluids, such as saliva, tears, sweat, semen and vaginal secretion. The main modes of transmission are either vertical, horizontal, or sexual [29, 30].

In this regard, the main transmission route, especially in high endemic regions, represents the perinatal transfer from mother to child (vertical transmission). The risk of a chronic infection in the newborn infant without appropriate immunization is around 70-90%, but even immunoprophylaxis does not offer a complete protection [31]. In contrast, in low-prevalence countries, HBV infection is predominantly acquired through either horizontal, by contact with blood or blood products, i.e. by transfusion or re-used injection material, or high-risk sexual exposures. Horizontal transmission usually occurs in adulthood but is facilitated by the fact that the virus is very stable and infectious on environmental surfaces (half-life > 22 days at 37 °C) [29, 32]. The chronicity rate after horizontal transmission is between 5 and 10% in older children and adults, while around 20 to 60% of infections in early childhood (1 to 5 years) are chronic [24]. Moreover, geographical distribution and transmission routes are also directly associated with the prevalence and epidemiology of HBV genotypes (as described below) [6].

1.2.4. Genetic Variability of Hepatitis B virus

High genetic heterogeneity is an important feature in the life cycle and disease progression of HBV [33]. In particular, the lack of a proof-reading function of the reverse transcriptase, together with an RNA intermediate as replication template facilitates a high rate of genetic variants, mutations and recombinants. In this regard, the nucleotide substitution rate for HBV is estimated to be 10-times higher, compared to other DNA viruses; the mutation rate in immune-suppressed HBV patients is assumed to be 100-fold higher as individuals having an occult HBV infection [21, 34]. Genomic stable variants, established over a longer time period were discriminated as genotypes and sub-genotypes, whereas several mutations mainly in the pre-core and basal core promoter (BCP) region emerge as a result of high replication rate or individual selection pressure [35]. It is estimated that the viral genome evolves between 10^{-3} and 10^{-6} error sites in the nucleotide sequence per year, whereas the location of the mutation sites varies among the different regions within the HBV genome. This is reasoned by selective constraints in the overlapping regions or secondary RNA structures in the nonoverlapping regions [36, 37].

1.2.4.1. Hepatitis B virus Genotypes and Sub-genotype

Stabil variants of HBV that arise over a long time period were formerly categorized as serotypes, according to the antigenic determinates (adw, adr, ayw or ayr) [38, 39]. However, since the phylogenetic analysis of the whole viral genome became possible, Okamoto et al. designate HBV into genotypes and sub-genotypes based on their molecular criteria [40]. Accordingly, the degree of nucleotide divergence discriminates HBV genotypes by a more than 8% intergroup divergence and further classifies sub-genotypes by a more than 4% and less than 8% intragenotype divergence. Up to date, nine genotypes have been identified, (genotypes A to I), whereas an additional genotype strain was recently isolated from a Japanese patient and has been designated as a putative tenth genotype [21, 37, 41]. Molecular genetically, the genotypes differ in their genome length and size of the open reading frame which also affects protein translation during the replication cycle. Importantly, HBV genotypes and sub-genotypes have a defined, geographical distribution and demonstrate a distinct demographic-ethnic pattern regarding the endemicity, transmission route and prevalence of liver disease (fig. 2) [42, 43].

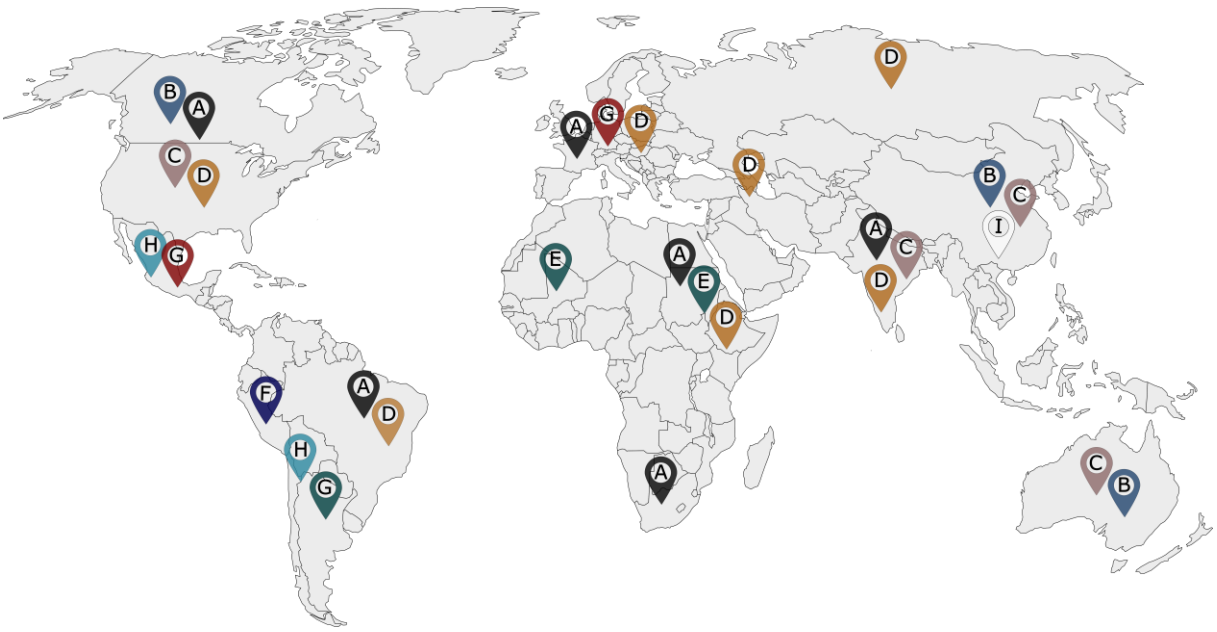

Figure 2: Geographical distribution of HBV genotypes worldwide. Genotypes A to I are indicated as capital letters, located in the region of their prevalence. (Underlying literature is reported by Velkov et al. [44].)

At present, 4 subgenotypes for genotype A have been described and share the unique feature of a 6-nucleotide insertion into the core region. The genotype is mainly represented in Africa, Northern and Central Europe, North America and South Asia [37, 45]. Genotype B is reclassified into 9 subgroups with main prevalence in South-East Asia (Japan and Pacific Islands) North America and Australia. The historically oldest genotype C is predominantly

endemic in South and East Asia, North America and indigenous people of Australia, by at least 16 identified sub-genotypes [44]. The geographical prevalence for genotype D however is not clearly defined, the 8 subvariants are widely distributed in Africa, Asia, Europe and America. The genome of genotype G represents a 33-nucleotide deletion in the pre-S1 domain and is overall the shortest genome, compared to the other genotypes [46, 47]. Genotype E is specifically characterized by a 3-nucleotide deletion in the preS1 domain but with generally low genetic diversity. The prevalence focuses on western and central African country. Furthermore, the genotypes F and H are mainly endemic in America, whereas the genotype G behaves as an aberrant genotype without a clear geographical association and occurs frequently as co-infection with other genotypes and the human immunodeficiency virus type 1 (HIV-1). The genome of genotype G has only little sequence divergence being a 36-nucleotide insertion in the core region and two stop codons in the pre-core region leading to a HBeAg negative phenotype and is furthermore unable to secrete HBsAg [37, 39, 44, 48]. Finally, the recently identified genotype I (respectively J) is suggested as a recombinant and was found in South/East Asia [49, 50]. Overall, the geographical pattern of HBV genotypes and phylogenetic comparisons of the sequences offers a valuable tool to reconstitute anthropological migration patterns and infection routes. Despite this, the migratory factor is a critical aspect in the modern world and might shift the overall global distribution of HBV genotypes with a major impact not only in the prevalence [18, 51]. Notably, HBV genotypes tremendously contribute to the chronicity of infection, prognosis, antiviral treatment response and the overall clinical outcome, however, this aspect is described in more detail in chapter 1.2.5.3.

1.2.4.2. Hepatitis B virus variants by mutations

Genetic variability by random point mutations emerges frequently during viral replication as a consequence of individual selection pressure. Therefore, the emergence of mutations promotes viral persistence, evasion of the host immune response, and therapeutic resistance, which are often associated with severe liver diseases [52]. Comprehensive studies recently identified common mutations in different genetic regions, occurring during specific phases of infections. In particular, mutations in the basal core promotor region (BCP) and in the precore region (PC) are broadly studied and responsible for the HBeAg seroconversion. In this regards, the coexistence of the BCP mutation together with the Quadruple mutation GCAC1809-1812TTCT was recently observed with an inactive carrier state and therefore discussed as an potential prognostic biomarker in HBV infection [53, 54].

In addition, mutations in the basal core promoter, especially by insertions or deletions are accompanied by a shift in the X gene frame. This subsequently leads to the production of HBx variants or truncated HBx-proteins, which are commonly detected in hepatocellular carcinoma (HCC) tissues [55]. Furthermore, based on a comparative study of Indian HBV isolates, it was

postulated that some HBx mutations occur particularly in certain genotypes/subgenotypes and fundamentally modulate the pathogenic properties of HBx [56]. Interestingly, a recent study identified emerging HBx mutants also in response to antiviral treatments with nucleotide or nucleoside analogs and with compensatory effects of the replication suppression [57].

1.2.5. Pathogenesis and treatment

1.2.5.1. Natural history of HBV infection

HBV itself is considered as non-cytopathic pathogen but causes necro-inflammatory liver diseases through hepatocyte-specific infections. The spectrum of hepatocellular injuries varies thereby in severity, ranging from acute to chronic hepatitis. Between 65-70% of HBV infections result in an acute infection, which is usually self-cleared within 6 months after infection [58, 59]. In this case, the infection is either asymptomatic or mildly symptomatic with a subclinical course of the disease that usually remains undetected. However, around one-third of acute infected patients develop clinical symptoms of hepatitis with nausea, jaundice, abdominal pain in combination with inflammation of the liver. Approximately 1% of acute infections develop a fulminant hepatitis, which is characterized by increased necrosis of the liver parenchyma and result in acute liver failure [58, 60]. Viral clearance is largely mediated by the adaptive immune response and involves the expression of antiviral cytokines, activation of cytotoxic T-lymphocytes (to eliminate infected hepatocytes) and finally the production of neutralizing antibodies by B-cell response to prevent the infection of new hepatocytes [61]. Typically, in clinical practice, the disease stage is discriminated by the quantitative detection of serological biomarkers [62].

Especially during the acute course of infection, HBV DNA, followed by HBsAg and HBeAg, are the initial viral markers that can be detected in the patient's serum. In addition, levels of serum alanine and aspartate aminotransferase (ALT, AST) begin to increase. HBeAg levels usually rise in correlation with high levels of viral replication but decline early after the main clinical symptoms have peaked. Therefore, the decrease in the amount of HBeAg in the serum and the presence of HBeAg-specific antibodies are considered as favorable serological markers, indicating the cure of infection. The recovery phase is also characterized by the seroconversion of HBcAg and HBeAg-specific antibodies, from IgM to IgG, and the development of HBsAg-specific antibodies, which arise in the late stage of acute infection and persist beyond the course of the infection process [58, 63].

Chronic hepatitis B (CHB) affects around 296 million people, whereas between 15 and 40% of patients developing severe symptoms of liver disease, ultimately making CHB one of the leading causes of death worldwide [64]. CHB is characterized by a continuous and detectable level of HBsAg and HBV-DNA beyond the initial 6 months after the primary infection, whereas the risk of a chronic course of infection is highly dependent on the age of exposure. Clinically, the course of chronic hepatitis is highly variable and dynamic and moreover, reflects a complex interplay between virus replication and the immune reactivity of the host. The course of chronic HBV infection can be divided into several phases, although not all patients proceed all stages (fig. 3) [58, 59, 65]. The immune tolerance phase (phase 1) represents the initial stage of chronic infection, indicated by a high viral replication activity. This results in elevated HBV-DNA titers and the presence of HBeAg, accompanied by moderate serum ALT-levels. The phase is characterized by a lack of active liver disease or liver inflammation processes and can manifest over years or even throughout life [65]. However, the high viral DNA levels facilitate the integration of viral DNA genome into the host hepatocyte DNA [66].

The transition from the immune tolerance to the immune clearance stage (phase 2) is indicated by an elevated HBV-specific T-cell activity accompanied by fluctuating levels of HBeAg, viral DNA and aminotransferase levels, as well as evidence for histological changes. Hereby it is believed, that heterogenous ALT-levels are the result of the T-cell mediated immune response and elimination of infected hepatocytes. Accordingly, this HBeAg-positive phase may last for years but emphasizes host immune pressure and disease progression. Typically, this phase attempts to regulate the viral replication activity and results at the end in the seroconversion from HBeAg to anti-HBe along with a significant drop in the ALT- levels and overall virus load [67–69].
Accordingly, this third phase represents an HBeAg negative state also named as “inactive HBsAg carrier” phase. It represents the favourable long-term outcome, since the replication levels decrease to a clinically not significant level, together with a moderate risk for liver disease. The 3rd phase could manifest for a lifetime, while in some cases a spontaneous viral reactivation, most likely as HBeAg-negative chronic hepatitis (HBeAg-negative HCB), occurs. This stage (phase 4) is usually characterized by a moderate viral replication rate, but elevated chronic inflammation and disease progression. It usually occurs by genetic mutations in the PC or BCP region [60, 70].

Finally, an occult hepatitis B infection (OBI) represents a clinical phase defined by the presence of replication-competent viral DNA in the liver but is most likely undetectable in the blood serum. Apart from the risk for an immunosuppression-related reactivation of viral replication, the potential for the development of HCC is still present in occult HBV carriers. The absence

of detectable HBsAg may also carry the risk of HBV transmission through contaminated blood donations [71, 72]. Apart from this, chronic HBV infection is also considered as main cause of Acute-on-chronic liver failure (ACLF), which is described as a complex clinical syndrome and characterized by acute hepatic dysfunction and severe extrahepatic organ failure in combination with an high short-term mortality [73].

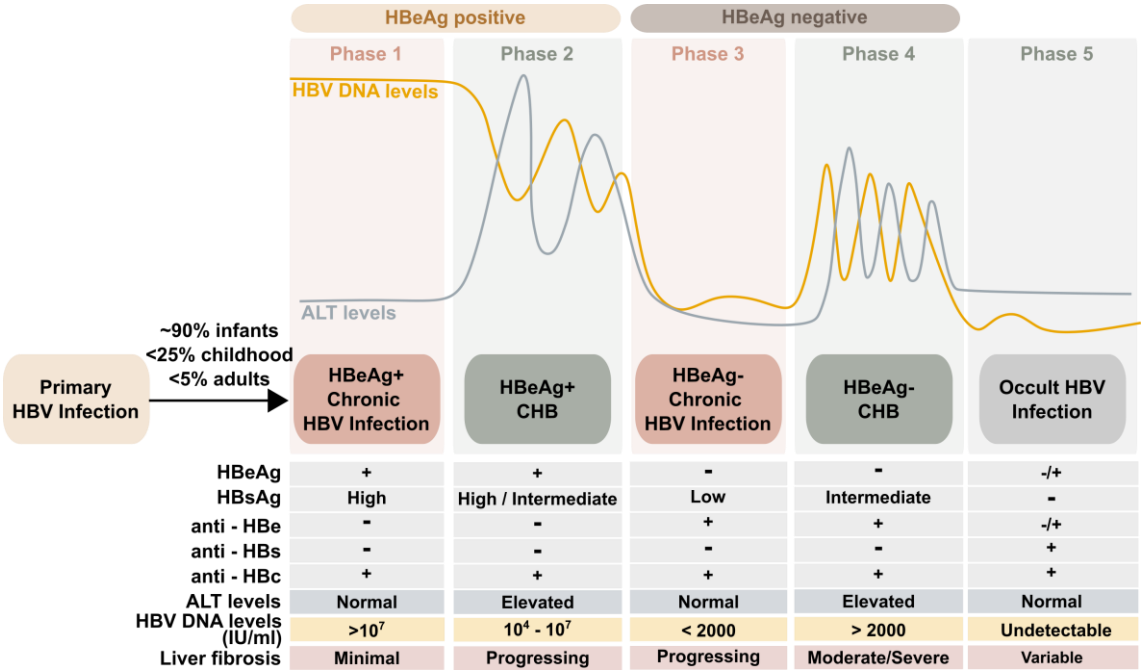

Figure 3: Natural history of chronic hepatitis B infection. The course of infection is described by five phases characterized by distinct levels of serological markers: immune tolerant phase (phase 1); immune reactive HBeAg positive phase (phase 2); inactive carrier phase (phase 3), HBeAg negative chronic hepatitis phase (phase 4) and occult HBV infection or HBsAg negative phase (phase 5). The yellow curve describes the HBV DNA-level during the course of chronic HBV infection, the grey line indicates the ALT-levels. ALT - alanine aminotransferase; CHB - chronic hepatitis B. (Figure is retrieved and modified from Bousali et al. [66])

Although the course of CHB patients remains asymptomatic for a long time, the persistence of infection ultimately accelerates the progression of liver cirrhosis and the development of HCC [74]. Complications of cirrhosis are represented by the development of a decompensated cirrhosis occurring with an acute onset of symptoms and emerging mortality risk [75]. In addition, an extrahepatic manifestation of CHB (mediated by immune modulators), includes a spectrum of lesions, which provides a systemic disease progression with high mortality [76]. Currently, HBsAg seroclearance considered the ultimate clinical outcome for CHB treatment trials and includes a very good prognosis and survival rate. However, a complete clearance phase through the elimination of the persistent covalently closed circular DNA (cccDNA, which serves as template for the viral replication) and removal of integrated viral DNA from the host genome remains a theoretical end phase [66, 77].

1.2.5.2. Prevention and treatment

To date, the currently available therapy for HBV-infected people is based on suppressing viral replication and monitoring and reducing clinical symptoms. Despite ongoing progression in antiviral therapy options, a complete cure is still not possible. Therefore, extensive immunization represents the cornerstone of efforts to prevent HBV infections and related diseases. As a pioneer in the history of vaccine development, the HBV vaccine of the second generation is based on a recombinant HBsAg immunogen and provides a safe and protective immunization against HBV infection [78]. Typically, three doses of vaccine are intramuscularly administered and achieve a 95% coverage with long-lasting immunity. Beyond that, however, the standard vaccination failed to elicit an immune response in around 5% of individuals. Although the reasons for these “non-responders” are still poorly understood, it is believed that the greatest likelihood of the lack of an immune response is due to genetic predisposition, chronic diseases and immunomodulatory drugs [79, 80].

A worldwide high coverage rate of HBV vaccination is accounted as the best strategy to prevent breakthrough infection. In order to this, in 2019, the WHO recommended a universal HBV vaccination program for all countries and even those with low prevalence. This includes first of all, the vaccination of all infants soon after birth as well as catch-up vaccinations of all adults and especially “high-risk” groups. With 180 countries contributing to the universal infant HBV vaccination program, the global coverage rate was estimated in 2010, by 75% [81, 82]. Further prevention strategies, particularly to prevent horizontal transmission, include sterilization of injection materials and education to avoid “high-risk” behavior. However, significant efforts to reduce HBV transmission have been made since the 1970s through routinely testing of blood products and transplant organs [81, 83].

The current goal of HBV therapy options remains until now in the suppression of viral replication, ameliorate progression of liver related as well as extra-hepatic complications and prevention of further transmission. Whereas an acute infection is most likely symptomatically treated, available, antiviral drugs against CHB are categorized into two groups: direct-acting antivirals and immune modulators. Often a combination of both is used and leads to a significantly improved clinical outcome [84].
Commonly, nucleos(t)ide analogs (NUCs) (lamivudine, adefovir, entecavir, tenofovir and telbivudine) in combination with interferon (IFN) treatment (common IFN or pegylated-IFN-α) are used [85]. However, NUC therapy has a high risk of developing viral resistance, whereas IFN treatments are associated with strong side effects and are not recommended for decompensated cirrhosis [86]. Newer drugs, targeting distinct steps in the viral life cycle provide promising approaches but are still under clinical development. Despite this, a

functional cure with undetectable serum HBV DNA-levels together with a loss of HBsAg would lead to an excellent long-term outcome but needs further investigations, especially by eliciting the cccDNA and integrated viral DNA [87].

1.2.5.3. Viral pathogenesis of Hepatitis B virus genotypes

Besides the geographical heterogenicity among HBV genotypes, there is growing evidence, that the genetic variants of HBV greatly influence the natural history, pathogenicity and clinical outcome of infection. In particular, in the past years, several studies investigated differences within the tendency to chronification, HBeAg seroconversion, HBsAg seroclearance, HCC development, viral load, molecular mechanisms and response to antiviral therapies [88, 89]. For examples, an acute infection with genotype A is considered with a higher risk of chronification, whereas genotype C is associated with lower rates of HBeAg seroconversion which accelerate the progression of liver inflammation, risk of HCC development and poor clinical outcome. The genotypes A and B have a higher rate of HBsAg seroclearance, accompanied with a better chance to prevent severe liver disease progression. Genotypes D and F have a high rate for HCC related deaths [44, 90]. With respect to the response to anti-viral therapies, patients infected with genotype A or B seems to be better susceptible to IFN-α therapy. Furthermore, preliminary studies assumed also a better response for the genotypes E, F and H, as compared to genotype G [90, 91]. Interestingly, regarding nucleos(t)ide analog based therapies, no significant association could be observed across the distinct genotypes [90]. A detailed comparison of clinical differences among the distinct HBV genotypes are listed below in table 1.

Table 1: Clinical characteristics among hepatitis B genotypes. Importantly, due to the unique distribution of genotypes in different geographical regions and demographic groups, data availability is partially inconsistent.

Clinical characteristics	Genotype				
	A	B	C	D	E-J
Tendency of chronicity	Higher	Lower	Higher	Lower	ND
Positivity of HBeAg	Higher	Lower	Higher	Lower	ND
HBeAg seroconversion	Earlier	Earlier	Later	Later	ND
HBsAg seroclearance	More	More	Less	Less	ND
Histologic activity	Lower	Lower	Higher	Higher	ND
Clinical outcome (cirrhosis and HCC)	Better	Better	Worse	Worse	Worse for genotype F

Response to interferon-α	Higher	Higher	Lower	Lower	Lower in genotype G
Response to nucleos(t)ide analogues	No significant differences				ND

ND, no available data. Table retrieved and modified from Lin et al. [88]

Furthermore, distinct mutation patterns in multiple regions of the viral genome specific to the different genotypes have been associated with different pathogenic traits. For example, mutations in the S-region correlate with immune escape mechanisms, whereas mutations in the preS or S gene are associated with an impaired HBsAg secretion [42, 92, 93]. A comparative in vitro study by Hassemer et al. analyzed the secretion and composition of HBsAg and identified enormous differences among the distinct genotypes. In this regard, especially genotype G fails to secrete HBsAg and provides risk for an underdiagnosis and undertreatment. Overall, this highlighted the relevance and potential obstacles to using HBsAg as a common diagnostic marker among HBV genotypes, especially for diagnosis and blood safety [94].

1.2.5.4. HBV-coinfection

Due to a shared bloodborne transmission route, co-infections with other viruses are frequently occurring while HBV infection. In particular, the hepatitis C virus is estimated to be present in 10-15% of chronic HBV patients and is reported to heavily accelerate the progression of severe hepatitis and fulminant liver failure [95]. Furthermore, around 10% of immunodeficient virus (HIV) infected patients also have a chronic HBV infection with a faster liver fibrosis progression and a lower rate of HBeAg seroconversion [96]. The viral hepatitis D virus (HDV) is a satellite virus and requires the presence of HBV for hepatic entry, intrahepatic spread and propagation. Chronic HBV/HDV coinfection arises in approximately 5% of HBV infected and corresponds with an severe clinical outcome and limited antiviral treatment options [97]. HBV co-infections with the Severe acute respiratory syndrome coronavirus 2 (SARS-CoV-2), a global pandemic beginning in 2019 with an international health emergency and more than 6 million deaths worldwide, also manifest and increase hepatic liver injury. Importantly, a study suspects persistent abnormalities in ALT levels in SARS-CoV-2 patients, which could lead to an increased risk of viral reactivation in the event of HBV co-infection [98, 99].

1.3. Molecular virology

1.3.1. Structure and morphology of virions and subviral particles

In the serum of infected patients, three types of HBV particles are detected: the mature HBV virion (Dane particle) and large amounts of subviral particles (SVP) in the shape of spheres and filaments (fig. 4) [100]. The infectious HBV virion is a spherical particle of 42 nm in diameter, and consists of an outer envelope, surrounding an inner icosahedral nucleocapsid which packages the polymerase and the viral DNA [8]. In particular, the HBV genome is approximately 3.2 kb in length and is most likely obtained as relaxed circular, double-stranded DNA. The (-)-strand is covalently attached to the viral polymerase. The icosahedral nucleocapsid is approximately 30 nm in diameter and encloses the viral genome. The HBc protein is highly conserved and self-assembled first as a homodimer, then oligomerizes to a complete capsid with an icosahedral symmetry consisting of either 90 (T=3 symmetry, 30 nm diameter) or 120 (T=4 symmetry, 32 nm diameter) dimers. However, infective virions mainly consist of a T=4 symmetry. The nucleocapsid is finally enveloped by a lipid membrane which is attributed by three surface glycoproteins – large (LHBs), middle (MHBs) and small (SHBs) [101–103]. Cryo-electron microscopy images of a reconstituted mature virion indicated furthermore, that the HBsAg spikes in the enveloped were arranged in a roughly trigonal lattice, which does not coincide with the spikes from by the core dimers. Based on this it was concluded, that the nucleocapsid and the envelope are only loosely associated [104].

Apart from the completely assembled, infectious viral particles, SUPs are produced in a 10^3 to 10^6-fold excess over mature particles and form spheres or filaments exclusively from the envelope proteins and lack any capsid or viral DNA. Spheres are approximately 20 nm in diameter and assemble mainly by SHBs proteins, whereas filaments are characterized by 22 nm diameter and variable length. Filaments incorporate larger amounts of LHBs as compared to spherical, subviral particles. Although the reason for the massive release of SVPs is still unclear, it is possible that the overproduction neutralizes the host's virus-specific immune response and thus favors the infection of new hepatocytes [100, 101]. Recent evidence indicated also further, non-infectious particles circulating in the blood of infected patients. These include either DNA-free (empty), double-stranded linear DNA (~10% of enveloped capsids) or RNA (~1% of enveloped capsids) containing enveloped particles. In addition, non-enveloped, naked capsids were found primarily in HBV-replicating cells (fig. 4) [105–107].

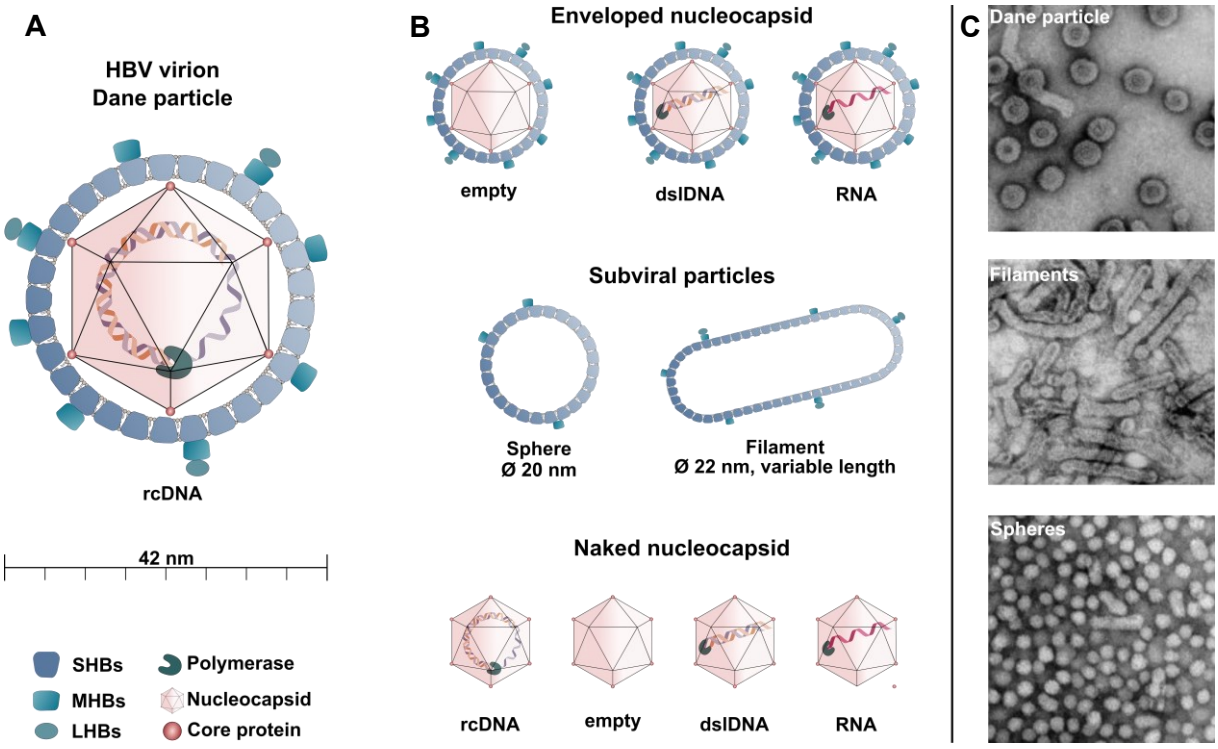

Figure 4: Schematic representation of HBV particles. (A) Infectious hepatitis B virion (Dane particle) consists of an envelope with LHBs, MHBs and SHBs proteins. The envelope encloses an inner nucleocapsid assembled by core proteins with an icosahedral structure. The capsid particle consists of a copy of the rcDNA with 3.2 kb in size and is associated with the viral polymerase. **(B)** Non-infectious HBV particles are rarely produced and include enveloped nucleocapsids, either empty, with dslDNA or RNA. Or naked nucleocapsid with rcDNA, empty, dslDNA or RNA. Large quantities of subviral particles are released as spheres or filaments with variable composition of surface proteins and different sizes. **(C)** Electron microscopy of the most common, circulating viral particles. (Images are retrieved from Gerlich et al. [6]). dslDNA – double stranded linear DNA; LHBs / MHBs /SHBs - large-, middle- and small surface protein; rcDNA – relaxed circular DNA, (Underlying literature is reported by Tsukuda et al. & Iannacone et al. [106, 107])

1.3.2. Viral nucleic acid and genome organization

A unique feature of HBV is the highly compact and efficiently organized genome structure [108]. With approximately 3.200 base pairs in length, the HBV genome represents the smallest genome among DNA viruses. The partially double-stranded character is composed by two asymmetric strands of fixed polarity, plus-strand DNA (incomplete, non-coding) and the negative strand DNA (complete, coding-strand). The circular configuration is archived by a biochemical repair mechanism between the 5’ end of the positive and negative strands. Whereas the 5’-end of the minus-strand is covalently linked to the viral polymerase, the 5’ end of the plus strand is capped by a 19 nt-long RNA oligonucleotide derived from the pregenomic RNA (pgRNA), and serves as primer for the plus-strand synthesis [109, 110]. In addition, the 5’ ends of both strands are mapped with two short repeat sequences of 11 nucleotides (nt)

(direct repeats - DR), which are crucial for genome circularization and viral replication initiation [111, 112].

The HBV genome contains four highly overlapping open reading frames (ORFs) and represents the gene sequence to encode seven viral proteins. The longest ORF (Pol) encodes for the viral polymerase, which represents the central enzyme in the genome replication and includes the three catalytic subdomains – the terminal protein domain (TP), reverse transcriptase with DNA-polymerase activity and the RNaseH [113, 114]. The second largest ORF (S) encodes the three different envelope glycoproteins, the large, middle and small surface antigen (HBsAg) followed by the precore/core ORF (C/preC), which refers to the HBV e antigen (HBeAg) or core protein respectively. The X-ORF (X) encodes the multifunctional HBx-protein (Fig. 5A) [21, 115].

The replication of the HBV genome occurs due to an RNA-intermediate and requires the nuclear machinery of the host cell. Accordingly, post-infection, the viral DNA is completed from the relaxed, circular DNA (rcDNA) into a covalently closed circular DNA (cccDNA). This serves as a template for transcription of the pregenomic RNA (pgRNA, 3.5 kb) and several subgenomic RNA (sgRNA, 2.4 kb, 2.1. kb and 0.7 kb), driven by four specific and unidirectional promotor sequences within the HBV genome (core, SPI, SPII and X) (Fig. 5B) [109, 110, 116]. With a length of 3.5 kb, the pgRNA exceeds the size of the genomic, rcDNA (3.2 kb) and contains therefore a terminal redundant copy of the viral genome (fig. 5) [113].

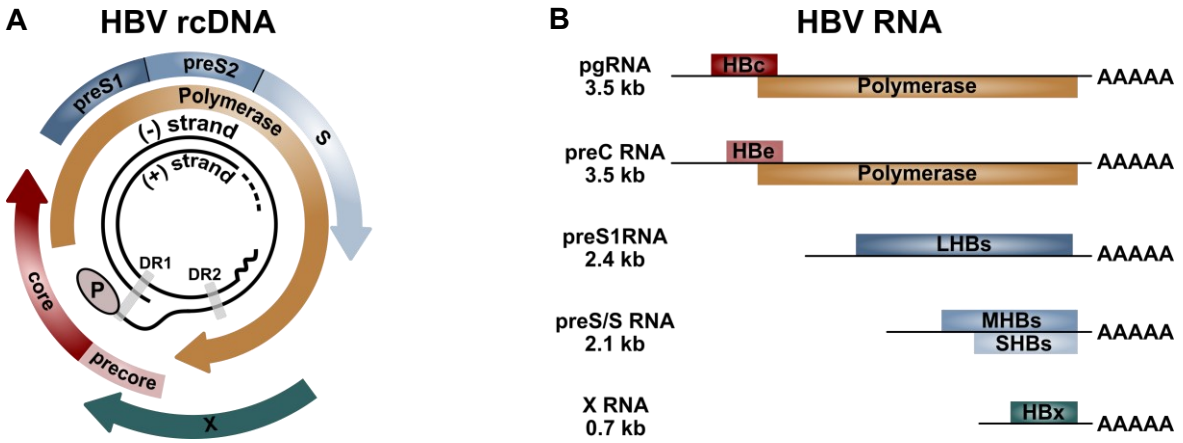

Figure 5: HBV genome organization. (A) The partial double-stranded circular DNA is made up of black lines with covalent bound viral polymerase (P, brown) at the 5' end of the (-) strand DNA. The heterogeneous character of the (+)-strand DNA is indicated by a dotted line, the RNA primer sequence at the 5' end is represented by a zigzag line. The direct repeat elements 1 and 2 (DR1 and DR2) are indicated by vertical bars (grey). The relative position of the open reading frames is placed outside: HBc and HBe – red arrow, viral polymerase – yellow arrow, LHBs, MHBs and SHBs (preS1, preS2 and S) - blue arrow and HBx green arrow. **(B)** Viral RNA transcripts produced from the cccDNA (black lines) and the encoded proteins (boxes). (Modified according Beck et al. & Tsukada et al. [106, 109])

1.3.3. Viral proteins

Based on the limited size of the viral genome, HBV synthesizes only a limited repertoire of structural and regulatory proteins. In light of this, three surface proteins (L-, M- and S-HBsAg) and the core protein (HBcAg) provide the structurally relevant proteins. The non-structural proteins encompassed the polymerase, which is required for the replication and the regulatory HBx protein with pleiotropic functions in viral and host pathways. In contrast, HBeAg is not part of the assembled virion and is secreted after synthesis from hepatocytes [113].

1.3.3.1. Surface proteins

The three hepatitis B envelope proteins are encoded by a single ORF, divided by three in-frame start codons. Based on this, an amino-terminal (N-terminal) preS1 (108-119 aa), a central preS2 (55 aa) and a carboxy-terminal (C-terminal) S-domain (226 aa) are translated. All three surface proteins are type II transmembrane proteins and harbor glycosylation sides, supporting disulfide bridge formation and particle secretion. The SHBs (24 kDa) contains only the S-domain and are present in all three surface proteins, the preS2 extension occurs in the MHBs (31 kDa), the additional preS1 is present only in the LHBs (39 kDa). Therefore, the different surface proteins differ only by their length and glycosylation sites within the N-terminal domain [6, 101]. Furthermore, the transmembrane topology, gained by the synthesis and secretion at the endoplasmic reticulum (ER) differs only in the N-terminal region. Importantly, during the translation process and translocation through the ER, part of the N-terminal S-domain forms an ER-luminal orientated loop between the first and the second transmembrane anchor region [117]. The loop is issued as “a” determinate and provides the major conformational epitope (99-170 aa) of the HBsAg and contains an additional glycosylation site at Asn 146 [118]. Unique for the LHBs, since the initial transmembrane domain is no longer used as a co-translational signal sequence, a post-translational mechanism causes in 50% a topological reorientation of the PreS1/PreS2 domain. This facilitates on the cytoplasmic site the interaction and envelope with the core protein, as well as interaction with intracellular signal transduction mediators. The opposite topology exposes the N-terminus on the surface of virions and facilitates a high-affinity NTCP-receptor (entry receptor of HBV) recognition [119]. Despite structural functions, HBsAg is also reported as a multifunctional protein and plays a crucial role in the host immune response and regulation of various cellular signaling pathways with contribution to HCC development In this regard, the PreS2-domain is known with an activator function and initiates the PKC; c-Raf-1/MAP2-kinase signaling cascade, which is finally associated with an elevated proliferation level in hepatocytes and promotion of carcinogenesis [120, 121].

1.3.3.2. Core protein

The HBV core protein (22 kDa) is highly conserved among different genotypes and forms the framework (nucleocapsid) of the viral particle. The primary sequence can be divided into an N-terminal assembly domain and an arginine-rich, C-terminal packaging domain [122]. Structural analysis, based on 3.3 Å resolution X-ray crystallography data, reveals mainly α-helices and a hairpin loop, which constitutes the spike tip (epitope) of the core protein, while dimerization [123]. Disulfide bonds among dimers stabilize the assembled nucleocapsid and provide on the one hand the caging of the viral genome and interaction with the envelope shell [103]. On the other hand, the core protein is required for initiation of the reverse transcription, pgRNA packaging and reduces spacing of the HBV nucleoprotein complex, while binding to the cccDNA [124].

1.3.3.3. Polymerase

The polymerase polypeptide (90 kDa) encompasses three functional domains and a variable spacer region. While the terminal protein domain (TP) is crucial for pgRNA packaging and initiation of viral replication, the C-terminal domain provides the reverse transcriptase activity and is further equipped with RNaseH in order to permit synthesis of the (-) DNA-strand [125, 126].Furthermore, Lupberger et al. identified a bipartite nuclear localization signal in the TP region of the polymerase that is crucial for nuclear import of the genome complex and thus for productive virus infection [114].

1.3.3.4. E antigen

The HBeAg (18 kDa) is an accessory protein of HBV and is produced by a posttranslational cleavage apart from the C-terminus of the precore-core protein at the ER. The HBeAg is secreted from infected hepatocytes and provides a crucial viral biomarker to monitor the course of natural infection. The antigen is not necessary for the viral infection, replication or assembly. While the biological function of HBeAg remains a long time unknown, recent evidence offers an immune modulatory contribution [127–129].

1.3.3.5. HBx-protein

The HBx protein is a non-structural viral protein of 154 aa in size (17 kDa) and is described as a multifunctional protein with pleiotropic function in several viral and cellular pathways. While the sequence of HBx indicates partially high homologs consensus among all mammalian Hepadnaviruses, it is absent in Avihepadnaviruses. Likewise, no sequence homologies to other proteins are known [130].

The primary sequence is subdivided into two functional domains, the N-terminal domain contains a negative-transactivator activity (1-50 aa), whereas the C-terminal region includes a transcriptional activator domain with numerous identified target regions, essential for host cell interactions. In particular, three regions (aa 54-70, 75-88 and 109-131) provide target sites for the interaction with mitochondria, a nuclear trans-activation site if offered between the aa 120 and 140. Furthermore, studies identified a zinc-binding motif, a conserved alpha-helix H-box motif and a BH3-like domain as key structured areas, responsible for the main functions of the protein [131–133]. Apart from this, until now, structural investigations failed to identify the three-dimensional structure of the HBx-protein [134]. The reason for this, remains in the molecular characteristics of the HBx. On the one hand, the expression level during the natural course of infection is relatively low, on the other hand reveals the recombinant expression of only minor amounts of soluble proteins (fig. 6) [133, 135].

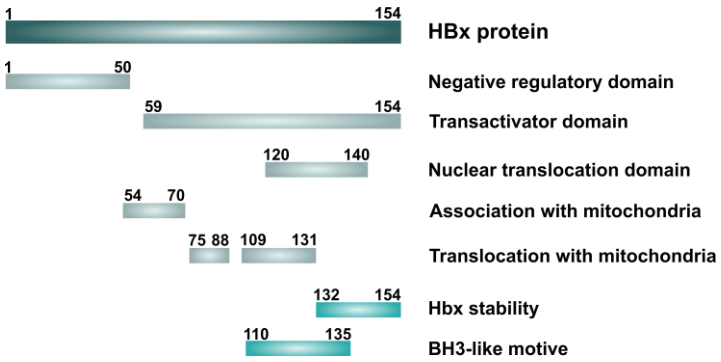

Figure 6: Functional domains of HBx protein. The 154 amino acid HBx is represented in dark green. Functional domains are indicated as light green boxes. Structural regions are coloured in turquoise. (Figure is retrieved and modified according Chuang et al. [132])

The subcellular localization of the HBx protein is mainly dependent on its relative abundance. At low expression levels, HBx is predominantly nuclearly localized. A cytoplasmatic accumulation with partially mitochondrial association is preferred among higher expression levels [136]. Long time, the relevance and functional contribution of HBx were under debate. Although the protein is not essential for the viral life cycle and replication mechanism, it is suspected to be responsible for direct and indirect contributions to severe liver transformation and pathogenesis [137].

In this regard, HBx is assumed to actively control the cccDNA pool within the cell and furthermore govern as well viral, as cellular promoters. In fact, a proteomic screening elucidated a total of 402 proteins (189 proteins with a specific trans-activator domain for HBx), interacting with the HBx protein [138]. By hijacking cellular functions, HBx initiates an immense deregulation of several cellular mechanisms and signaling pathways, which ultimately promote hepatocarcinogenesis. Therefore, HBx is accounted as one of the driving forces in the progression of virus-induced liver transformation and HCC development (Fig. 7) [137, 139].

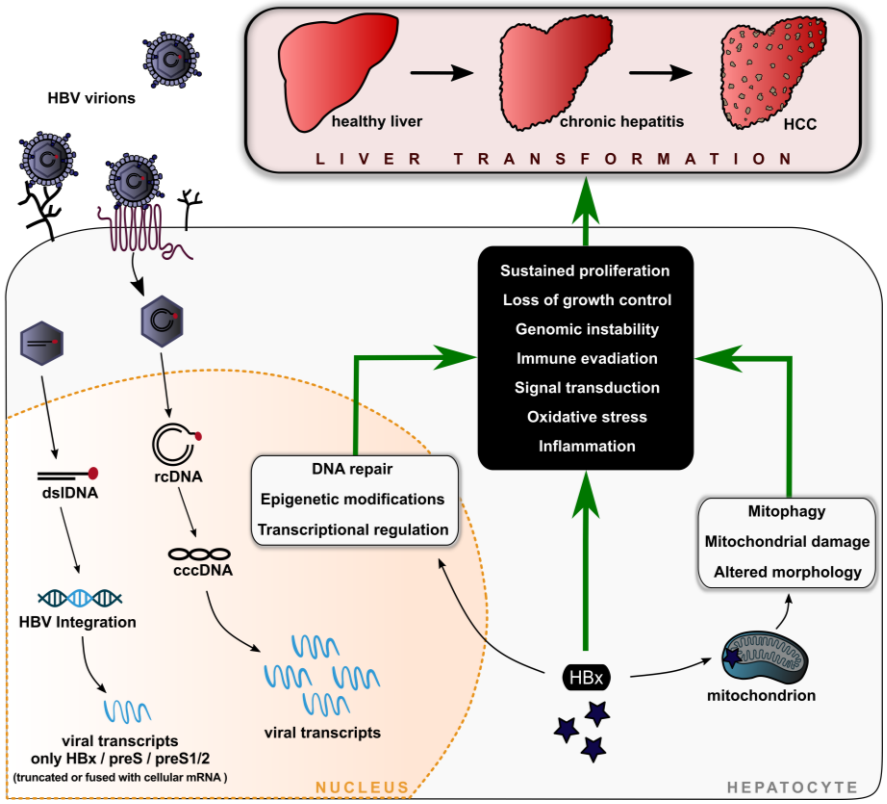

Figure 7: Schematic overview of HBx-mediated liver transformation processes. HBx is synthesized either from integrated viral transcripts or from cccDNA based subgenomic viral RNA. According to their subcellular localization, nuclear, cytoplasmic or mitochondrion-associated, HBx is attributed to a variety of cellular signaling pathways, and the deregulation of host cellular functions, which contributes to liver-related pathogenesis. DsIDNA – double stranded linear DNA; HSPG - heparan sulfate proteoglycans; NTCP - Sodium taurocholate co-transporting polypeptide; rcDNA – relaxed circular DNA (Figure published in Schollmeier et al. [139])

Based on the subcellular localization of HBx, HBx-induces changes in both nuclear, cytoplasmic and mitochondrial-associated proteins and signaling pathways. In particular, nuclear HBx mainly occurs at low expression levels, which in terms reflects the early phase of HBV infection and modifies the gene expression of viral and cellular genes through epigenetic modifications (methylation/demethylation), chromatin remodeling or binding and modulation of non-coding RNAs [140]. In light of this, important HBx-mediated epigenetic modulations are represented by hypermethylation within promotor regions of CpG-island areas of tumor suppressor genes, but also genome-wide hypomethylation of proto-oncogenes [141, 142]. HBx binding sites were also identified in several non-coding RNAs which have further consequences in the immune response, cell proliferation and inflammation processes [143]. In addition, HBx is also reported to hijack chromatin-modifying enzymes in order to benefit functional, epigenetic control of the viral cccDNA [143]. Overall, the direct correlation between malignant tumor transformation and HBx-mediated, epigenetic landscape offers an interesting aspect as a “biomarker” to monitor HBV-related tumorigenesis [144].

Cytosolic HBx interferes with key cellular signaling pathways with fulminant effects on cell survival, metabolism, inflammation, genomic instability, and other signal transduction pathways. In particular, modulatory effects through HBx were reported for example in nuclear factor-κB (NF-κB), Wnt/β-catenin, Janus kinase (JAK) / STAT, PI3K/AKT, Ras/Raf-mitogen-activated protein kinase (MAPK) and Src-kinase pathways. The complex and extensive contribution in cellular pathways and network interactions are reasonable for aberrant hepatocellular metabolism, proliferation, immune response and other cellular functions, which ultimately facilitates liver disease and cancer progression [137, 145]. The best characterized cytoplasmic interaction of HBx is reported with the DNA damage-specific DNA-binding protein 1 (DDB1), which mediates the degradation of the structural maintenance of chromosomes protein 5/6 (Smc5/6) complex and subsequently supports the viral replication from the cccDNA [146].

Particular focus is given also to the HBx-driven induction of oxidative stress, connected with a broad impact on cellular energy metabolism and hepatic inflammatory response. In light of this, in response to HBx-mediated ER stress and aberrant energy metabolism an elevated level of radical oxidative stress (ROS) arises in the cytoplasm. Consequently, hepatocytes respond with expression of distinct inflammatory mediators. This triggers on the one hand interleukins and related cytoprotective signaling pathways, such as NF-κB/AKT, and on the other hand the activation of the NLR family pyrin domain containing 3 (NLRP3) inflammasome with further consequences for inflammation processes and HCC development [147–151]. In addition, Kelch-like ECH-associated protein 1 (Keap1), an oxidative stress sensor, provides an important defense mechanism by interacting with the HBx protein and leading to activation of NF-E2-related factor 2 (Nrf2) / antioxidant response element (ARE) signaling pathway and further to a negative regulation of HBV replication [101, 152].

Apart from this, HBx is also known to associate with mitochondrion-specific proteins and exert sustained effects in the mitochondrial dynamic, signal transduction and overall mitochondrial metabolism. HBx-mediated mitochondrial turnover is also considered a key factor in hepatocarcinogenesis [153]. However, detailed interactions of HBx with mitochondria and underlying mechanisms are described in more detail in chapter 1.5.

1.4. Viral life cycle

HBV is a highly hepatotropic virus, whereas a single virion is sufficient for establishing a viral infection. This is only possible by an efficient transport of the pathogen across the bloodstream to the liver, avoiding immune control and persisting within the target cell. Although the exact mechanism of how the virus travels through the bloodstream and enters hepatocytes remains

to be established, a recent study provides evidence for an association between HBV and liver-targeted lipoproteins to hijack the physiological lipid transport mechanism to target and enter hepatocytes [154, 155]. Furthermore, the initial uptake of HBV into the liver organ is taken place through a barrier of fenestrated liver sinusoidal endothelial cells (LSECs), probably by squeezing through the fenestrae [155, 156]. To gain excess through the liver parenchyma, HBV is attached in the Disse-space (interspace of both LSEC and parenchyma cell layers) by heparan sulfate proteoglycans (HSPG), which is essential for the uptake through the basolateral membrane of liver parenchyma cells by NTCP receptor binding (fig. 8A) [157, 158]. Followed by a unique mechanism, in which the viral genome is replicated through an RNA intermediate and newly assembled virions secrete via multi-vesicular bodies (MVB), as described in detail below (fig. 8B) [101].

1.4.1. Attachment and Entry

The NTCP receptor, originally discovered as hepatocyte-specific bile acid transporter, was recently identified as an HBV entry receptor. This step is preceded by a reversible, low-affinity binding of HSPG, followed by the high-affinity HBV binding on the NTCP receptor, which binds specifically the myristoylated N-terminal part of the preS1 surface domain. The interaction triggers then the internalization in an endocytosis-dependent mechanism [11, 158, 159]. This process is probably supported by direct interaction with the epidermal growth factor receptor (EGFR) and other, till now undiscovered host entry co-factors [160]. Endosomal proteolytic processing enables the dissociation of the viral envelope and the release of the nucleocapsid from the vesicular membrane. The nucleocapsid further interacts with host microtubules and is thereby actively mediated through the cytoplasm and imported into the nucleus [161, 162].

1.4.2. Nuclear import and viral replication

The entry of the nucleocapsid into the nucleus takes place through the nuclear core complex (NCP) and is mediated in an importin-dependent manner. Hereby, the nucleocapsid is caged into the NCP-basket and induces the disassembly of the core capsid, followed by the release of the rcDNA [162, 163]. In this regard, a previous study reported, that the nuclear entry and dispersion of the capsid is facilitated by small ubiquitin-like modifiers conjugation (SUMOylation) among the core protein [164]. The partially rcDNA is now processed by cellular factors and completed to a circular supercoiled cccDNA. This process is supported by DNA polymerases, DNA ligases and topoisomerases [165–167]. The cccDNA maintains in the nucleus and contributes therefore in the persistence of the viral infection and serves as a template for the viral RNA synthesis. In particular, the transcription of the cccDNA reveals into the pgRNA (3.5 kb), which is an intermediate for the viral replication and further sgRNAs of

different lengths. This step is highly regulated by histones, which are recruited to cccDNA and control transcriptional activity through post-translational modifications [101, 168].

1.4.3. Encapsidation and egress

After the release of the pgRNA into the cytoplasm, the translation of the polymerase and core protein started and assembled together in a core capsid. This step is mediated by binding of the polymerase to the epsilon motive in the pgRNA, which serves first, as an encapsidation signal and provides further the priming sequence to initiate the maturation process of the capsid by reverse transcription from pgRNA to rcDNA. Now the maturated capsids can be either re-imported into the nucleus and enrich the pool of cccDNA in the nucleus, or assembled with mature, viral surface proteins to be released from hepatocytes [169, 170]. Apart from this, a minor fraction of nucleocapsids containing dslDNA, viral RNA, or are empty. These particles can follow up the same route as the rcDNA containing capsids, however, are not infections. Importantly, however, dslDNA-containing capsids provide the dominant substrate for a viral DNA integration process into the host genome [171]. Although the integrated sequence is unable to replicate the entire HBV sequence, it still contributes to the transcription of viral mRNA of HBsAg or HBx transcripts and thus increasing the number of synthesized viral proteins [172].

Besides this, the sgRNA encodes for the three surface proteins and the regulatory HBx protein. To gain interaction and envelopment with the nucleocapsid, the surface proteins are co-transcriptionally anchored in the ER membrane and thus facilitate the enclosure of the capsid and interaction with the LHBs surface proteins. Finally, the release process of viral particles, naked capsids and SVP is tightly regulated by the cellular membrane sorting machinery [101, 173]. In particular, the release of infectious viral particles is mediated through MVBs and the Endolysosomal sorting complex required for transport (ESCRT)-pathway [174]. This pathway is supported by co-factors such as γ2-adaptin, Vsp4 and α-taxilin [173, 175]. Besides this, a recent study evidence also intact HBV virion in released exosomes as an alternative release route [176]. Subviral particles are released as spheres via the general secretory pathway, whereas the LHBs containing filaments are also secreted via ESCRT/MVB pathway [177, 178]. HBV naked capsids also egress through an ESCRT-independent pathway but require Alix and hepatocyte growth factor-regulated tyrosine kinase substrate (HGS) [179, 180].

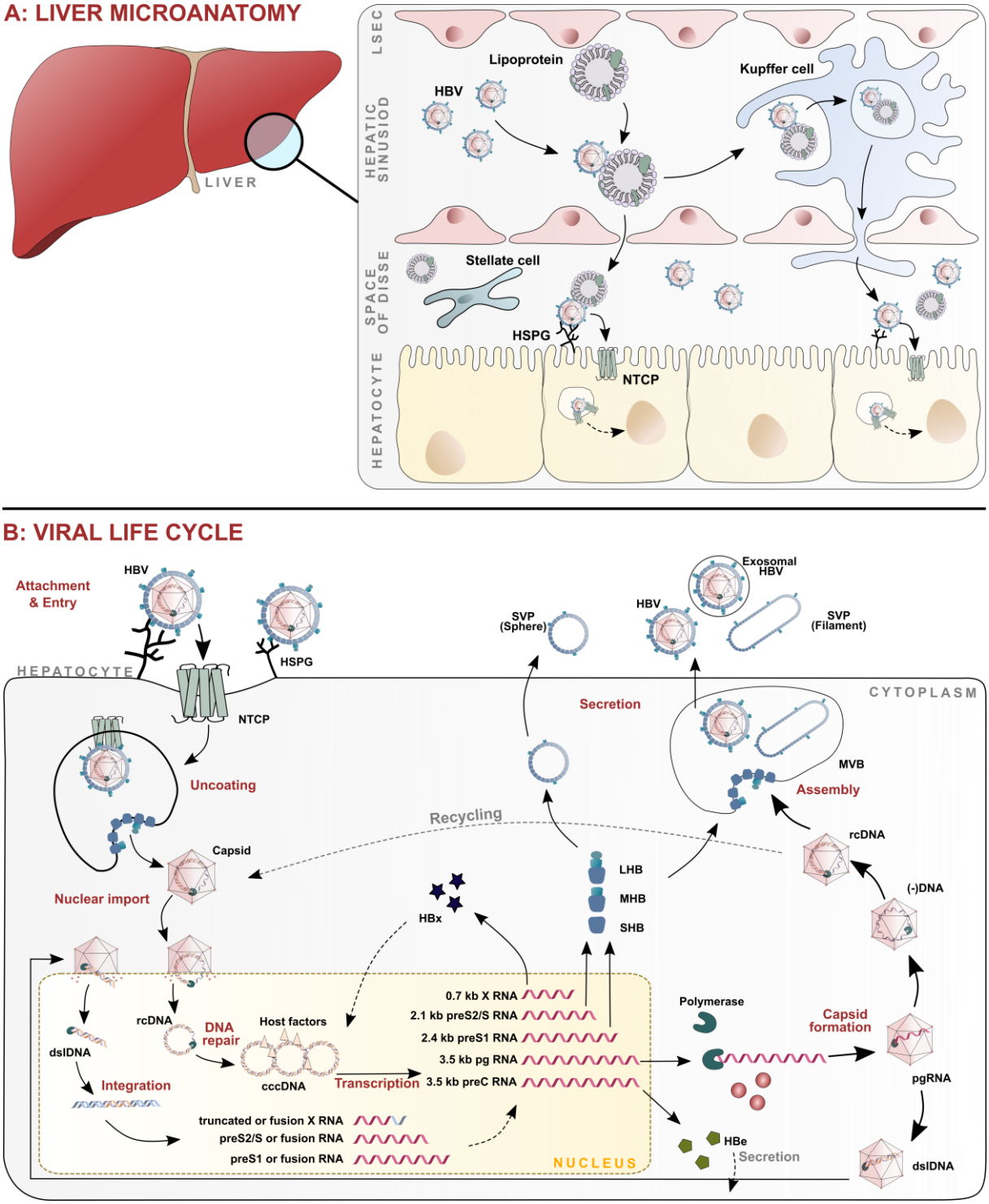

Figure 8: Liver microanatomy and viral life cycle during HBV infection. (A) Infectious HBV particles circulating through the bloodstream towards the hepatic sinusoid. The first barrier is given by the liver sinusoidal endothelial cell (LSEC) and is overcome either by lipoprotein mediated squeezing or by shuttling via kupffer-cell entering. Once entering the Dissé-space, the virus is attached to HSPG and directed towards the liver parenchyma cell membrane via NTCP-receptor binding. (Underlying literature is reported by Protzer et al. & Esser et al. [154, 155]) **(B)** Schematic overview of the HBV life cycle includes attachment and entry, uncoating, nuclear import, DNA repair and integration, transcription, capsid formation, assembly and secretion. DslDNA – double stranded linear DNA; HSPG - heparan sulfate proteoglycans; LSEC - liver sinusoidal endothelial cell; MVB – multivesicular bodies; NTCP - Sodium taurocholate co-transporting polypeptide; pgRNA – pregenomic RNA; rcDNA – relaxed circular DNA. (Underlying literature reported by Tsukuda et al. & Zhao et al. [106, 172]).

1.5. Mitochondria in virus infection

Mitochondria are found in all eukaryotic cells (except blood cells) and play a crucial role in regulating multiple cellular processes, such as metabolic pathways, apoptosis, cell proliferation and innate immune signaling. These highly dynamic organelles sense environmental insults, inflammations and other messenger molecules and rapidly respond with structural changes and protein expression. However, an elevated mitochondrial turnover triggers a cascade of reactions and leads to a global mitochondrial dysfunction with a fundamental impact on cellular homeostasis, which is further attributed to a variety of diseases [181]. In this regard, mitochondria are the main source of ROS, which is associated with pathological consequences in case of an imbalance between production and elimination [182]. Accumulating evidence also demonstrated a close nexus between virus infections and profound mitochondrial alterations. Against this background, the physiology and pathology of mitochondria in viral infections are increasingly coming into focus and offer the opportunity to develop mitochondria-targeted antiviral therapies [183].

1.5.1. Mitochondria biogenesis and function

Mitochondria are double-membraned organelles and contain their own double-stranded, circular DNA (mtDNA), which encodes 13 polypeptides from 37 genes. In addition, approximately 1500 nuclear-encoded proteins contribute to mitochondrial functionality [184]. The innermost compartment of the mitochondrion, the mitochondrial matrix contains the mtDNA and is the site of several enzymatic reactions that contribute to the replication as well as protein syntheses from mtDNA [185]. Furthermore, the matrix represents the main side of key metabolic processes and reactions, such as oxidative phosphorylations (OXPHOS) or fatty acid oxidation (FAO) and the tricarboxylic acid cycle (TCA) [186–188].

The inner mitochondrial membrane (IMM) extends into the matrix and forms cristae in which the electron transport chain and the ATP synthase takes place. The IMM is permeable to oxygen, carbon dioxide and H_2O and embeds a series of protein complexes (complex I - IV) and acts as electron carrier. Once electrons are transferred from an electron donor through the electron transport chain, protons are shuttled from the mitochondrial matrix towards the IMM in the intermembrane space. This generates an energy potential along the IMM, which is returned via ATP synthase and ultimately produces ATP and H_2O. The latter is due to the reaction of protons from the electron transport chain with molecular oxygen. A common byproduct of this reaction is ROS, which is formed when electrons leak from the electron transport chain and reduce the surrounding molecular oxygen. In fact, mitochondria represent

the main source of ROS production in the cell which are usually (under healthy conditions) rapidly detoxified by a variety of antioxidant enzymes and mechanisms [187, 189].

The outer mitochondrial membrane (OMM) consists of a porous phospholipid bilayer that is permeable to small molecules. In addition, the membrane houses multiple pores and channels to allow the traffic of larger molecules [190]. An important pore-forming channel is thereby the voltage-dependent anion channels (VDAC; 3 isoforms), which conducts metabolites through the membrane and regulates the integrity of the OMM [191]. Furthermore, the OMM associates with the ER (the main intracellular Ca^{2+} storage) and maintains the calcium homeostasis of the cell [192].

1.5.1.1. Mitochondrial network dynamic

To maintain mitochondrial homeostasis, the mitochondria within a cell form a dynamic tubular network, composed of long filaments with branching structures. The merging and branching of these networks from smaller filaments or single mitochondria is called fusion and is associated with the rapid equilibrium of matrix components and recycling of mitochondrial metabolites [187]. In contrast, this process can be converted by a fission process and leads to an asymmetric fragmentation with unconnected, small round mitochondria. This process is of great importance to remove non-functioning mitochondria or mutations in the mtDNA and maintain a healthy phenotype. Accordingly, the mitochondrial network undergoes a continuous modification through fusion and fission to prevent mitochondrial dysfunction and is ultimately the result of two opposite processes, which are highly coordinated and regulated by large GTPases. In particular, GTPase dynamin-related protein (Drp1) in combination with the mitochondrial fission 1 protein (FIS1) the mitochondrial fission factor (MFF) facilitates the fission process, while the dynamine-like GTPase – Opa1, together with Mitofusin 1 and 2 (MFN1/2) forces the fusion process. Given this, the mitochondrial membrane potential ($\Delta\Psi_m$) plays a crucial role in the perception of mitochondrial physiology and the corresponding shift in balance. In addition, increased ROS levels have been postulated as a direct inducer towards fission [193–195]. In this context, various kinases and phosphatases have been identified as hubs for mitochondrial signaling, which have major implications for their localization and function [196].

1.5.1.2. Molecular mechanism of mitophagy

Since defective mitochondria are associated with enormous pathogenic consequences, fragmented mitochondria become immediately eliminated by mitophagy, which describes a selective form of autophagy and is considered as important mitochondrial quality control

mechanism [197]. This process is characterized by mitophagy initiation, targeting for recognition by ubiquitin (Ub), recognizing by a microtubule-associated protein light chain 3 protein (LC3) and engulfment into autophagolysosomes and final fusion with lytic compartments and degradation by hydrolases [198]. Yet, two distinct pathways have been identified to tether compromised mitochondria to the autophagic machinery [199].

The best-characterized pathway is mediated by the PTEN-induced putative kinase 1 (PINK1). The Pink1/Parkin pathway is initiated by accumulation and activation (phosphorylation) of PINK1 at the OMM, thereby recruiting Parkin, which in turn is activated by an autoinhibited enzyme to a ubiquitin-dependent E3 ligase. Upon activation, Parkin becomes polyubiquitinated, along with several other OMM proteins and triggers the interaction with the LC3-decorated membrane of phagophores and incorporation within the autophagosomal system [200]. Furthermore, mitophagy can also be initiated independently of Parkin. The receptor-mediated mitophagy relies hereby on the contribution of mitochondrial receptors, which contain a conserved LC3-interaction region (LIR) and directly recruit LC3 and autophagosomes for elimination. Typical receptors with a direct LIR sequence are located either on the IMM or OMM and include among others, the BCL2 interacting protein 3 (BNIP3), Nip3-like protein X (NIX), and the FUN14 domain-containing protein 1 (FUNDC1) [201].

Beyond the tight balance of mitochondrial dynamics, several factors such as cellular stress, cancer or especially viral infections contribute to an aberrant mitochondrial physiology and pathology with consequences for cellular apoptosis, intracellular calcium signaling and innate immune system stimulation (fig. 9) [183].

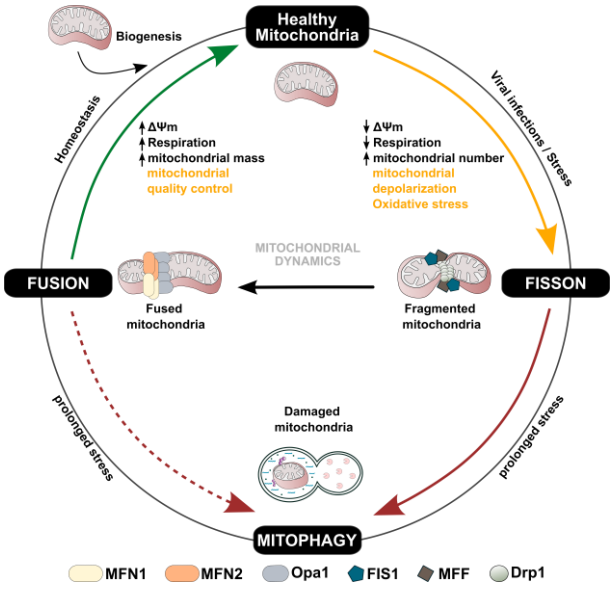

Figure 9: Mitochondrial network dynamics. Mitochondrial network represents a balance between fission, fusion and mitophagy depending on the physiological state of the cell and mitochondria. Fusion is mediated by Opa1 and MFN1/2, to maintain homeostasis. Viral infections and cellular stress induce fission by FIS1, MFF and Drp1 and lead to fragmentation of mitochondrial network. Prolonged stress induces a breakdown of damaged mitochondria

through mitophagy. Drp1 - dynamin-related protein 1; FIS1 - mitochondrial fission 1 protein; MFF – mitochondrial fission factor; MFN – mitofusin; Opa1 - mitochondrial dynamin like GTPase. (Graphic is retrieved and modified according Elesela et al. [202])

1.5.2. Mitochondria in hepatic infections

HBV is known to interact with numerous of mitochondrial proteins and induces thereby a profound change in the mitochondrial morphology and homeostasis, which further associated with a direct impact on mitochondrial and cellular signaling pathways and the innate immune response. In particular, the liver cells contain up to 500-4000 mitochondria and play therefore a key role in the liver-related physiology [153]. Importantly, HBV infections leading to an adjacent membrane depolarization and mitochondrial dysfunctionality and is believed to play a momentous role in HBV-mediated HCC formation. Furthermore, the interaction between HBV and mitochondrial proteins supports the viral life cycle (replication), prevents the induction of mitochondria-associated antiviral signaling mechanisms, and likely prevents global cell death as a survival mechanism [181]. In this context, HBV polymerase, HBsAg, nuclear protein and HBx protein were found to interact with mitochondrial proteins, despite the main contribution with significant impact on liver pathophysiology is caused by the HBx protein [153].

1.5.2.1. HBx mediated impact on mitochondrial dynamic

The viral protein HBx is known to interact with several mitochondrial proteins and has significant effects on mitochondrial-mediated pathways. This includes the modulation of several signaling pathways, ROS production, calcium signaling, induction of cellular apoptosis and innate immune response. Overall, the profound modulation of mitochondrial physiology by HBx ultimately could facilitate chronic liver failure and the development of HCC (fig. 10) [203]. With this in mind, three regions in the HBx sequence were identified to target mitochondria, one putative transmembrane region is located between the amino acids 54 and 70 and is important for the mitochondrial association, the later domains between 75 and 88, and 109 and 131 are required for mitochondrial targeting. Furthermore, interaction with HBx often results in a perinuclear clustering of mitochondria as a consequence of reduced intracellular transport along microtubular structures [204].

In particular, the HBx protein is known to interact directly with Drp1 and enormously shift the mitochondrial network toward the fission process. This step is also considered as an initial step to promote and increase degradation through mitophagy [205]. In addition, a key co-localization is also given between HBx and the VDAC3, which leads to a loss of the mitochondrial transmembrane potential and depolarization of the mitochondrion [206]. As a consequence, the organelle becomes permeable for several mitochondrial metabolites such

as cytochrome c (Cyt c), mtROS and mtDNA. On the one hand, this leads to an increased induction of mitophagy, whereas HBx is assumed to trigger the PINK1/Parkin-mediated mitophagy signaling pathway; On the other hand, excessive release of mitochondrial metabolites is strongly associated with mitochondrial dysfunction [147, 197, 207].

Increased mtROS levels contribute to increased cellular oxygen stress, which in turn leads to the initiation of hepatic inflammatory processes, but also induces feedback loop effects in the respiratory chain complex, which further increases ROS [207]. The release of mtDNA causes the activation of signaling pathways (e.g. Nrf2, NF-κB/p-AKT, AP-1 and STAT4) or stimulates inflammatory mediators as damage-associated molecular pattern (DAMP) [208].

Upon mitochondrial destabilization and in direct response to mitochondrial oxidative stress, the NLR family pyrin domain containing 3 (NLRP3) inflammasome is activated and induces the caspase 1-dependent secretion of several cellular pro-inflammatory mediators, such as interleukin 1β (IL-1β), IL6 and IL18. Likewise, upregulation of pro-inflammatory cytokines upon HBx-mediated ROS and mtDNA release triggers anti-apoptotic behavior, probably to enhance viral persistence [209, 210]. In addition, mitochondrial antiviral signaling protein (MAVS), a host antiviral defense mechanism, is also affected by HBx, as HBx suppresses the retinoic acid-inducible gene I (RIG-I) and thereby downregulating the antiviral immune response. However, this process appears to be dependent on the genotype of the respective HBx protein [211].

Furthermore, the emerging influence of the HBx protein on numerous mitochondrial signaling pathways and the profound alteration of mitochondrial function (as summarized in fig. 10) provides the opportunity to establish new biomarkers to monitor virus-induced liver pathogenicity but also offers options for drug development [139, 212].

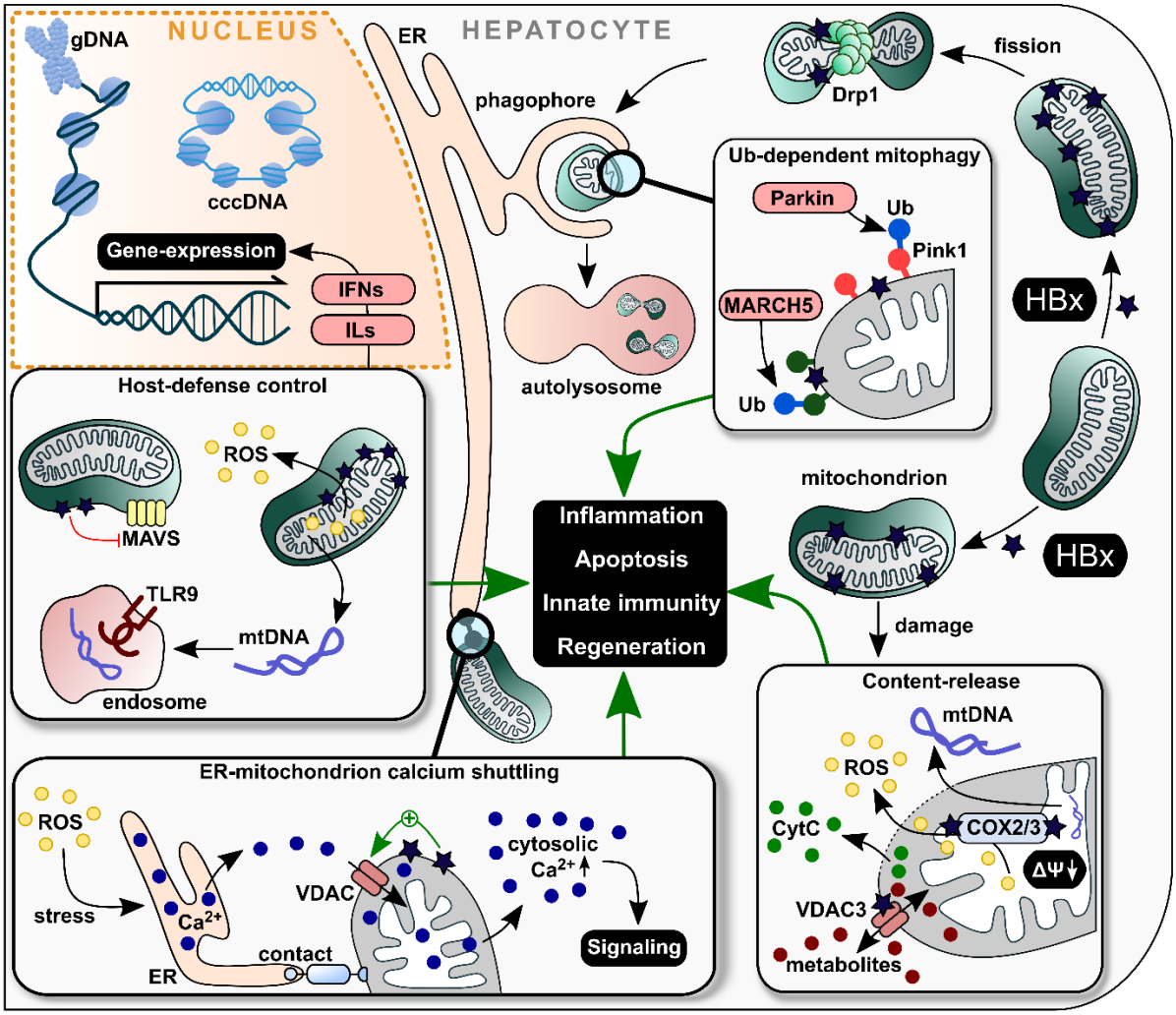

Figure 10: Schematic overview of HBx-mediated mitochondrial dysfunction. HBx interacts with several mitochondrial proteins and induces fundamental effects on mitochondrial and cellular processes. HBx-mediated effects are clustered in host-defense control mechanisms, Calcium signaling, Ub-dependent mitophagy through the PINK1/Parkin mediated pathway and release of mitochondrial metabolites and contribute to liver-related disease progression. Ca2+ - calcium ions; cccDNA - covalently closed circular DNA; COX2/3 - cyclooxygenase 2/3; CytC - cytochrome complex C; Drp1 - dynamin-related protein 1; ER - endoplasmic reticulum; gDNA - genomic DNA; IFN - interferon; IL - interleukin, MARCH5 - membrane-associated RING-CH 5 protein; MAVS - mitochondrial antiviral signaling protein; mtDNA - mitochondrial DNA; PINK1 - PTEN-induced kinase 1; ROS - reactive oxygen species; TLR9 - toll-like receptor 9; Ub - ubiquitin; VDAC3 - voltage-dependent anion channel (Figure published previously in Schollmeier et al. [139])

2. Context and specification of this study

With approximately 269 million chronically infected individuals and up to 0.8 million deaths per year, the hepatitis B virus remains a major global health problem worldwide [18]. Although available treatment options are capable to supress viral replication, there is still a need for curative therapy. In light of this, some important aspects of the viral life cycle and the complex interaction with host signaling pathways are still poorly understood. Furthermore, in recent years, the genetic variability of HBV has been increasingly considered as an emerging factor in clinical outcomes and therapeutic responses. In particular, molecular mechanisms among different HBV genotypes still remain a riddle but need urgent attention for possible implications for diagnosis and treatment [6, 56].

Furthermore, several studies in the past have described that mitochondria are an “emerging battlefront” in viral infections, as viral proteins hijack host mitochondrial proteins and signaling pathways to promote viral survival and replication. Additionally, there is a direct correlation between mitochondrial dysfunction and the progression of liver diseases, the targeted tissue for HBV [181, 183].

Against this background, this study aims to investigate a comparative characterization of the intergenotypic differences of the viral HBx protein and the associated effects on host molecular mechanisms. A particular focus was also placed on the genotype-related impact of the HBx-protein on morphological and functional implications on mitochondria dynamics and the interaction with associated host proteins. Overall, this work aims to broaden the current understanding of the distinct HBV genotypes and their contribution to HBx-related pathogenicity.

3. Materials and Methods

3.1. Materials

3.1.1. Cell lines – Eukaryotic

Table 2: Eukaryotic cell lines used.

Strain	Description	Source	Identifier
Huh7	Human hepatoma cell line Nakabayashi et al. 1982 [213]	AG Hildt, PEI	N/A
HepG2	Human hepatoma cell line	AG Hildt, PEI	N/A

3.1.2. Cell lines – Prokaryotic

Table 3: Prokaryotic cell line used.

Strain	Genotype	Source	Identifier
Escherichia coli DH5α	F– φ80lacZΔ M15 Δ (lacZYA-argF) U169 recA1 endA1 hsdR17 (rK– mK+) phoA supE44 λ-thi–1gyrA96 relA1	Invitrogen	EC0112

3.1.3. Plasmids

Table 4: Plasmids used.

Plasmid	Description	Manufacturer	Identifier
pcDNA 3.1(-)	Mammalian expression vector with CMV promotor activity (empty control vector)	Invitrogen	V79520
pcDNA_HBx(gtA)	Mammalian expression vector of viral HBx of genotype A	AG Hildt, PEI	N/A
pcDNA_HBx(gtA)_HA	Mammalian expression vector of viral HBx of genotype A with C-terminal hemagglutinin-tag (HA-tag)	AG Hildt, PEI	N/A
pcDNA_HBx(gtB)_HA	Mammalian expression vector of viral HBx of genotype B with C-terminal HA-tag	AG Hildt, PEI	N/A

pcDNA_HBx(gtC)_HA	Mammalian expression vector of viral HBx of genotype C with C-terminal HA-tag	AG Hildt, PEI	N/A
pcDNA_HBx(gtD)_HA	Mammalian expression vector of viral HBx of genotype D with C-terminal HA-tag	AG Hildt, PEI	N/A
pcDNA_HBx(gtE)_HA	Mammalian expression vector of viral HBx of genotype E with C-terminal HA-tag	AG Hildt, PEI	N/A
pcDNA_HBx(gtG)_HA	Mammalian expression vector of viral HBx of genotype G with C-terminal HA-tag	AG Hildt, PEI	N/A
pcDNA_HBx(gtA)_ eGFP	Mammalian expression vector of viral HBx of genotype A with C-terminal green fluorescent protein (GFP)	Created by this work.	N/A
pcDNA_HBx(gtB)_ eGFP	Mammalian expression vector of viral HBx of genotype B with C-terminal GFP	Created by this work.	N/A
pcDNA_HBx(gtD)_ eGFP	Mammalian expression vector of viral HBx of genotype D with C-terminal GFP	Created by this work.	N/A
pcDNA_HBx(gtE)_ eGFP	Mammalian expression vector of viral HBx of genotype E with C-terminal GFP	Created by this work.	N/A
pcDNA_HBx(gtG)_ eGFP	Mammalian expression vector of viral HBx of genotype G with C-terminal GFP	Created by this work.	N/A
pNQO1_luc	Encoding firefly luciferase under NAD(P)H Quinone Dehydrogenase 1 driven promoter	AG Hildt, PEI	N/A
pAP1_luc	Encoding firefly luciferase under activator protein 1 driven promoter	AG Hildt, PEI	N/A
mKeima-Red-Mito-7	Mammalian expression vector of mitochondrial localization side fused to mKeima fluorescent protein	Addgene M. Davidson	56018

pYFP_Parkin	Mammalian expression vector of human Park2 fused to yellow fluorescent protein	Addgene R. Youle [214]	23955

3.1.4. Oligonucleotides

3.1.4.1. Light cycler oligonucleotides

Table 5: Light cycler oligonucleotides used.

Name	Gene ID (NCBI)	Sequence
Human-RPL27_fw	6155	5'-AAA GCT GTC ATC GTG AAG AAC-3'
Human-RPL27_rev	6155	5'-GCT GCT ACT TTG CGG GGG TAG-3'
Human_NLRP3_fw	114548	5'-GGT GGA GTG TCG GAG AAG-3' [215]
Human_NLRP3_rev	114548	5'-CTG TCA TTG TCC TGG TGT CT-3' [215]
Human_TOMM20_fw	9804	5'-TTT GGG GAG GGT AGA AAC GC-3' [216]
Human_TOMM20_rev	9804	5'-TTC AGA GCC AAG TGA CAC CC-3' [216]
Human_IL6_fw	3569	5'-GGA GAC TTG CCT GGT GAA AAT CAT CAC-3'
Human_IL6_rev	3569	5'-AGC AGG CTG GCA TTT GTG GTT G-3'
Human_TNFα_fw	7124	5'-GTT CCT CAG CCT CTT CTC CTT CCT G-3'
Human_TNFα_rev	7124	5'-ACA ACA TGG GCT ACA GGC TTG TCA C-3'
Human_ATF4_fw	468	5'-CCC TTC ACC TTC TTA CAA CCT C-3' [217]
Human_ATF_rev	468	5'- GTC TGG CTT CCT ATC TCC TTC A-3' [217]
Human_IL1β_fw	3553	5'-GAG CTC GCC AGT GAA ATG ATG-3'
Human_IL1β_rev	3553	5'-TAG TGG TGG TCG GAG ATT CG-3'
Human_PTEN induced kinase 1_fw	65018	5'-GGC CTT GGC TGG GGA GTA TG-3'
Human_PTEN induced kinase 1_rev	65018	5'-GCG GAG AAC CCG GAT GAT GT-3'
Human_Parkin_fw	5071	5'-GTG TTT GTC AGG TTC AAC TCC A-3'
Human_Parkin_rev	5071	5'-GAA AAT CAC ACG CAA CTG GTC-3'

3.1.4.2. Cloning oligonucleotides

Table 6: Oligonucleotides used for cloning.

Name	Sequence
HBx_gtA_NheI_fw	5'-CTA GCT AGC ATG GCT GCT AGG CTG TAC TGC-3'
HBx_gtB/D/G/E_NheI_fw	5'-CTA GCT AGC ATG GCT GCT AGG CTG TGC TGC-3'
HBx_gtA_HindIII_rev	5'- CCC AAG CTT TTA GGC AGA GGT GAA AAA GTT GCA TG-3'
HBx_gtA/B/D/E_HA_HindIII_rew	5'-CCC AAG CTT TTA GGC ATA ATC TGG CAC ATC ATA AGG GTA GGC AGA GGT GAA AAA GTT GCA TG-3'
HBx_gtG_HA_HindIII_rev	5'-CCC AAG CTT TTA GGC ATA ATC TGG CAC ATC ATA AGG GTA GGC AGA GGT GAA AAA GTT ACA TG-3'
HBx_fw_fusion primer	5'-TCG AGC GGC CGC CAC TGT GCT GG A TAT GGC TGC TAG GCT GTA CTG C-3'
HBx_gtC_fw_fusion primer	5'-TCG AGC GGC CGC CAC TGT GCT GGA TAT GGC TGC TAG GGT GTG CTG C-3'
HBx_rew_fusion primer	5'-GGA TCC TCC GGA TCC TCC GAT ATC GGC AGA GGT GAA AAA GTT GCA TG-3'
HBx_gtD_rew_ fusion primer	5'-GGA TCC TCC GGA TCC TCC GAT ATC GGC AGA GGT GAA AAA GTG GCA AG-3'
HBx_gtG_rew_ fusion primer	5'-GGA TCC TCC GGA TCC TCC GAT ATC GGC AGA GGT GAA AAA GTT ACA TG-3'
eGFP_fw_fusion primer	5'-GAT ATC GGA GGA TCC GGA GGA TCC GTG AGC AAG GGC GAG GAG-3'
eGFP_rew_fusion primer	5'-TCC AGT GTG GTG GAA TTC TGC AGA TTT ACT TGT ACA GCT CGT CCA TGC-3'

3.1.4.3. Sequencing oligonucleotides

Table 7: Oligonucleotides used for sequencing.

Name	Sequence
pcDNA_CMV_promotor_fw	5'-CGC AAA TGG GCG GTA GGCGTG-3'
pcDNA_BGH_rev	5'-TAG AAG GCA CAG TCG AGG-3'

3.1.5. Enzymes

Table 8: Enzymes and related buffers used.

Name	Manufacturer	Identifier
EcoRv-HF	New England Biolabs	R3195
HindIII-HF	New England Biolabs	R3104
NheI-HF	New England Biolabs	R3131
Phusion High-Fidelity DNA Pol	New England Biolabs	M0530
Q5 HotStart DNA Polymerase	New England Biolabs	M0491
RevertAid H Minus Reverse Transcriptase	Fermentas	EP0451
RQ1 RNase 10 × reaction buffer	Promega	M199A
RQ1 RNase-free DNase	Promega	M198A
Stop solution (for RQ1 DNase)	Promega	M610A
T5 exonuclease	New England Biolabs	M0663
Taq DNA Ligase	New England Biolabs	M0208

3.1.6. Reagents for cell culture

Table 9: Reagents used for cell culture.

Name	Manufacturer	Identifier
Accutase	Thermo Scientific™	00-4555-56
Dimethyl sulfoxide (DMSO)	Genaxxon	M6323.0250
Dulbecco's Modified Eagle's Medium (DMEM) (4.5 g/L glucose, w/o L-Glutamine)	Sigma-Aldrich	D6546
Fetal bovine serum superior (FCS)	Bio & Sell GmbH	FBS.S 0615
FluoroBrite™ DMEM	Gibco™	A1896701
L-Glutamine	Bio & Sell GmbH	K 0283
Phosphate Buffered Saline (PBS) w/o Ca^{2+} & Mg^{2+}	Paul-Ehrlich-Institute	N/A
Penicillin	Paul-Ehrlich-Institute	N/A
Streptomycin	Paul-Ehrlich-Institute	N/A
Trypsin/EDTA (0.05% Trypsin)	Paul-Ehrlich-Institute	N/A

3.1.7. Antibodies and fluorescence dyes

3.1.7.1. Primary antibodies

Table 10: Primary antibodies used.

Antibody	Species/Clonality	Dilution		Manufacturer	Identifier / RRID
Anti GAPDH	mouse monoclonal	WB:	1:2000	Santa Cruz	RRID:AB 62778
Anti p62	guinea pig polyclonal	IF:	1:100	ProGen	RRID:AB 2687531
Anti-COX2	mouse monoclonal	WB:	1:1000	Santa Cruz	Cat# sc-514489
Anti-COX4	mouse monoclonal	WB:	1:1000	Santa Cruz	RRID:AB 2904544
Anti-GFP	rabbit polyclonal	WB:	1:1000	Thermo Scientific™	RRID:AB 221569
Anti-HBx	mouse monoclonal	WB: IF:	1:1000 1:200	Thermo Scientific™	RRID:AB 325418
Anti-HA Tag	mouse monoclonal	WB: IF:	1:1000 1:50	Thermo Scientific™	RRID:AB 10978021
Anti-HA-FITC	mouse monoclonal	FCM:	1:50	Miltenyi	RRID:AB 2784357
Anti-HA-Tag	rabbit monoclonal	IF:	1:1000	Cell Signaling	RRID:AB 1549585
Anti-HA-Tag	goat polyclonal	IF:	1:200	Novus	RRID:AB 10124937
Anti-LC3	rabbit polyclonal	WB:	1:1000	Biozol	RRID:AB 2274121
Anti-Parkin	rabbit polyclonal	WB:	1:1000	Cell Signaling	RRID:AB 10693040
Anti-PINK1	rabbit monoclonal	WB:	1:1000	Cell Signaling	RRID:AB 11179069
Anti-SLC10A1	rabbit polyclonal	FCM:	1:100	Bioss	Cat# bs-1958-APC
Anti-TOM20	mouse monoclonal	WB: IF:	1:1000 1:200	Santa Cruz	RRID:AB 628381
Anti-TOM20	rabbit monoclonal	IF:	1:250	Abcam	RRID:AB 2889972
Anti-VDAC3	rabbit polyclonal	IF:	1:100	Thermo Scientific™	RRID:AB 2804554
Anti-β-Actin	mouse monoclonal	WB:	1:10.000	Sigma	RRID:AB 476743

RRID Research Resource Identifiers

3.1.7.2. Secondary antibodies

Table 11: Secondary antibodies used.

Antibody	Dilution	Manufacturer	Identifier (RRID)

Donkey monoclonal anti-mouse (H+L), Alexa Fluor™ 488	1:10.000	Thermo Scientific™	RRID:AB 141607
Donkey polyclonal anti-goat (H+L), Alexa Fluor™633	1:10.000	Thermo Scientific™	RRID:AB 2762827
Donkey polyclonal anti-mouse (H+L), Alexa Fluor™ 546	1:10.000	Thermo Scientific™	RRID:AB 2534012
Donkey polyclonal anti-rabbit (H+L), Alexa Fluor™ 546	1:10.000	Thermo Scientific™	RRID:AB 2535739
Donkey polyclonal anti-rabbit (H+L) Alexa Fluor™ 488	1:10.000	Thermo Scientific™	RRID:AB 2535792
ECL Donkey polyclonal anti-rabbit-IgG HRP	1:10.000	GE-healthcare	RRID:AB 2722659
IRDye®680CW (H+L) donkey anti-mouse	1:10.000	LI-COR	RRID:AB 2814912
IRDye®680RD (H+L) donkey anti-rabbit	1:10.000	LI-COR	RRID:AB 2716687
IRDye®800CW (H+L) donkey anti-rabbit	1:10.000	LI-COR	RRID:AB 2715510
IRDye®800CW (H+L) donkey anti-mouse	1:10.000	LI-COR	RRID:AB 2716622

RRID Research Resource Identifiers

3.1.7.3. Fluorescence reagents

Table 12: Fluorescence reagents used.

Dye	Dilution	Manufacturer	Identifier
4´,6-diamidino-2-phenylindole (DAPI)	1:100	Carl Roth	6335.1
Hoechst33342	1:1000	Life technologies	H3570
Phalloidin Atto633	1:1000	Sigma-Aldrich	68825

3.1.8. Reagents

Table 13: Reagents used.

Name	Manufacturer	Identifier
Bradford reagent	Sigma-Aldrich	B6916
DNA Gel Loading Dye (6×)	Thermo Scientific™	R0611
dNTP-Mix (10 mM)	Thermo Scientific™	R0192
FuGENE® HD Transfection Reagent	Promega	E2311
GeneRuler 1 kb DNA Ladder	Thermo Scientific™	SM0314
Immobilon western Chemiluminescent HRP Substrate	Merck Millipore	WBLUIF

Page Ruler Prestained protein ladder	Thermo Scientific™	26616
RNA-Solv® Reagent	Omega Bio-Tek	R6830-02
Random Hexamer Primer	Thermo Scientific™	SO142
RevertAid H Minus reverse transcriptase	Thermo Scientific™	EP0451

3.1.9. Commercial Kits

Table 14: Commercial Kits used.

Name	Manufacturer	Identifier
Complex IV Human Specific Activity Microplate Assay Kit	Abcam	ab109910
Murex HBsAg ELISA Kit	DiaSorin	9F80-05
Fixation and Permeabilization Solution Kit	BD biosciences	554722
Mitochondria Isolation kit for cell culture	Thermo Scientific™	89874
MitoProbe™ JC-1 Assay-Kit	Thermo Scientific™	M34152
OxyBlot Protein Oxidation Detection Kit	Merck Millipore	S7150
STK reagent kit	PamGene	32201
PTK reagent kit	PamGene	32112
SYBR® Green Real-Time PCR Master Mix	Thermo Scientific™	K0221
QIAGEN Plasmid Maxi-Kit	QIAGEN	12162
QIAquick Gel Extraction Kit	QIAGEN	28704
QIAquick PCR Purification Kit	QIAGEN	28106

3.1.10. Inhibitors

Table 15: Inhibitors used.

Inhibitor	Target	Manufacturer	Identifier
Aprotinin	Serine protease	AppliChem	A2132
Leupeptin	Serine and cysteine proteases	AppliChem	A2183
Pepstatin	Aspartyl protease	AppliChem	A2205
PMSF	Serine protease	AppliChem	A0999
Halt™ Phosphatase-Inhibitor Cocktail	Phosphatases	Thermo Scientific™	87785
Halt™ Protease-Inhibitor Cocktail (100x)	Protease-Inhibitor	Thermo Scientific™	87786

3.1.11. Chemicals

Table 16: Chemicals used.

Name	Manufacturer	Identifier
6-Aminohexanoic acid	Carl Roth	3113
Agarose LE	Genaxxon	M3044
Ammoniumperoxydisulfate (APS)	Carl Roth	9592
Ampicillin	Carl Roth	K029
Bovines serum albumin (BSA), Fraction V	PAA	K45-001
Bromophenol blue	Merck	108122
Coomassie-Brillantblau R-250	Carl Roth	112553
Dimethylsulfoxid (DMSO)	Genaxxon	M6323
D-Luciferin sodium salt	Synchem	BC 218
Double distilled water	Paul-Ehrlich Institute	N/A
Ethanol 96% (v/v)	Carl Roth	5054
Ethidiumbromide	AppliChem	A1152
Ethylendiaminotetraacetic acid (EDTA) 0.5 M (pH 8.0)	Paul-Ehrlich Institute	N/A
Formaldehyde 37.5% (v/v)	Carl Roth	4979
Glycerol	Carl Roth	3783
Isopropanol	Carl Roth	0080
Kanamycin	Carl Roth	T832
Methanol 96% (v/v)	Carl Roth	CAS 67-56-1
Mowiol 40-88	Sigma-Aldrich	324590
Polyethyleneglycol 8000	VWR	C0159
rCutSmart buffer	New England Biolabs	B6004S
Roti®-Block	Carl Roth	A151
Skim milk powder	Carl Roth	T145.4
Sodium chloride (NaCl)	Carl Roth	3957
Sodium dodecyl sulfate (SDS)	Carl Roth	0183
TEMED	Carl Roth	2367
Trichlormethan/Chloroform	Carl Roth	4423
Triton X-100	Sigma-Aldrich	T9284

β-Mercaptoethanol	Sigma-Aldrich	M6250

3.1.12. Buffers and media

Table 17: Buffers and media used. If not indicated otherwise, all buffers and solutions were prepared with ddH_2O.

Name	Ingredients
Anode buffer I	20% (v/v) Ethanol 0.3 M Tris
Anode buffer II	20% (v/v) Ethanol 25 mM Tris
APS-solution	10% (w/v) APS
Assembly Master Mix	320 µL Isothermal Master Mix 10 U/µl T5 exonuclease 2 U/µl Phusion DNA Pol 40 U/µl Taq DNA Ligase ad 1 ml H_2O
Blocking solution for IF	5% (w/v) BSA in TBS-T
Cathode buffer	20% (v/v) Ethanol 40 mM 6-Amino-hexanonic acid
DMEM / RPMI1640 complete	10% (v/v) FCS 2 mM L-Glutamine 100 µg/ml Streptomycin 100 U/mL Penicillin in DMEM High Glucose or RPMI-1640 medium
Isothermal Reaction Mix	1 M Tris-HCl pH7.5 1 M MgCl2 10 mM dNTP Mix 50 mM DTT 1.5 g PEG-8000 100 mM NAD ad 6 ml H_2O
Luciferase lysis buffer	25 mM Tris/HCl 2 mM DTT 2 mM EGTA 10% (v/v) Glycerol 0.1% (v/v) Triton X-100 pH 7.5
Luciferase substrate	20 mM Tris/HCl 5 mM $MgCl_2$ 0.1 mM EDTA 33.3 mM DTT 470 µM D-luciferin 530 µM ATP pH 7.8

Luria Bertani Medium (LB)	1% (w/v) Bacto-Trypton 0.5% (w/v) Yeast extract 1% (w/v) NaCl
Milk-blocking solution	10% (w/v) Skim milk powder in TBS-T
Mowiol mounting medium	100 mM Tris/HCl 10% (w/v) Mowiol 25% (w/v) Glycerol 2.5% DABCO pH 8.5
Phosphate buffered Saline (PBS) w/o Mg2+ and Ca2+	137 mM NaCl 2.7 mM KCL 8.1 mM Na_2HPO_4 1.5 mM KH_2PO_4 pH 7.4
RIPA buffer	50 mM Tris/HCl 150 mM NaCl 0.1% (w/v) SDS 1% (w/v) Sodium deoxycholate 1% (v/v) Triton X-100 pH 7.2
SDS-loading buffer 4x	4% (w/v) SDS 125 mM Tris/HCl 10% (v/v) Glycerol 10% (v/v) β-Mercaptoethanol 0.02% (w/v) Bromophenol blue pH 6.8
SDS-running buffer (10x)	0.25 M Tris/Base 2 M Glycine 1% (w/v) SDS pH 8.3
SDS-separating gel buffer	1.5 M Tris 0.4% (w/v) SDS pH 8.8
SDS-stacking gel buffer	0.5 M Tris 0.4% (w/v) SDS pH 6.8
TAE-buffer (50x)	2 M Tris-Base 1 M Acetic acid 50 mM EDTA pH 8.0
TBS-T (10x)	500 mM Tris/HCl 1.5 M NaCl 0.5% (v/v) Tween-20 pH 7.8

3.1.13. Devices

3.1.13.1. Electrophorese and blotting systems

Table 18: Electrophorese and blotting systems used.

Device	Function	Manufacturer
Electrophorese power supply EPS 301	Power supply	GE Healthcare
Mighty small II vertical electrophoresis system SE250	Electrophoresis chamber	GE Healthcare
Mighty small multiple gel caster SE 200	Gel caster	GE Healthcare
TE77 ECL semi dry Transfer Unit	Blotter	GE Healthcare

3.1.13.2. Microscopes

Table 19: Microscopes used.

Device	Function	Manufacturer
Axiovert 40C	Inverted transmitted-light microscope	Carl Zeiss AG
TCS SP8	Confocal Laser Scanning Microscope	Leica Microsystems

3.1.13.3. Flow cytometer

Table 20: Flow cytometer used.

Device	Function	Manufacturer
MACSQuant 10	Flow cytometer	Miltenyi

3.1.13.4. Further devices

Table 21: Further devices used.

Device	Function	Manufacturer
Accu-jet® pro	Pipette controller	Brand
Bacterial incubator Typ B6760	Incubator	Heraeus
CO_2-Incubator BBD 6220	Incubator	Thermo Scientific™
Heraeus Fresco 17	Centrifuge	Thermo Scientific™
ImageQuant800™ system	CCD Imager	Cytiva Europe
Infinite M1000	Microplate reader	Tecan

LI-COR Odyssey	Infrared Imager	LI-COR Biosciences
LightCycler® 480 Instrument II	RT-PCR	Roche
Microcentrifuge	Centrifuge	Carl Roth
NanoDrop™ One	UV/VIS Spectrophotometer	Thermo Scientific™
Orion II microplate lumiometer	Luminometer	Berthold Tecnologies
PamStation®12 System	Kinase profiling	PamGene
pH-Meter 766 Calimatic	pH-Meter	Knick
Rocking platform WT16	Roller	Biometra
SonoPuls MS73	Sonicator	Bandelin
Steril GARD III Advance	Sterile bank	The baker company
Stuart Roller Incubator SRT9	Roller	Bibby Scientific
Thermocycler	PCR	Analytic Jena
Thermomixer compact	Heat block	Eppendorf
UV transilluminator	UV-Imager	INTAS
Vortex®Genie 2	Vortexer	Scientific Industries
Water bath 1228-2F	Water bath	VWR

3.1.14. Consumables

Table 22: Consumables used.

Name	**Manufacturer**
Cell culture flask (T75, T175)	Greiner bio-one
Falcon tubes (15 mL, 50 mL)	Greiner bio-one
Coverslips 18 mm	Thermo Scientific™
Filtered pipette tips (10 µL, 100 µL, 1mL)	Sarstedt
IBIDI® µ-Slide 2-Well	IBIDI®
LightCycler® 480 Multiwell plate 96	Roche
Roti®-Fluoro PVDF-Membran	Carl Roth
Glass slides	Carl Roth
Neubauer counting chamber	Marienfeld
Parafilm	Sigma-Aldrich

Protein Tyrosine Kinase PamChip®	PamGene
Serine threonine Kinase PamChip®	PamGene
Serological pipettes	Greiner
Whatman filter papers, D 32 mm, Grade 1	GE Healthcare
FACS tubes	Sarstedt
Cell culture plates (6, 12, 96 wells)	Greiner bio-one
RotiLabo® syringe filters (0.22 / 0.45 µm)	Carl Roth
Reaction tubes (1,5 ml / 2 ml)	Eppendorf

3.1.15. Software

Table 23: Software used.

Software	Manufacturer
Bionavigator v6.3.67	PamGene
Citavi v6	Swiss Academic Software GmbH
Fiji ImageJ	Open-source https://fiji.sc/
Infinite	Berthold Tecnologies
KOBAS v3.0	KEGG Orthology Based Annotation System
FlowJo v10	BD biosciences
GraphPad Prism v8.3	GraphPad
Image Studio Lite	LI-COR Biosciences
Inkscape	Open-source https://inkscape.org/de/
LasXCore	Leica
MACSQuantify	Miltenyi
Mitochondrial Network Analysis Tool (MiNA) Python scripts for Fiji	Open-source https://github.com/StuartLab/MiNA
MS Office	Microsoft
SnapGene Viewer	GSL Biotech LLC
Tecan iControl Software	Tecan

3.2. Methods

3.2.1. Cell-biological methods

3.2.1.1. Prokaryotic cell culture

E. coli K12 strain DH5α was used for overnight-culture to produce a high number of bacteria transformed with the plasmid of interest. Usually, 250 ml LB-medium was cultured at 37 °C by 300 rpm on a shaker for approximately 16 h. For the selection of transformed bacteria, 25 µg/ml kanamycin or 100 µg/ml ampicillin was supplemented into the medium. Bacteria were harvested by centrifugation at 6000 g and 4 °C for 10 min and used for plasmid preparation. An aliquot was stored as cryostock in 40% (v/v) glycerol at -80 °C.

3.2.1.2. Mammalian cell culture

Human hepatoma-derived Huh7 cell line were used as a model system for *in vitro* studies. This adherent cell line was established 1982 by Nakabayshi & Sato and demonstrates an epithelial-like, tumorigenic morphology [213]. Cells were cultured in Dulbecco´s modified Eagle´s medium (DMEM, 4.5 g/L glucose) supplemented with 10 % fetal calf serum, 2 mM L-glutamine, 100 U/ml of penicillin and 100 µg/ml streptomycin and maintained at 37 °C with a humidified atmosphere containing 5% (v/v) CO_2. HepG2 cells were cultured in RPMI-1640 medium supplemented and maintained as described before. Passaging of cells was accomplished every second or third day when reaching a confluence of 70 – 80%, performed by using Trypsin/EDTA at 37 °C for 5 min.

All laboratory work with genetically modified organisms (GMO) and biohazard material was performed by a Biosafety Level 2 (BSL2) and documented accordingly.

3.2.1.3. Transient transfection

FugeneHD DNA transfection Reagent was applied for transient transfection or co-transfection of Huh7 cells according to the manufacturer's protocol. Cells were seeded 6 h prior to transfection in multiwell plates (6-well plate with 3x 10^5 cells/well; 12-well plate with 1x 10^5 cells/ well) or cell culture dishes (TC-100 with 1.5x 10^6 cells). The transfection reagent were premixed in Opti-Mem using a 3:1 Ratio (Reagent:DNA) and incubated for 10 min at room-temperature prior to adding dropwise on the cell. A medium exchange was performed 16 h post-transfection, transfection with pcDNA plasmid DNA into another batch of cells in parallel served as a control sample. As not indicated otherwise, cells were harvested 72 h post-transfection (h. p.t.) as described below and resulting in a routinely observed transfection efficiency of 40 – 55% (based on flow cytometry analysis).

3.2.1.4. Cell lysis

3.2.1.4.1. RIPA lysates

Cells were seeded in a 6-well plate and lysed 72 h post-transfection using 200 µl RIPA buffer, supplemented with protease inhibitors. Samples were collected and sonicated with 25% power for 10 sec on ice. Cell debris was removed by centrifugation at 14.000 g for 5 min at 4 °C and the protein concentration was quantified by Bradford assay (as explained in chapter 3.2.3.1.).

3.2.1.4.2. Luciferase lysates

Luciferase assay lysates were performed 48 h post-transfection. Cells were washed twice with PBS and incubated on ice for 10 min in the presence of 200 µl luciferase lysis buffer. The cell lysates were collected in tubes and clear spin at 14.000 g for 5 min and 4 °C to remove cell debris.

3.2.1.4.3. PamStation lysates

Transiently transfected cells designed for kinome profiling through PamStation, were harvested 72 h post-transfection by adding 100 µl M-PER™ Mammalian Protein Extraction Reagent including Halt™ Protease Inhibitor Cocktail and Halt™ Phosphatase Inhibitor Cocktail. Cells were incubated for 10 min on dry ice and scraped afterwards carefully into a prechilled tube. Subsequently, samples were centrifuged for 15 min at 16.000 g at 4 °C and aliquoted with 10 µl per tube. Immediately, lysates were stored at -80 °C, one aliquot was used for protein quantification using a BCA protein quantification assay (as explained in chapter 3.2.3.1.).

3.2.2. Molecular biological methods

3.2.2.1. Transformation of competent bacteria

Plasmid DNA was introduced into chemically competent *E. coli* (K12 strain DH5α) by heat-shock method. In brief, competent bacteria cells were thawed for 30 min on ice followed by adding 50 ng plasmid DNA. Heat shock was performed by incubation at 42 °C for 90 sec and immediately storage on ice for 5 min. Cells were preincubated in 500 µl pre-warmed LB-medium without antibiotics at 37 °C and 500 rpm shaking for 30 min before being plated on LB-agar plated containing suitable antibiotics for selection purposes and incubated overnight at 37 °C.

3.2.2.2. Isolation of plasmid DNA

Plasmid DNA extraction was achieved by using the QIAGEN Plasmid Maxi Kit according to the manufacturer's instructions. Briefly, harvested bacteria pellet was resuspended in a chemical detergent-based buffer in order to accomplish cell breakdown. Subsequently, plasmid DNA was extracted on Maxi-Prep Spin columns by gravity flow. The purified plasmid DNA was eluted in ddH_2O and stored at -20 °C. The DNA concentration was measured with a UV/Vis Spectrometer at λ = 260 nm, the quality of the preparation was determined by measuring the absorbance at λ = 280 nm as well as by test digestion with HindIII restriction enzyme and subsequent size-dependent separation on a 1% Agarose gel.

2.2.2.3. Cloning of HBx-HA plasmids

The expression construct of HBx with an N-terminal HA-tag was generated by cloning the HBx coding sequence in frame with an HA-tag into a pcDNA3.0(-) vector. The X-ORF of GtA, GtB, GtC GtD, GtE and GtG were PCR-amplified from the respective genotypes of HBV replicon plasmids using Q5 polymerase according to the manufacturer's protocol and with the following parameters (table 24).

Table 24: Amplification program for HBx-HA cloning.

Temperature [°C]	Time	Cycles	Program
98	30 sec	1	Initial denaturation
98 65 72	10 sec 30 sec 60 sec	30	Denaturation Annealing Extension
72	10 min	1	Final Extension
4	hold	1	Cooling

Subsequently, 10 µl of the PCR reaction was proofed regarding the size of the fragments in a 1.5% Agarose gel and purified using the QIAquick PCR purification kit according to the instructions. The purified fragments as well as the pcDNA3.0 empty vector were HindIII-HF and NheI-HF digested for 20 min at 37 °C, followed by heat-inactivation of the reaction at 80 °C for 10 min. Gel-extracted fragments consisting of insert and vector backbone were finally ligated together using a 3:1 ratio in the presence of T4-ligase for 20 min at room temperature. The sequences of all clones were confirmed by sequencing (Eurofings genomics) using primers flanking to the multiple cloning sites of the backbone vector. The pcDNA_HBx_gtA_(no tag) tag were cloned accordingly, but without an addition tag-sequence in the reverse primer.

3.2.2.4. Cloning of HBx-eGFP plasmids using Gibson assembly

The expression construct of HBx with an N-terminal eGFP-tag was generated by Gibson assembly method. The X-ORF of GtA, GtB, GtC GtD, GtE and GtG, as well as the eGFP coding region, were PCR-amplified with 20-40 bp homologous sequences between the respective neighbor fragments by using Q5 polymerase according to the following parameters (table 25).

Table 25: Amplification program for HBx-eGFP cloning.

Temperature [°C]	Time	Cycles	Program
98	60 sec	1	Initial denaturation
98 52 72	30 sec 30 sec 60 sec	30	Denaturation Annealing Extension
72	5 min	1	Final Extension
4	hold	1	Cooling

The desired PCR fragments were identified by size by running a 1.5% Agarose gel electrophoresis and gel extracted with QIAquick Gel Extraction Kit according to the protocol. The Gibson assembly was performed with 50 ng of each insert and 50 ng of EcoRV-HF digested pcDNA3.1(-) backbone. The DNA fragments were premixed to a total volume of 5 µl in ddH_2O, added to 15 µl of Assembly Master Mix, incubated for 1 h at 50 °C and subsequently used for transformation in competent bacteria under selection conditions. The sequences of all clones were confirmed by sequencing (Eurofings genomics) using primers flanking for the multiple cloning sites of the backbone vector.

3.2.2.5. Agarose gel extraction

Agarose gel electrophoresis was performed to separate nuclei acids according to their size in an agarose matrix. Therefore, between 1 and 1.5% (w/v) Agarose was melted in 1x TAE buffer and polymerized in a horizontal gel cast in the presence of 0.1 µg/ml ethidium bromide. Samples were mixed with 6x DNA loading dye and loaded within the gel chambers. Electrophoretic migration was achieved at 80 V, a commercial protein ladder was used as a marker for the identification of the protein size. For detection, the used ethidium bromide intercalates with the major groove of DNA, and was visualized under UV light (254 nm) and documented with the INTAS-Imaging Systems.

3.2.2.6. Isolation of total DNA

Total RNA was extracted from whole cell-lysate using RNA-Solv® Reagent according to the provided protocol of the company. In brief, cells were washed twice with PBS and incubated for 10 min in the presence of 400 µl RNA-Solv® on ice. Subsequently, RNA was isolated by Phenol/Chloroform, before being precipitated with isopropanol. The RNA pellet was air-dried and resuspended in 15 µl DEPC-H_2O. The RNA concentration and quantity were determined with a UV-Vis spectrometer and stored at -80 °C.

3.2.2.7. cDNA synthesis

Isolated RNA was converted into first-strand cDNA using RevertAidTM H minus Reverse Transcriptase. Before head, DNA contaminations were digested by adding 1 Unit RQ1 RNase-free DNase for 1 h at 37 °C and inactivated by adding RQ1 DNase Stop solution (10 min at 65 °C). 5 µM Random Hexamer Primer was added to the sample and incubated 15 min at 65 °C. Finally, reverse transcription takes place in the presence of 1 µM dNTPs and 200 Units Revert Aid H minus Reverse Transcriptase with an RNA concentration of 0.25 µl/µl. The reaction was performed for 10 min at room temperature, 60 min at 42 °C and subsequent heat inactivation at 72 °C for 10 min. Synthesized cDNA was stored at -20 °C.

3.2.2.8. Quantitative Real-Time qPCR

The mRNA expression level was determined by RT-qPCR based on a SYBER-Green system. In the presence of primers flanking for the gene of interest (GOI) and a cDNA concentration equivalent to 7.5 ng/µl input RNA, Maxima SYBER-Green qPCR Kit was performed according to the manufacturer's instructions on a LightCycler480 Instrument II with the following parameters (table 26). An additional H_2O and non-reversed transcribed RNA served as internal control. The amplification was performed in duplicates in conical, heat-sealed MicronAmp Optical 96-well microtiter plates and results were carried out as Cp (crossing points) values calculated as fold changed values of the control achieved by the $\Delta\Delta C_T$ method [218].

Table 26: RT-qPCR program for genomic transcripts.

Temperature [°C]	Time [sec.]	Slope Time [°C/s]	Cycles	Program
95	600	4.4	1	Denaturation
95 56 72	15 30 30	4.4 2.2 4.4	45	Cycling/ Quantification

95 56 97	60 30 continuous	4.4 2.2	1	Melting
37	30	2.2	1	Cooling

3.2.3. Protein-biochemical methods

3.2.3.1. Protein quantification

The protein concentration was determined either according to Bradford (1976) or, for more precise determination, with the Pierce™ BCA Protein Assay Kit. For the determination according to Bradford, the spectral shift to 595 nm (absorbance maximum) of the Coomassie Brilliant Blue G-250 dye (Bradford-Reagent) was measured depending on the protein concentration [219].

The BCA Protein Assay Kit was performed according to the manufacturer's protocol. In brief, a two-component system standing with a carbonate buffer containing BCA-reagent and a cupric sulfate solution was incubated with 25 µl sample for 30 min at 37 °C. The working solution demonstrated in the presence of proteins a color shift and is calorimetrically detected at 562 nm. The absolute protein concentration was determined within the linear range of a BSA-standard curve.

3.2.3.2. SDS-PAGE electrophoresis

The SDS-PAGE was used to separate proteins dependent on their molecular weight as described before by Leammli, (1970) [220]. Between 50 and 80 µg protein was denatured in SDS-loading dye for 5 min at 95 °C and subsequently separated by electrophoresis in a discontinuous SDS-Polyacrylamide gel at 80-100 V. A commercial protein ladder was used as a marker for identification of the protein size. The gels were used for immune detection as described below (chapter 3.2.4.1.).

3.2.3.3. Luciferase Reporter-gene Assay

Prior to lysis, cells were transiently co-transfected with the indicated luciferase reporter gene plasmid DNA (NF-κB or AP-1) and the respective HBx plasmid DNA in a 1:3 ratio. Chemiluminescence of prepared luciferase lysates (chapter 3.2.1.4.2.) was carried out in a white microtiter plate measured in an Orion II microplate luminometer. Luciferase substrate was added with a built-in liquid dispenser and measured over a course of 10 sec. Relative light intensities were normalized to the total protein amount calculated by Bradford assay and related finally to the experimental control sample.

3.2.3.4. Mitochondria membrane potential assay

Mitochondrial membrane potential was performed with the JC-1 probe assay-Kit as described previously [221]. JC-1 is a lipophilic, cationic dye and is used to monitor the state of mitochondria polarization. The fluorescent dye is able to enter the mitochondrial membrane in a concentration-dependent manner and forms reversible complexes (J aggregated), which are detectable due to excitation and emission in the red spectrum (585/590 nm). By contrast, a loss of mitochondrial membrane potential leads to a loss of the electrochemical gradient through the mitochondrial membrane and subsequently loss of aggregation of JC-1 molecules. JC-1 dye remains as monomers and exhibits a green fluorescence emission (510/527 nm). A ratio of red/green fluorescence reflects the electrochemical gradient over the membrane and thus the polarization status of the mitochondria. In this study, transiently transfected cells within a 6 well-plate were washed twice with PBS and detached from the well 72 h p.t. by adding 500 µl Accutase. A total amount of 1x 10^6 cells were resuspended in 1 ml JC-1 dye diluted in PBS (final concentration 2 µM) and incubated for 20 min at 37 °C in the dark. Samples were washed twice by centrifugation (800 g for 5 min) and fluorescence intensity was measured by using a MACSQuant10 flow cytometer. Channels with 488 nm excitation and 529 nm as well as 590 nm emission filters were applied to observe JC-1 aggregates or JC-1 monomer depending on the mitochondria membrane potential of the cell. A total amount of 2x 10^4 cells was recorded and analyzed using FlowJo software (v10, FlowJo). Results were calculated as a ratio between red (JC-1 aggregates) to green (JC-1 monomer) mean fluorescence intensities and normalized to the control sample.

3.2.3.5. Complex IV activity determination

The cytochrome c-oxidase is part of the respiratory chain within the inner mitochondrial membrane and serves as a marker for the integrity of the mitochondrial membrane, but also to determine mitochondrial stress and the energy level through the cytochrome c-oxidase activity. The cytochrome c-oxidase activity assay used in this study is based on a calorimetric method, measuring the decreased absorption of reduced cytochrome c through oxidation at the cytochrome c-oxidase at 550 nm. Therefore, Huh7 cells were seeded in TC100 cell culture dishes and were HBx-transfected as described previously. Cells were trypsinized 72 h p.t. and washed twice with PBS by centrifugation at 800 g for 5 min. Subsequently, mitochondria were isolated by using the Mitochondrial Isolation Kit. In brief, cells were disrupted by a detergent-based method and mitochondrial fraction was achieved by differential centrifugation, yielding in a pure mitochondrial fraction with minimal impairment of mitochondrial integrity. The protein concentration was determined by Bradford assay (chapter 3.2.3.1.) and 10 µg mitochondria were used for the Complex IV Human Enzyme Activity Microplate Assay Kit. The cytochrome c-oxidase is immunocaptured in the provided 96-well microplate, pre-bound with monoclonal

antibody and activity was determined by monitoring the absorbance at 550 nm over time. Subsequently, the rate of enzyme activity was calculated as a slope between two points within the linear range and was correlated to the control sample.

3.2.3.6. Mt-Keima mitophagy assay

Mitophagy detection was carried out by co-transfection with the mKeima-Red-Mito-7 plasmid. The Keima-fluorophore exhibits a bimodal excitation under neutral and acid pH conditions. Together with a mitochondrial target sequence, the fluorophore is connected to mitochondria and indicates the formation of mitolysosomes and therefore mitophagy through the differential excitation in the acid environment. For this purpose, Huh7 cells were cultured in IBIDI® chamber-slides and were transiently co-transfected with the respective HBx-eGFP plasmid and the mKeima-Red-Mito-7 plasmid in a 1:1 ratio. Subsequently, 72 h p.t, nuclei were stained with Hoechst33342, diluted in culture medium for 10 min at 37 °C. Cells were washed twice with PBS and covered with 400 µl of FluoroBrite™ DMEM medium for immediate imaging by live-cell imaging on a confocal laser scanning microscope as described below (chapter 3.2.5.). Dual-excitation radiometric of mt-Keima fluorescence was observed via two sequential excitations (458 nm and 561 nm) and using a 570 to 690 nm emission range. A 488-nm excitation was used to identify HBx-positive cells via eGFP-tag. A minimum of 11 double-positive cells were imaged and further processed by employing FIJI software (detailed description below in chapter 3.2.6.3.).

3.2.3.7. Kinome profiling

The PamGene technology was applied in order to investigate protein kinase activity in cellular lysates. The assay is based on measuring peptide phosphorylation by protein kinases and is used for predictions of enriched signal transduction pathway activity. Either phosphotyrosine kinase (PTK) or serine-threonine kinase (STK) PamChip® microarrays were used. The microarrays consist of a highly porous ceramic membrane on which 144 (STK) or 196 (PTK) peptides, harboring specific phosphorylation sites, are immobilized. Active kinases present in the sample phosphorylate their target sites of the provided peptides and were captured by fluorescently labeled anti-phospho-antibodies with a CCD camera. The analysis is based on a computational prediction of upstream kinase activities calculated from the differentially phosphorylated peptides as described elsewhere [222].

For this study, an equal number of cellular lysates (see chapter 2.2.1.4.3.) were loaded on STK and PTK PamChip microarrays and measured with the respective reagent kit using the PamStation®12 instrument according to the manufacturer's protocol. All samples were investigated in experimental and technical duplicates. Upstream kinase activities were processed by using the BioNavigator software, a median final statistic above 1.2 was assumed

as significantly enriched compared to the pcDNA control sample. The database tool KEGG Orthology Based Annotation System (KOBAS, v3.0) was utilized for Kyoto Encyclopedia of Genes and Genomes (KEGG) pathway enrichment analysis [223]. In brief, the gene list of predicted, statistically enriched kinome data, (Mean Final score above 1.2) was applied to conduct pathway enrichment analysis. The analysis was performed using the default module settings. Enriched KEGG terms with a *p*-value above 0.05 were clustered and visualized in a bubble blot [224].

3.2.4. Immunological methods

3.2.4.1. Western blotting and immunodetection

Proteins separated by SDS-Page were transferred on a methanol-activated PVDF membrane with semi-dry blotting method by applying a current of 1.3 mA/cm² for 1 h, as described previously [225, 226]. After blocking in 1x RotiBlock or 5% (w/v) skim milk, the blots were probed overnight at 4 °C with respective primary antibodies, followed by a 1 h incubation time at room temperature with HRP- or IRDye® - conjugated secondary antibodies raised against the desired primary antibody epitopes. In case of the HRP conjugated detection system, ECL detection substrate were added dropwise on the membrane and imaged using the ImageQuant800^{TM} Imaging system. IRDye® based system was investigated with the LI-COR Odyssey Infrared Imager with wavelength adjusted to IRDye 680RD (Ex672/Em694) or IRDye® 800CW (Ex774/Em789) fluorescent spectra.
Band intensities were quantified with the Image Studio light software. The determined values were subtracted from the local background surrounded by the region of interest, normalized to the respective reference protein (GAPDH or β-actin) and subsequently calculated to the corresponding experimental control in order to achieve the fold-change value.

3.2.4.2. Measurement of protein oxidation

For quantification of intracellular ROS levels, protein carbonylation was investigated by using the OxyBlot™ protein oxidation detection Kit according to the manufacturer's protocol. The kit is based on an immunoblot method to detect modifications on proteins in form of carbonyl groups introduced by oxidative reactions with oxygen free radicals and other reactive species. Cells were lysed as described before (chapter 3.2.1.4.1.), except for lysis buffer which where supplemented with 2% β-Mercaptoethanol to prevent oxidation of proteins after cell lysis. A total amount of 40 µg DNP-derivatized protein was separated by 12% SDS-PAGE electrophoresis followed by DNP-detection through WB-analysis. The primary anti-DNP was incubated for 1 h at room temperature, followed by HRP-linked secondary antibody incubation. Protein bands were developed using an ECL detection reagent and imaged with the

ImageQuant800^{TM} Imaging system. Band intensities were quantified with the ImageStudio light software and normalized to anti-β-Actin, which was used as a loading control.

3.2.4.3. Indirect immunofluorescence

Huh7 cells were seeded on glass coverslips in a 12-well plate and transiently transfected with HBx-HA plasmid DNA or together with reporter plasmid DNA and fixed 72 h post-transfection in 4% Formaldehyde in PBS for 10 min at room temperature. Subsequently, cells were washed twice with PBS and permeabilized with 0.5% Triton X-100 in PBS for 10 min, followed by blocking with 5% BSA in PBS for 30 min. Primary antibodies were diluted in a blocking solution and samples were incubated for 1 h at room temperature in a humid chamber. Afterward, slides were washed three times, each 5 min in PBS to remove unbound primary antibody and primary antibody epitopes were detected by incubation with respective secondary antibodies conjugated with AlexaFluor488, AlexaFluor546 or AlexaFluor633. Secondary antibodies were diluted accordingly in a blocking solution together with 250 ng/ml 4',6-Diamidin-2-phenylindole (DAPI) for nuclei staining and incubated for 1h at room temperature. Finally, samples were washed 3x 5 min with PBS and mounted on glass slides using Mowiol.

3.2.5. Microscopy and image acquisition

3.2.5.1. Confocal laser scanning microscopy

Intracellular localization and distribution as well as fluorescence intensities of the stained protein epitopes were imaged with a confocal laser scanning microscope, the Leica TCS SP8 System with a DMi8 microscope. All images were captured with a 100× magnification oil immersion objective (numerical aperture = 1.4) and a pinhole setting at 1 airy unit (AU) for giving an optical section thickness of 0.7 µm. Image acquisition was achieved with the LasX Control software.

3.2.5.2. 3D High-resolution microscopy

Three-dimensional data were obtained with a z-stack scan, a compilation of multiple focal planes processed to a multidimensional cell structure, in combination with lightning technology. Lightning enables super-resolution confocal microscopy by an adaptive, modular process to gain more refined and detailed structural information compared to confocal microscopy. About 10 µm thick Z-stacks of 10 to 20 slices were acquired and processed using the 3D viewer of LasX control software.

3.2.6. Quantification and statistical analysis

3.2.6.1. Fluorescence co-localization analysis

Analysis of co-localization in fluorescence microscopy images was applied to observe the spatial overlap between two different fluorophore-labeled antigens, using the tMOC (threshold Mander's overlap coefficient) calculation with FIJI software. The tMOC value ranges from 0 to 1, whereas a coefficient of 1 indicates complete co-localization, independent from the overall intensity of the used fluorophores. A minimum of 18 cells of each condition was used for statistical analysis.

3.2.6.2. Fluorescence intensity quantification

Total fluorescence intensity per cell was calculated in fluorescence microscopy images with Fiji software. The calculated integrated density was corrected by subtraction of the area of the selected cell multiplied by the mean fluorescence of background readings and expressed as CTCF. A minimum of 10 cells of each condition was used for statistical analysis.

3.2.6.3. Quantification of double-positive particles

The number of double-positive particles within a cell was processed by particle analysis with FIJI. First, respective fluorescence microscopy images were manually set with a threshold to convert it to binary. Then, an overlapping image consisting of only pixels, which are present in both channels was created and used for subsequent particle counting. The ratio of double positive cells to the total number of particles counted was calculated as a percentage in each cell.

3.2.6.4. Mitochondrial network analysis

In order to quantitatively describe the mitochondrial morphology, the Fiji-supported Mitochondrial Network Analysis tool (MiNa) was applied. The method was published first by Valente et al. [227]. The source code for MiNA is provided by the developer in the GitHub repository [228]. Fluorescence microscopy images, stained for the mitochondrial outer membrane marker protein (Tom20) were processed with the tool to investigate changes in the mitochondrial structure in HBx-positive cells. In detail, running the tool converted the image into a binary mitochondrial overlay and a skeleton model based on the respective image, and used to determine the desired parameters for the mitochondrial network. In this work, the mitochondrial footprint and the mean network count were investigated. The first parameter reflects the area of detected mitochondrial signal (in μm^2), the last parameter indicates the

bifurcation of the mitochondrial network as the mean count of connected lines. A minimum of 12 cells of each construct were used for statistical analysis.

3.2.6.5. Statistical analysis

Unless stated otherwise, all data are expressed as mean value ± SEM of the indicated number of independent experiments (n). At least a minimum of three approaches were performed. Data analysis was evaluated with GraphPad Prism Software with a statistical comparison of two datasets by an unpaired, two-tailed student's t-test. A *p*-value of less than 0,05 was considered to be statistically significant and is indicated by an asterisk. Data sets presented as fold change values were calculated to the respective control sample in each independent experiment and were arbitrarily set as 1.

4. Results

4.1. Characterization and validation of the experimental design

The study of the viral HBx protein represents a major challenge due to its low level of expression, its small size and its overall flexible and inherent nature. In particular, the genetic variability within different genotypes has an influence on the antigenic properties of HBx. Because of this, the experimental setup was designed primarily on the human hepatoma cell line Huh7 together with an HBx overexpression system. The introduction of an HA or eGFP reporter-tag at the C-terminus of HBx enables an equivalent detection strategy and comparative characterization of genotypes across host cell pathways. To validate the capability of the used constructs, western blot analysis and immunofluorescence microscopy were conducted.

4.1.1. HBx protein expression and cellular distribution are not affected by a reporter tag

To confirm the expression of HBx as well as the respective tag (HA or eGFP), Huh7 cells were transiently transfected with HBx GtA either with or without a tag and verified by western blot analysis. In addition, the localization was confirmed by confocal laser scanning microscopy, immunostained with a HBx-specific antibody. A co-staining with the respective tag verifies the presence of the HBx-protein and a sensitive detection of the protein of interest.

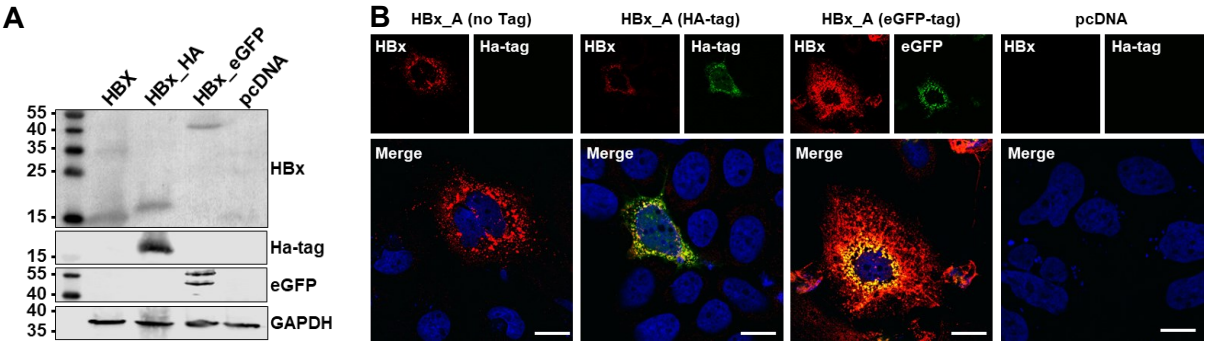

Figure 11: Detection and localization of HBx are independent from the reporter tag. Huh7 cells were transiently transfected with HBx_gtA (no tag), HBx_gtA-HA, HBx_gtA-eGFP or empty plasmid DNA as control and harvested 72 h. p.t. **(A)** Representative Western blot of viral HBx in total cell lysates. HBx protein levels were detected by a HBx-specific antibody. Tags were detected by eGFP fluorescence or HA-specific antibody, GAPDH detection was used as internal loading control. **(B)** Representative CLSM images were fixed with Formaldehyde and immunostained for HBx with an HBx-specific antibody (red), HA-tag/eGFP (green) and nuclei counterstained with DAPI (blue). Scale bar indicates 20 µm.

Western blot analysis and CLSM detection confirms equal protein synthesis and localization between the different HBx constructs. Also, the HA or eGFP tag is detectable and presents no

visible differences, compared to the tag-free construct. Furthermore, the HBx staining directly overlaps with the respective fused reporter, as shown by the yellow areas in the respective immunofluorescence images (fig. 11).

4.1.2. The cellular compartmentalization of the HBx protein depends on the protein level

In addition, the intracellular compartmentalization of the HBx protein were determined over the time by CLSM analysis. Therefore, Huh7 cells were transiently transfected with HBx_GtA-HA and harvested after different timepoints after transfection.

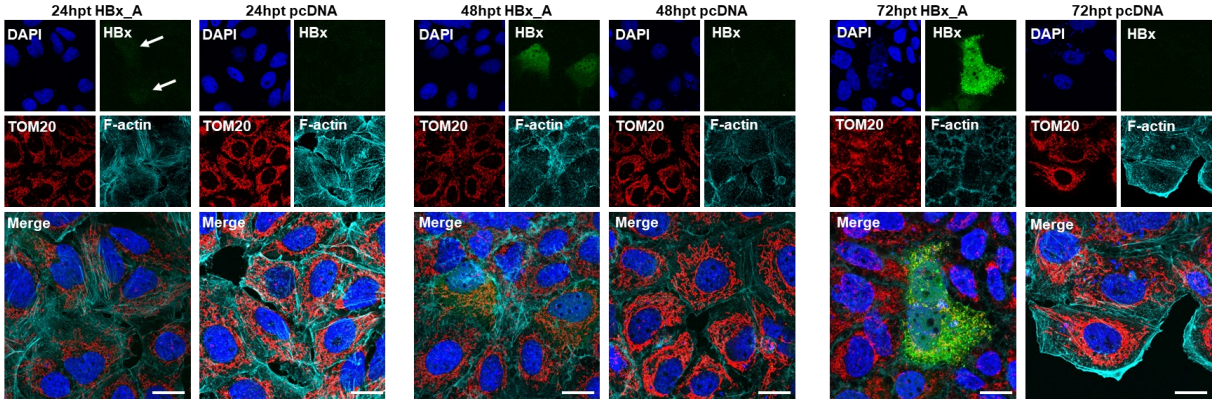

Figure 12: Intracellular compartmentalization of HBx varies among different timepoints after transfection. Representative CLSM images of Huh7 cells, transiently transfected with HBx_gtA-HA or empty plasmid DNA. Cells were harvested 24h, 48h or 72h p.t. and immunostained for HBx with an HA-specific antibody (green), TOM20 antibody (red) to image the outer mitochondrial membrane. Cells were counterstained with Phalloidin-Atto633 for F-actin and DAPI for nuclei staining (blue). Scale bar indicates 20 µm. White arrows indicate HBx staining.

Based on CLSM staining, the intracellular localization of HBx depends on different time points after transfections, mainly representing different levels of protein within the cell. After 24 h p.t. the amount of HBx protein is rather low and localizes exclusively in the nucleus (white arrow, fig. 12, left panel). 48h after transfection, HBx still localizes mainly in the nucleus, but also partially in the cytoplasm. At both time points, the mitochondrial network appears with intact, tubular network structures that extend throughout the entire cytoplasm. After 72 h p.t. and at high levels of HBx, a predominantly cytoplasmic compartmentalization occurs (reflecting persistent HBV infection) and enables the possibility of interaction with mitochondrial organelles. The mitochondria appears with condensed and perinuclear aggregation, but only in the HBx-transfected cells (fig. 12).

Overall, the HBx constructs used in the present study synthesizes and localizes the viral HBx protein in a comparable manner to the unlabeled control. The intracellular localization is time-dependent, whereas a cytoplasmic compartmentalization and mitochondrial accessibility mainly occurs in this setting 72h after transfection.

4.2. Cellular characterization between genetic variants of HBx reveals significant differences in quantity, localization and host kinome profile

The viral HBx protein is accounted as a multifunctional protein with pleiotropic effects on host signaling pathways and a major contribution in the progression of liver-specific carcinogenesis [137]. However, the impact of the different HBV genotypes especially with regard to the HBx protein is poorly understood. Therefore, an initial characterization of the HBx protein was set up to investigate differences among the distinct genotypes of HBx in vitro.

4.2.1. HBx protein amount and cellular distribution vary among distinct genotypes

To elucidate the subcellular distribution and relative expression levels of HBx within transiently transfected Huh7 cells, confocal laser scanning microscopy (CLSM) using high-resolution lightning application and a Western blot analysis was performed. The HBx protein was detected through a C-terminally introduced HA-tag, which enables the specific visualization of full-length HBx and overcomes detection inhomogeneities due to genotype-related sequence differences (fig. 11).

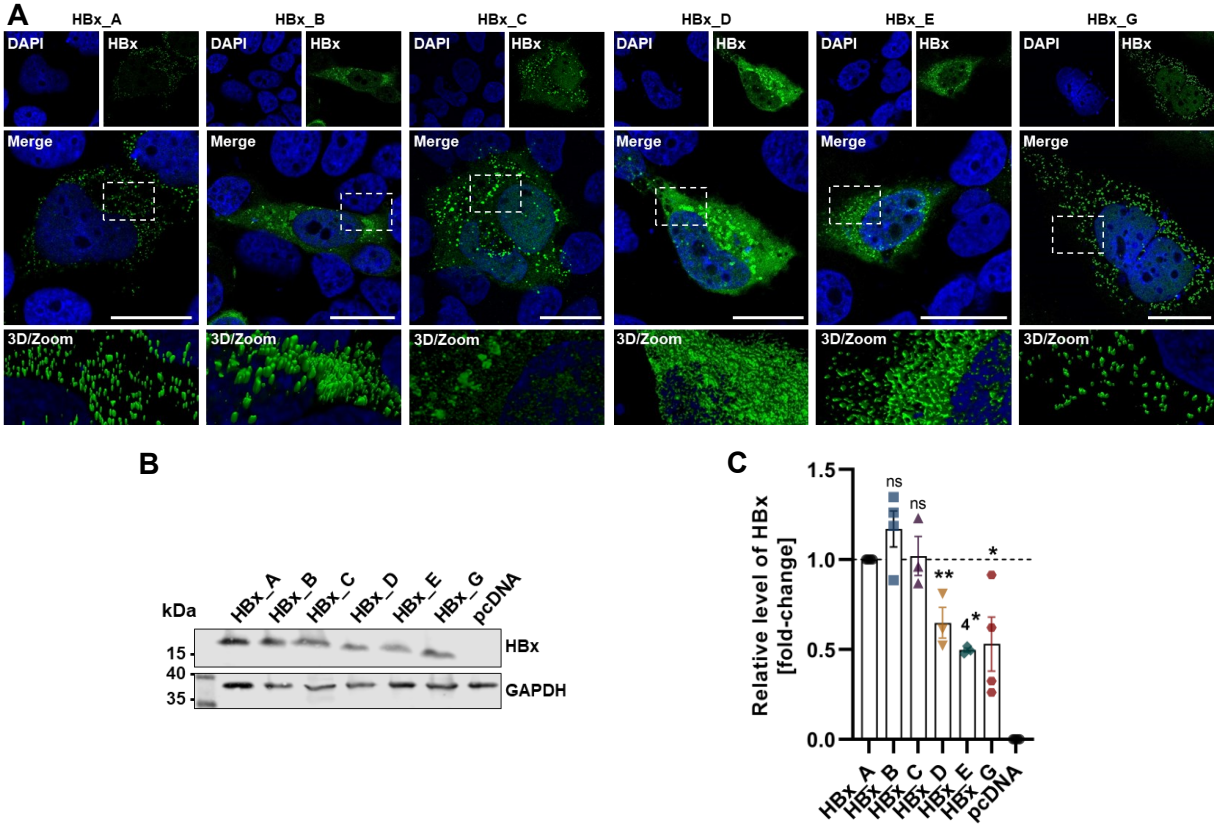

Figure 13: Cellular distribution and protein amount of HBx varies among different HBV genotypes in transiently transfected Huh7 cells. Cells were transiently transfected with HBx plasmid DNA (genotype A, B, C, D, E or G) or pcDNA (empty plasmid control) and harvested 72 h. p.t. **(A)** Representative CLSM images fixed with Formaldehyde and immunostained for HBx with an HA-specific antibody (green). Nuclei were counterstained with DAPI (blue), dashed rectangle indicates zoom section for 3D-high resolution images. Scale bar indicates 20 µm.

(B) Representative Western blot of viral HBx in total cell lysates. HBx protein levels were detected by an HA-specific antibody, GAPDH detection was used as internal loading control. **(C)** Quantification of relative HBx protein amounts in (B) referred to genotype A. Statistic is indicated as mean ± SEM based on N>3 independent experiments using unpaired t-test related to genotype A with * $p < 0.05$; ** $p < 0.01$; **** $p < 0.0001$.

Based on the CLSM images, a mainly cytoplasmic distribution is observable for all tested genotypes, however, they differ among their subcellular distribution. In particular, the genotypes (Gt) A, C and G display a clear dot-like structure, distributed over the whole cytoplasmic space. Against that, the genotypes B, D and E demonstrated a homogenous distribution in combination with a perinuclear accumulation of HBx, which is more pronounced in genotypes B and D, respectively (fig. 13A).
The analysis of HBx protein levels reveals to a higher protein amount for Gt A, B and C, as compared to the other used genotypes. In fact, it was found that the amount of HBx in genotype E was reduced by about 50% on average, compared to Gt A. Overall, the genotypes partially showed a high variance within the experimental replicates, especially for genotypes B and D, which indicate an increased tendency towards insoluble or aggregated proteins (fig. 13B-C).

Overall, the viral HBx protein shows an extranuclear localization in all HBx genotypes examined, but with clear differences in terms of the cytosolic distribution pattern and beyond that, on the protein expression levels.

4.2.2. Kinome profile analysis reveals a significant, HBx genotypes-dependent impact on host signaling pathways

To gain further knowledge of the regulatory effects of HBx on host pathway interactions, a kinome profile analysis was performed. This method is based on the detection of peptide phosphorylations by protein kinases and thus recognizes modifications in the kinome profile compared to a control sample. Furthermore, changes in the upstream kinase activity facilitate the identification of signal transduction and pathway alterations. To initially identify regulated pathways by HBx, predicted target genes of HBx-genotype A in Huh7 transfected cells were identified and used for a pathway enrichment analysis. In light of this, predicted genes with a mean final score above 1.2 were applied in the KEGG Orthology Based Annotation System (KOBAS) and calculated to identify significantly enriched Kyoto Encyclopedia of Genes and Genomes (KEGG) -pathways. Enriched pathways with a *p*-value above 0.05 were categorized, whereas the top 5 ranged KEGG terms were given in the data analysis report (fig. 14).

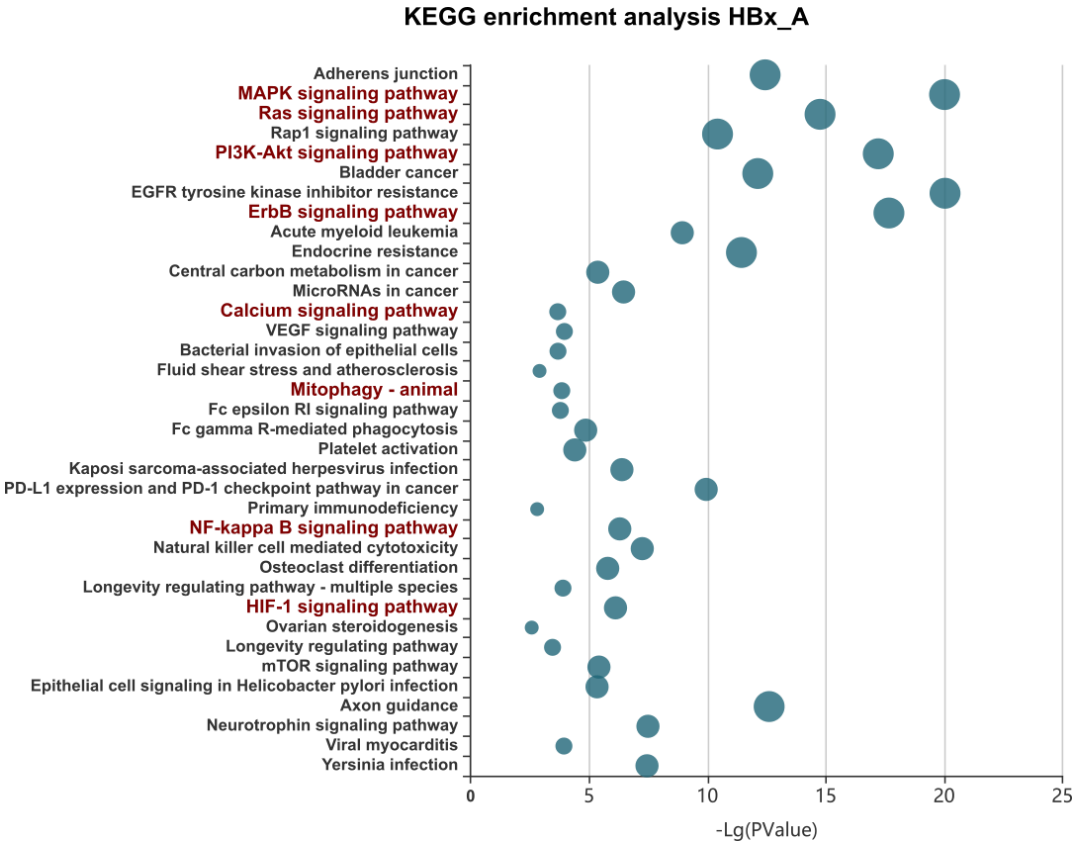

Figure 14: HBx-genotype A impairs mitochondrial associated signaling pathways. Huh7 cells were transiently transfected with HBx plasmid DNA of different HBV genotypes or pcDNA control vector and harvested 72 h p.t. Kinase activity was determined by PamStation analysis, whereas predicted kinases with a mean final score above 1.2 were applied for KEGG pathways enrichment analysis by using the KOBAS databank. Bubble blot indicates significantly enriched KEGG terms (*p*-value > 0.05) and ranked accordingly to the highest enrich ratio. Each bubble represents an enriched KEGG term. The node size represents the *p*-value of enrichment (from small to large): [0.05,1], [0.01,0.05], [0.001,0.01], [0.0001,0.001], [1e-10,0.0001], [0,1e-10], means bigger bubbles indicating smaller *p*-values. Mitochondrial-associated regulatory signaling pathways were highlighted in red.

The pathway enrichment analysis of HBx genotype A showed significant regulatory effects in several KEGG pathways. In particular these include especially, alterations in central regulatory transduction pathways such as MAPK-, Ras- and PI3K- signaling. Interestingly, the analysis reveals also a significant contribution in mitophagy, ErbB signaling, calcium signaling, NF-κB and HIF-1 signaling, pathways which are directly associated with pleiotropic impact on the mitochondrial biogenesis and associated innate immune response. Accordingly, these data suggest a strong interaction between HBx genotype A and mitochondrial biogenesis (fig. 14).

To further elucidate these observations and compare putative enriched kinases with other HBx genotypes, kinome analysis of HBx genotypes A, B, C, D, E and G were investigated. In particular, Src kinase family, ABL, EGFR, ErbB2, Akt, JNK, ERK1/2, p38 MAPK, GSK3β, PKA and PKC were identified previously by Lim et al. [196] as dominant kinases in mitochondrial associated regulatory pathways and were annotated if they were significantly deregulated in the respective genotype analysis (fig. 15).

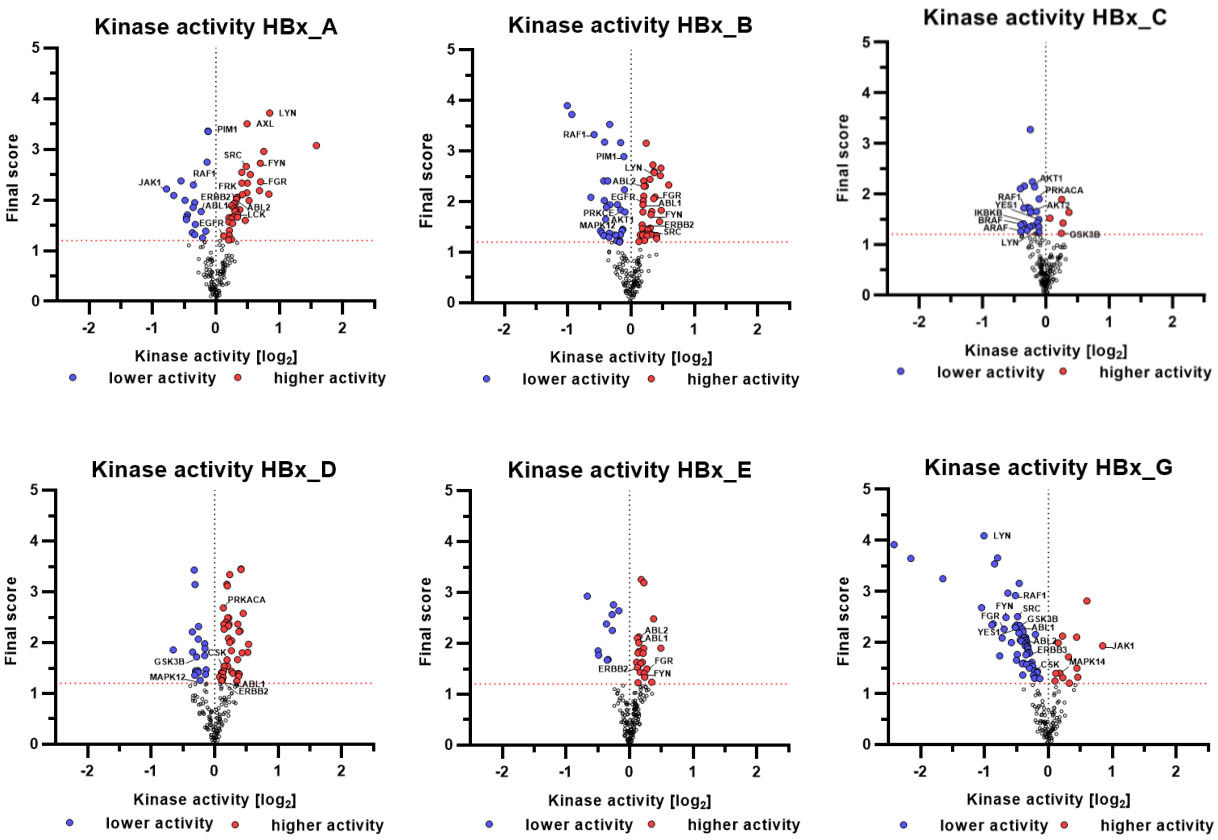

Figure 15: HBx protein of different genotypes display distinct regulatory effects in the kinome profile. Huh7 cells were transiently transfected with HBx plasmid DNA of different HBV genotypes or pcDNA control vector and harvested 72 h p.t. Kinase activity was determined by PamStation analysis and calculated for each HBx genotype compared to the control. Volcano plots shows the predicted kinase activity of each HBx genotype. The blue dots display significant downregulated kinases, the red dots represent significant upregulated kinases. A mean final score below 1.2 was conducted to be not significant and are colorless. Significant activated kinases with known function in mitochondrial morphogenesis and biogenesis were labelled by name.

On the kinome analysis profile it became evident, that the HBx protein alters the biological functional kinase activity of the host cell. Furthermore, however, significant differences were observed among the distinct genotypic variants of HBx. In particular, HBx Gt E showed only minor changes in the overall kinase activity profile, whereas genotypes A and B caused strong upregulation of kinase activity. Contrary, Gt G revealed a significant downregulation in the

kinome analysis. A particular focus on mitochondrial-associated kinases also revealed differences in a genotype-dependent manner. For example, Scr-kinases were significantly upregulated for HBx-Gt A and B, but significantly down-regulated in case of HBx Gt G. In addition, genotypes A and B indicated a downregulation in RAF1 and Erb2, Gt G is also accompanied with a strong kinase activity of JAK1 and MAPK14. Interestingly, HBx of genotypes D and E represented only a minor deregulation in mitochondrial associated kinases (fig 15).

Taken together, all genotypes exert a significant influence on host signaling pathways. However, the kinome profile differ greatly between the different HBx genotypes and indicates major differences in the overall cellular function, but particularly in kinases related with mitochondrial functions.

4.3. HBx induces profound changes in mitochondrial morphology and abundance in a genotype-dependent manner

In the preceding section, HBx was evident to provide elevated changes in the mitochondrial kinome and indicated furthermore a high heterogenicity across the HBx genotypes. In general, viral-induced changes in mitochondrial homeostasis are strongly associated with mitochondrial dysfunction and disease progression. The initial step in the cascade of several mitochondrial-associated misfunctions is provided by a change in the mitochondrial network structure and fragmentation of the reticular tubular structure in order to maintain the overall cellular physiology and cell survival. Despite it is already evident that HBx interacts with mitochondrial-associated proteins and shifts the regulatory mechanisms towards an elevated fission [205], the impact of different genotypes in this regard is largely unknown but is further investigated in this study.

4.3.1. HBx trigger the mitochondrial network structure towards fission genotype dependently

In order to investigate changes in the mitochondrial network structure in dependency of the genetic variants of HBx, CLSM analysis with high resolution-lightning tool was applied. Therefore, Huh7 cells expressing HBx of different genotypes were co-stained for HBx (via HA-tag) and the mitochondrial marker protein TOM20. Control transfected cells (empty vector plasmid) were used as reference, indicating a healthy mitochondrial phenotype (fig. 16).

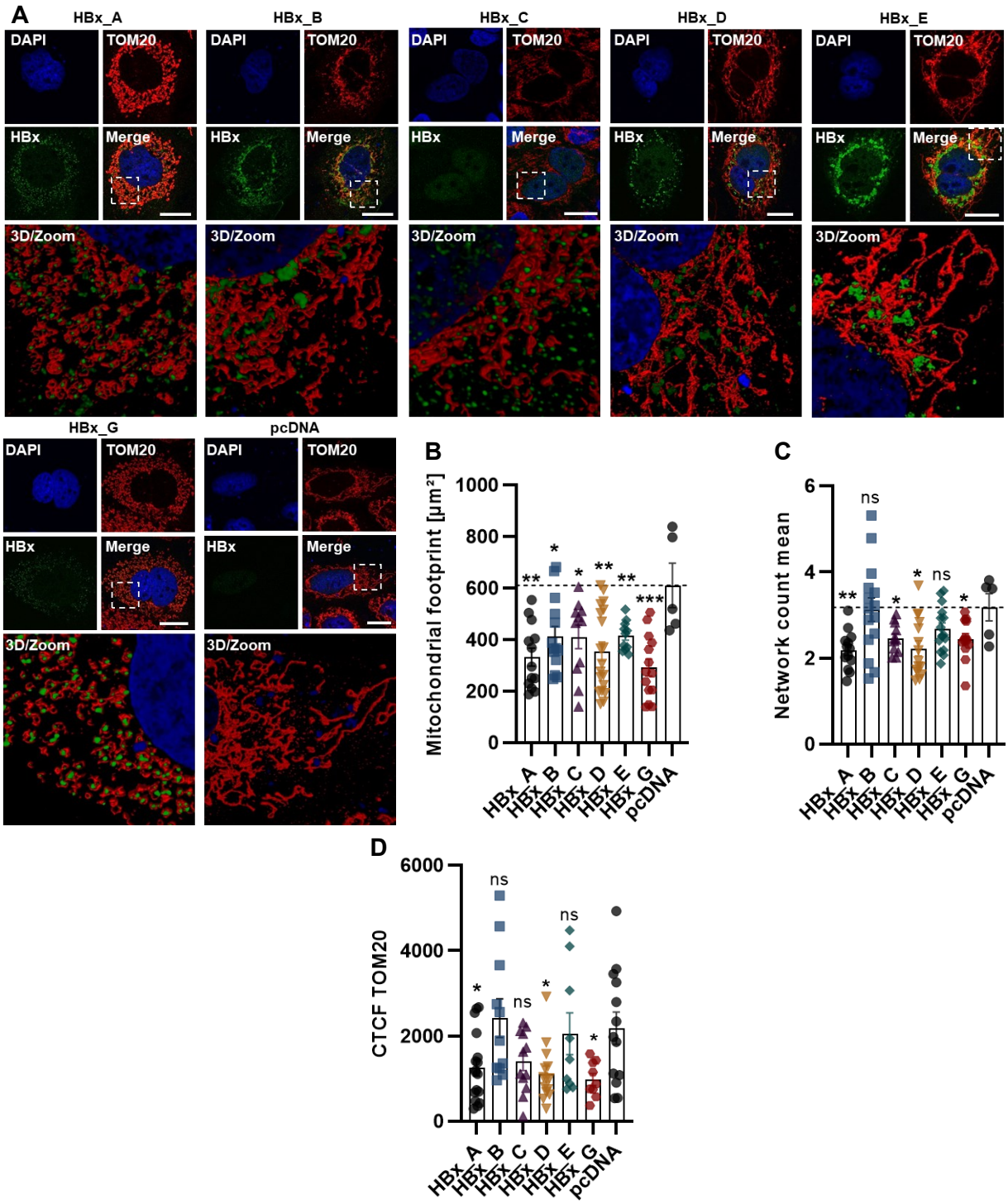

Figure 16: HBx genotype A and G heavily induce global mitochondrial fragmentation. (A) Representative CLSM images of HBx transfected Huh7 cells. Cells were fixed 72 h p.t., pcDNA transfected cells serves as control. Cells were immunostained for HBx via HA-specific antibody (green) and TOM20 (red), nuclei were counterstained with DAPI. Dashed rectangles indicate the zoom section for 3D-high resolution images. Scale bar indicates 20 µm. **(B-C)** Quantification of mitochondrial network structure in (A) using MiNa network analysis tool. Mitochondrial footprint reflects the area of mitochondrial structures in μm^2; the network count mean indicates the mean number of branching mitochondria. The statistic based on more than 12 single-cell quantifications per genotype, for pcDNA N=5 cells were analyzed. **(D)** Quantification of TOM20 signal intensities in (A) calculated as corrected total cell fluorescence CTCF. At least 10 cells per genotype/control were quantified. Data are indicated as mean ± SEM with unpaired t-test related to pcDNA sample with * $p < 0.05$; ** $p < 0.01$; *** $p < 0.001$.

Using single-cell analysis, structural differences between HBx transfected and pcDNA transfected cells were observed. The pcDNA transfected cells reflect an intact network of mitochondrial structures evident by a reticular framework of connected mitochondria with highly elongated and branched filaments. In contrast, HBx generally induces a reduction in footprint and network allocations. In addition, a comparison within the genotypes reveals clear differences in the extent of the changed networks. The HBx Gt B and E only induce moderate changes in the mitochondria dynamics, visible through slightly shorter filaments and less interconnections. However, Gt C and D shows some degree of mitochondrial fragmentation, while HBx genotypes A and G show noticeable amounts of damaged mitochondria, evident by high levels of fragmentation, resulting in isolated mitochondria that also have a swollen, round shape and no visible branches (fig. 16A). This observation was confirmed by a quantification of the mitochondrial network, given by an overall decline in the mitochondrial foot print for HBx, as compared to the control, yet with significant more reduction for the genotypes A, G and slightly C and D. The mean network count revealed a tremendous decline in the average amount of network interconnections for the HBx Gt A, C, D and G, but not for Gt B or E (fig 16B-C). Obviously, it can also be observed that in the case of severe fragmentation, the HBx protein appears with a perinuclear accumulation and in close proximity to the mitochondria, while in the case of moderate changes in the mitochondrial network, the HBx protein only located in-between of mitochondrial structures and without an obvious, direct association. Furthermore, a high number of disrupted mitochondria in the HBx-genotypes A, D and G are accompanied with a significand decline in the TOM20 protein levels (fig. 16D).

In summary, the different genotypes of HBx employ different capacities to induce mitochondrial fragmentation and alter the entire mitochondrial network within the cells. Particularly, in genotypes A and G, profound changes were detected together with an enormous decrease in the structure and protein content of TOM20.

4.3.2. HBx reduces the mitochondrial mass depending on the HBV genotype

In order to further elucidate the reduction in the mass of mitochondrial proteins, Western blot analysis was performed. To gain further insight in the underlying regulatory mechanisms of the HBx-dependent effect, we analyzed the protein amount of the nuclear-encoded mitochondrial TOM20 and cytochrome c oxidase subunit IV (COX-IV) protein. The TOM20-protein is part of the outer mitochondrial membrane, whereas COX-II is part of the respiratory chain complex and localized at the inner mitochondrial membrane. In addition, the Cytochrome c oxidase subunit 2 (COX-II) was chosen as example for and mitochondrial encoded protein. Cells treated with a mitochondrial decoupler (CCCP) were used as a control to induce mitochondrial

damage and an obvious decline in the mitochondrial mass. To access regulatory effects on gene-expression levels, a RT-qPCR analysis was performed (fig. 15).

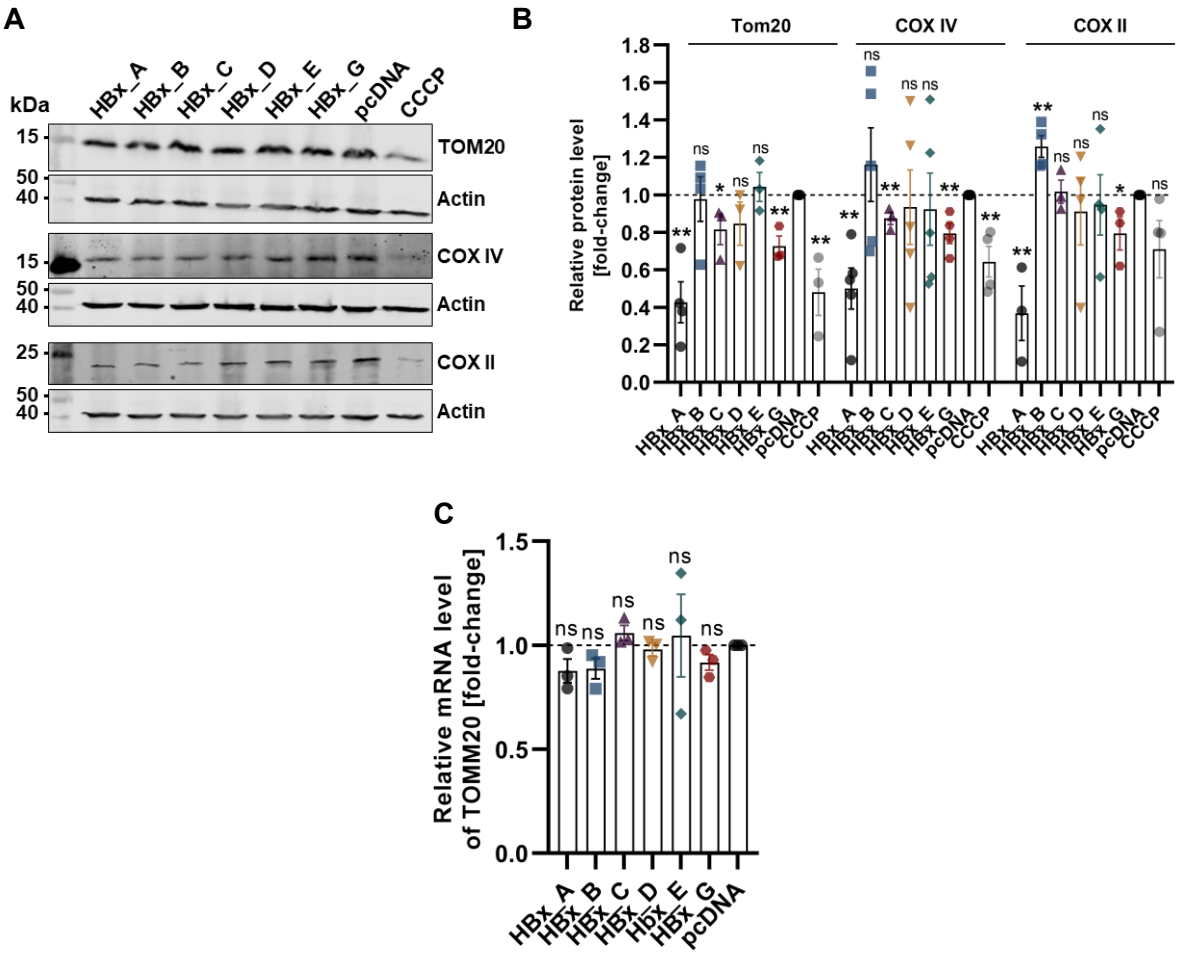

Figure 17: The mitochondrial protein amount, but not the mRNA level is modulated by HBx in a genotype-dependent manner. Huh7 cells were transiently transfected with HBx plasmid DNA (genotype A, B, C, D, E or G) or pcDNA (empty plasmid control) and harvested 72 h. p.t. **(A)** Representative Western blot of TOM20, COX-II and COX-IV in total cell lysates. Actin detection was used as internal loading control. **(B)** Quantification of relative protein amounts in (A) referred to pcDNA control. Statistic based on N>3 independent experiments. Cells treated with Carbonyl cyanide m-chlorophenyl hydrazine (CCCP) were includes as positive control to induce mitochondrial damage. **(C)** Relative changes in intracellular mRNA levels of TOMM20 assessed by RT-qPCR analysis. N=3. All data are indicated as mean ± SEM with unpaired t-test related to pcDNA sample. * $p < 0.05$; ** $p < 0.01$.

Consistent across all analyzed mitochondrial proteins and regardless of whether nuclear or mitochondrial encoded, a significant reduction in protein levels were observed for the HBx Gt A and G. In the case of Gt A, a decrease of up to 50% was measured, compared to the control. For the other HBx genotypes used, there was no significant decrease in protein amounts observable. HBx Gt C shown a decrease in Tom20 and COX IV protein amount, but no significant reduction compared to the control for COX II levels (fig. 17A & B). Likewise, the amount of intracellular mRNA levels was unchanged across all HBx genotypes and also in

comparison to the control. This indicates a gene-expression independent deregulation of the mitochondria by HBx (fig. 17C).

Taken together, and consistent with the immunofluorescence data, HBx induces profound genotype-dependent changes in mitochondrial protein abundance, which are thought to be regulated exclusively by protein-related mechanisms.

4.3.3. HBx effects mitochondrial dynamics genotype-dependent in HepG2 cells

Besides Huh7 cells, the human hepatoma cell line HepG2 provides another suitable system for HBV related in vitro studies. Since Huh7 cells represents an overall higher transfection efficiency, the HepG2 cell line expresses a higher degree of liver-specific proteins and thus more retains hepatic functions and the overall physiological context [229].

To exclude a cell line-specific bias in the previously observed genotype-related effects on mitochondrial dynamics, mitochondrial structures were additionally examined in the context of HBx-transfected HepG2 cells.

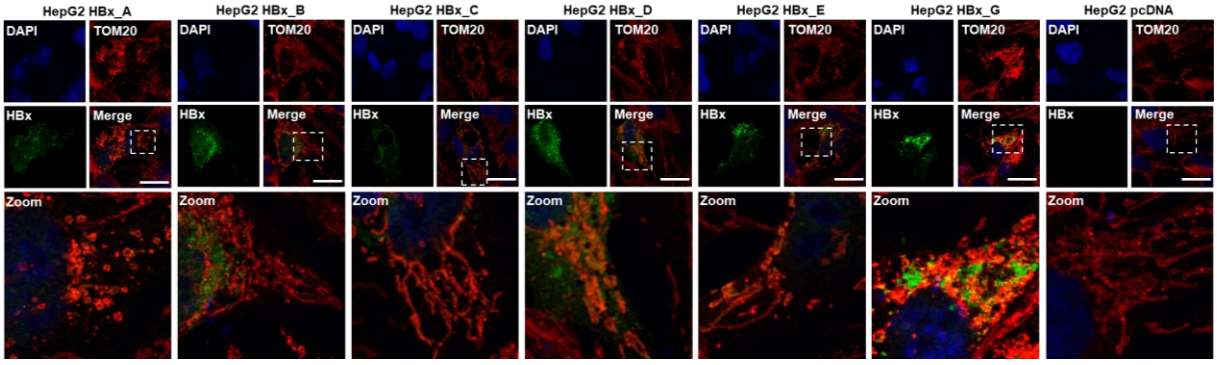

Figure 18: HBx induce mitochondrial fragmentation in HepG2 cells. Representative CLSM images of HBx transfected HepG2 cells. Cells were fixed 72 h p.t., pcDNA transfected cells serves as control. Cells were immunostained for HBx via HA-specific antibody (green) and TOM20 (red), nuclei were counterstained with DAPI. Dashed rectangles indicate the zoom section. Scale bar 20 µm.

CLSM analysis of HBx transfected HepG2 cells shows a strong fragmentation in the mitochondrial network, mainly for Gt A and G, whereas HBx Gt C and D represents a lower amount of branched structures. HBx Gt B and E retains mostly the elongated tubular network, comparable with the pcDNA transfected cells.

Overall, genotype dependent changes in the mitochondrial structures by HBx are consistently visible among different hepatoma cell lines.

4.4. HBx alters mitochondrial function and homeostasis in a genotype-dependent manner through association with VDAC3

HBx evidently represents a key factor in mitochondrial disruptions by including profound changes in the mitochondrial network structure and reduction in the mitochondrion-specific protein amounts, especially in some intergenotypic variants. According to this, we also suspected a potential serious impact on mitochondrial function and homeostasis. Central to this assumption is the interaction of HBx with VDAC3 and a resulting possible modulation of the opening state of the channel and release of essential mitochondrial metabolites [206].

4.4.1. Genetic variants of HBx interact with VDAC3 to varying degrees

To address this question, Huh7 cells were transiently transfected with the HBx plasmid DNA of different genotypes and analyzed by CLSM to obtain the association of HBx with the VDAC3 depending on the respective genotypes of HBx (fig.19).

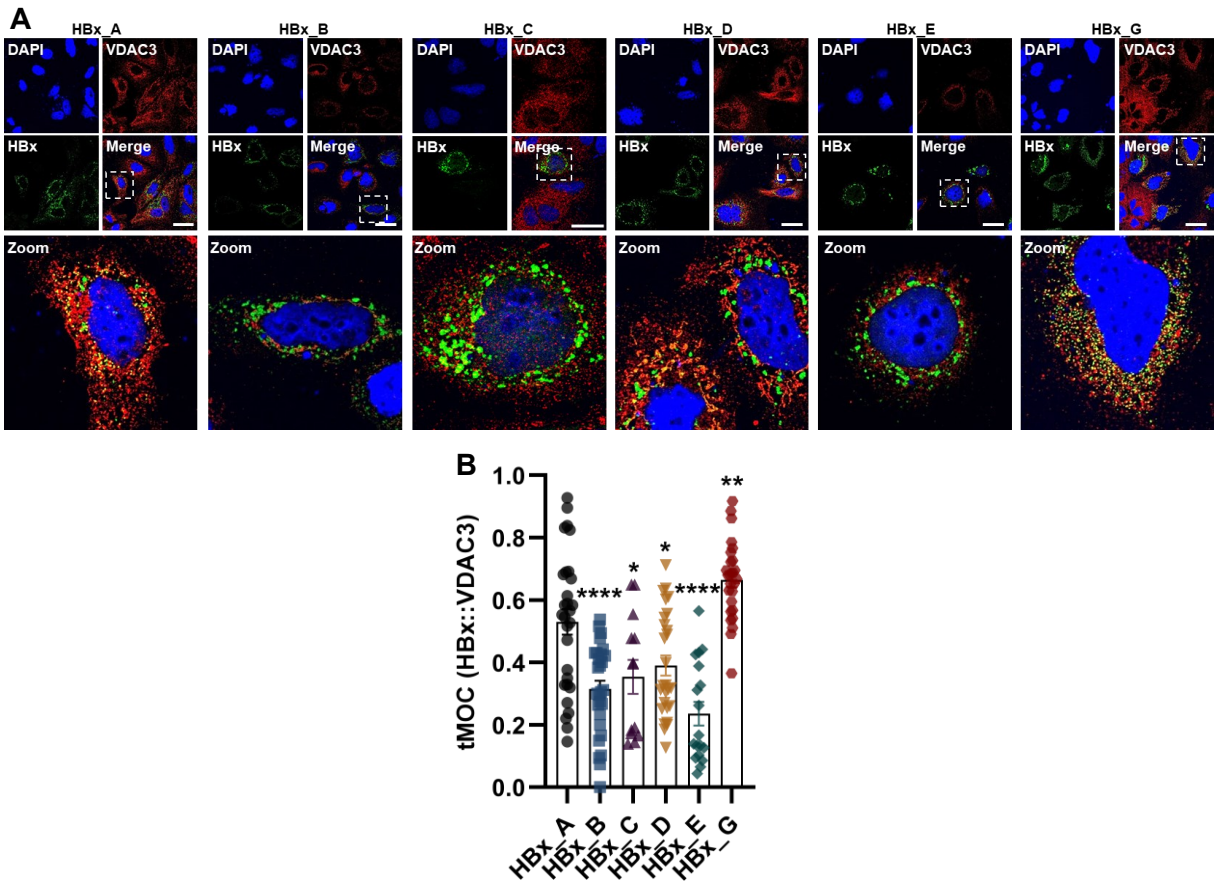

Figure 19: HBx colocalizes with the VDAC3 in a genotype-dependent manner. (A) Representative CLSM images of HBx transfected Huh7 cells. Cells were fixed 72 h p.t. and immunostained for HBx, using a HA-specific antibody (green) and VDAC3 (red), nuclei were counterstained with DAPI. Dashed rectangles indicate the zoom sections. Scale bar indicates 40 µm. **(B)** Quantification of pixel co-localization between HBx and VDAC3 in (A) as thresholded Mander's overlap coefficient (tMOC). At least 18 cells per condition were analyzed. Data are indicated as mean ± SEM with unpaired t-test related to HBx Gt A. * $p < 0.05$; ** $p < 0.01$;**** $p < 0.0001$.

All HBx variants analyzed, showed direct colocalization with the VDAC3, however strong differences in the degree of co-localization were observed (fig. 19A). In addition to the previously observed moderate effects for HBx Gt B and E, they exhibited accordingly the lowest co-localization with an average tMOC value between 25% and 35%, while a tMOC value of approximately 40% was determined for HBx Gt C and D. Notably, HBx of Gt A and G exhibit the highest co-localization with an average tMOC value between 55% and 70% (fid. 19B).

4.4.2. Genotype-dependent interaction between HBx and the VDAC diminish the $\Delta\Psi_m$-level and cytochrome c oxidase activity

Studies of mitochondrial membrane potential, a key indicator of the physiological state of mitochondria, were carried out using the membrane potential-sensitive JC-1 dye. The dye is a positively charged fluorophore and accumulate normally in the electronegative interior of mitochondria, indicated by red fluorescence emission. A loss of membrane potential shifts the JC-1 dye in a monomeric form, indicated by a green fluorescence emission. In this study, changes in the membrane potential were investigated by measuring changes in the JC-1 fluorescence intensities by flow cytometry analysis. Huh7 cells were therefore transfected with plasmid DNA of HBx from different genotypes and compared to control transfected cells. The degree of depolarization was calculated by red/green fluorescence intensity ratio (fig. 20).

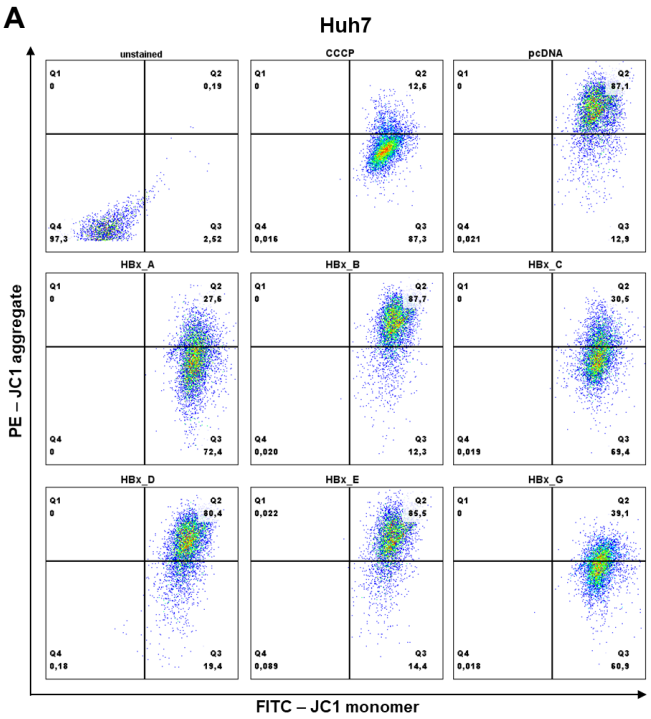

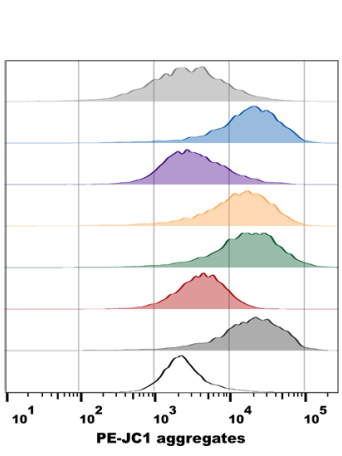

	Sample	Geometric Mean - PE
	F:HBx_A	2544
	F:HBx_B	15317
	F:HBx_C	3248
	F:HBx_D	11033
	F:HBx_E	14519
	F:HBx_G	3884
	F:HBx_pcDNA	16240
	F:HBx_CCCP	2400

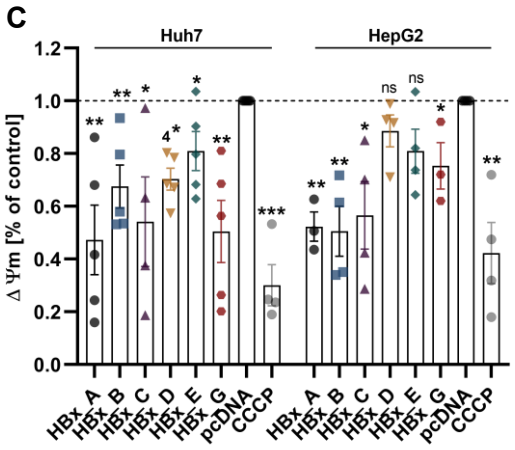

Figure 20: Genetic variants of HBx have distinct impact on the mitochondrial membrane potential. Huh7 or HepG2 cells were either HBx or pcDNA transfected and stained 72 h. p.t. with the JC-1 mitochondrial membrane-sensitive dye. CCCP treated cells were used as positive control, indicating elevated mitochondrial dysfunction and subsequent loss of ΔΨm. **(A)** Representative dot blots display JC-1 monomers in the FITC-channel on the x-axis and JC-1 aggregates on the y-axis of PE-channel. **(B)** Representative histogram of (A) with calculated geometric mean fluorescence intensities of PE. **(C)** Quantification of Huh7 and HepG2 cells; the ratio of red (JC-1 aggregates) to green (JC-1 monomers) mean fluorescence intensities represent the final mitochondrial membrane potential relative to the control. Statistic based on N>3 independent experiments, indicated as mean ± SEM and unpaired t-test related to pcDNA sample with * $p < 0.05$; ** $p < 0.01$; *** $p < 0.001$. CCCP stands for Carbonyl cyanide m-chlorophenyl hydrazine and served as positive control.

Interestingly, a significant loss of mitochondrial membrane potential could be observed for all HBx-expressing cells (fig. 20). Importantly, however, a decline between 20 and 40% was observed for the HBx genotypes B, D and E compared to the control group, yet this effect was again significantly more pronounced for the genotypes A, C and G. A similar effect was also detectable in the HepG2 cell line (fig. 20C).

As part of the respiratory chain complex, the activity of the cytochrome c complex is in direct response to an aberrant mitochondrial membrane potential and was therefore further investigated (fig. 21).

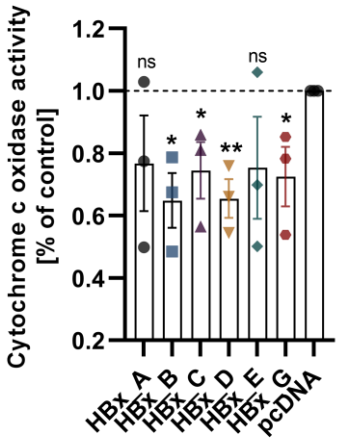

Figure 21: The cytochrome c activity is altered by HBx, dependent on the genotype. Cytochrome c activity assay gain form isolated mitochondria of Huh7 transfected cells and was calculated within the linear range of substrate turnover. Statistic based on N=3 independent experiments, indicated as mean ± SEM and unpaired t-test related to pcDNA sample with * $p < 0.05$; ** $p < 0.01$.

The cytochrome c activity was reduced among all tested HBx genotypes as compared to the control. Despite the change for the Gt A and E was not considered to be significant, HBx of the genotypes B, C, D and G reveals a significant decline in the activity (fig.21).

Overall, these data show a tremendous genotype-dependent contribution to HBx-induced aberrant mitochondrial membrane potential and cytochrome c activity and accordingly suggest increased mitochondrial dysfunction. Consistent with the influence on mitochondrial morphology, the strongest effects were investigated for HBx, derived from genotypes A and G.

4.5. HBx-mediated perturbation of mitochondrial integrity induces oxidative stress and pro-inflammatory responses

The interaction between HBx and mitochondrial-associated components and especially manipulation of the mitochondrial membrane integrity and respiratory chain function is associated with major mitochondrial dysfunctions and furthermore, increased production of ROS. As key source of ROS production, mitochondria account as central regulatory compartment in order to maintain the overall cellular homeostasis. In addition, manipulations of the oxidative status have emerged with pleiotropic effects on key pro-inflammatory mediators of the host [187, 210]. Based on the previous knowledge, it is assumed that a genotype-dependent influence on the ROS system and the associated inflammatory processes through HBx prevails.

4.5.1. HBx genotypes influence the intracellular ROS level

To investigate the impact of HBx genotypes on the radical oxygen levels, the protein carbonylation of HBx, and control transfected cells were investigated by Oxyblot analysis (fig. 22).

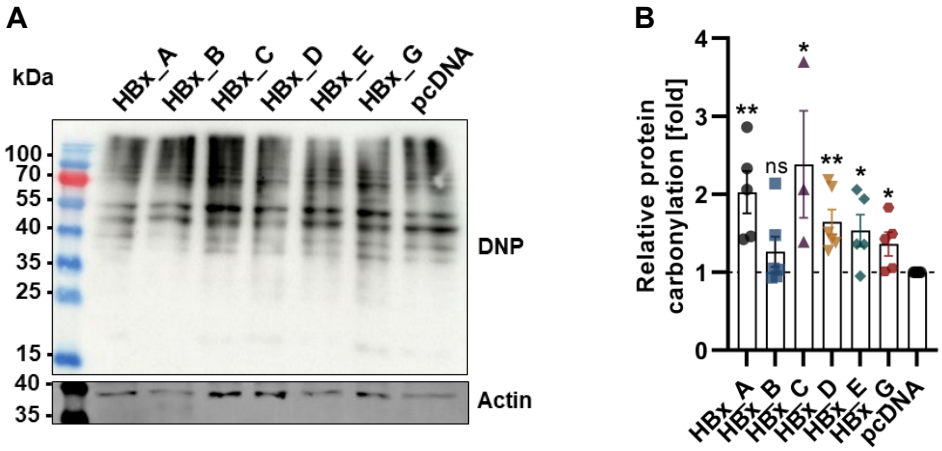

Figure 22: The intracellular ROS level is modulated depending on the genotype. (A) Representative Oxyblot of whole cell lysates from of either Gt A, B, C, D, E, G or empty plasmid DNA transfected Huh7 cells. Derivatized carbonyl groups in the proteins were identified by an anti-DNP antibody, β-Actin was used as internal loading control. **(B)** Relative change of DNP-derivate signal intensities in (A), values referred to pcDNA control. Statistic based on N>3 independent experiments, indicated as mean ± SEM and unpaired t-test related to pcDNA sample with * $p < 0.05$, ** $p < 0.01$.

The expression of HBx leads to and induction in the total amount of cellular ROS level (fig. 22A). In particular, most significant changes in the oxidative status were investigated in these genotypes, which were observed in the aforementioned data with an elevated impact in the mitochondrial structure and function. Notably, the most pronounced effect was determined for HBx Gt A and C (fig. 22B).

4.5.2. HBx-induced ROS levels trigger cytoprotective gene-expression and inflammatory processes

In order to examine the effects on various ROS-related cellular response mechanisms in more detail, the impact on AP-1 or NF-κB-dependent gene expression was examined using Luciferase assay of AP-1 and NF-κB promotor activity. In addition, a possible ROS-induced effect on the host immune system was determined using RT-qPCR. In light of this, NLRP3, IL6 and ATF6 were used as examples for central mitochondria-associated immune modulators (fig. 23).

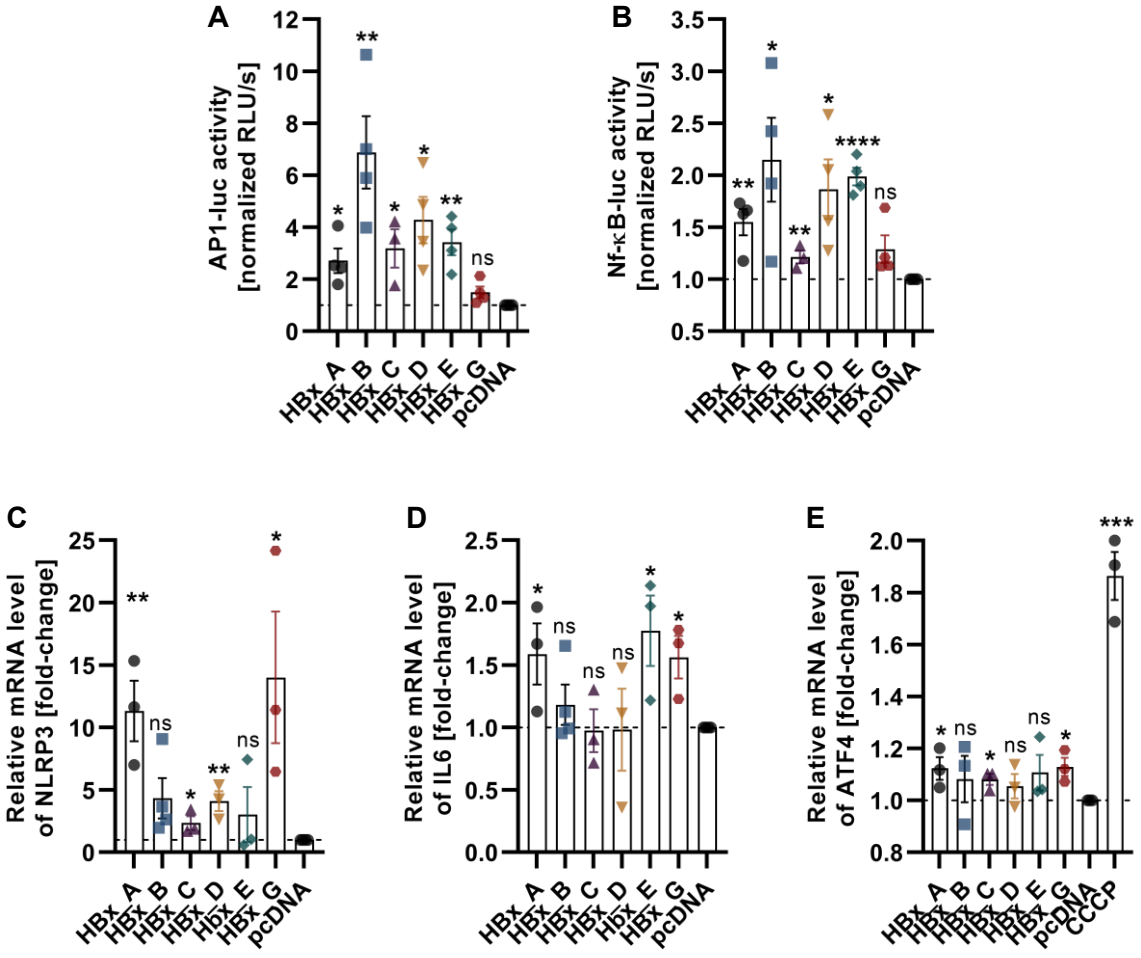

Figure 23: Induction of AP-1 or NF-κB-dependent gene-expression and inflammatory response varies among the genetic variants of HBx. (A-B) Relative change in AP-1 or NF-κB promoter driven luciferase activity of HBx transfected cells. Data are indicated as normalized RLU/s of luciferase activity compared to control sample. **(C-E)** Relative change in intracellular NLRP3, IL6 or ATF4 mRNA levels of HBx transfected cells assessed by RT-qPCR. Data are indicated as fold-change referred to pcDNA transfection control. Statistic based on N>3 independent experiments, indicated as mean ± SEM, unpaired t-test with * $p < 0.05$, ** $p < 0.01$, **** $p < 0.0001$.

Interstingly, the highest induction of AP-1 and NF-κB was observed in HBx-GtB and D, the genotypes with previously moderate influence in the mitochondrial dynamic. In contrast, Gt A and G indicated only moderate effects (fig. 23A-B). Furthermore, NLRP3 a key inflammatroy regulator after mitochondrial destabilisation [209], was found to be profound activated in the

HBx Gt A, C and G, while the latter later two show strikingly strong effects (fig. 23C). Mitochondrial cytokine induction represented by IL6, significantly increased in genotypes A, E and G, but not in gtB, C and D (fig. 23D). The activating transcribtion factor 4 (ATF4) is a transcription factor and a key regulator in the mitochondrial stress response [230]. Accordingly ATF4 mRNA levels are elevated compared to the control for HBx Gt A, C and G (fig. 23E).

Taken together, these results indicate that HBx-induced and in particular, genotype-dependent mitochondrial dysfunction has a causal relationship with the induction of mitochondrial oxidative stress and moreover, pro-inflammatory induction.

4.6. Genetic variants of HBx highly influence the removal of dysfunctional mitochondria by mitophagy

Rapid turnover of damaged mitochondria is an essential mechanism for cells to maintain cellular homeostasis and control cell survival. The process of removing non-functional mitochondrial structures is a selective form of autophagy, called mitophagy and involves several cellular components of the endo-lysosomal system. This process provides the terminal step in the mitochondrial life cycle, however deregulation in the process is believed to promote (liver-) disease progression [181, 231].

4.6.1. HBx induces mitophagy in a genotype-dependent manner

To address this question, we examined the impact of the genotype-dependent effect of HBx using an mtKeima-based mitophagy reporter assay. The reporter plasmid contains a mitochondrial localization site together with a pH-sensitive fluorophore and were co-transfected with eGFP-tagged HBx plasmid DNA of different genotypes. Engulfment of mitochondria into the acidic environment of lysosomes is represented by a shift in excitation spectra and was analyzed 72 h. p.t by live-cell CLSM (fig. 24).

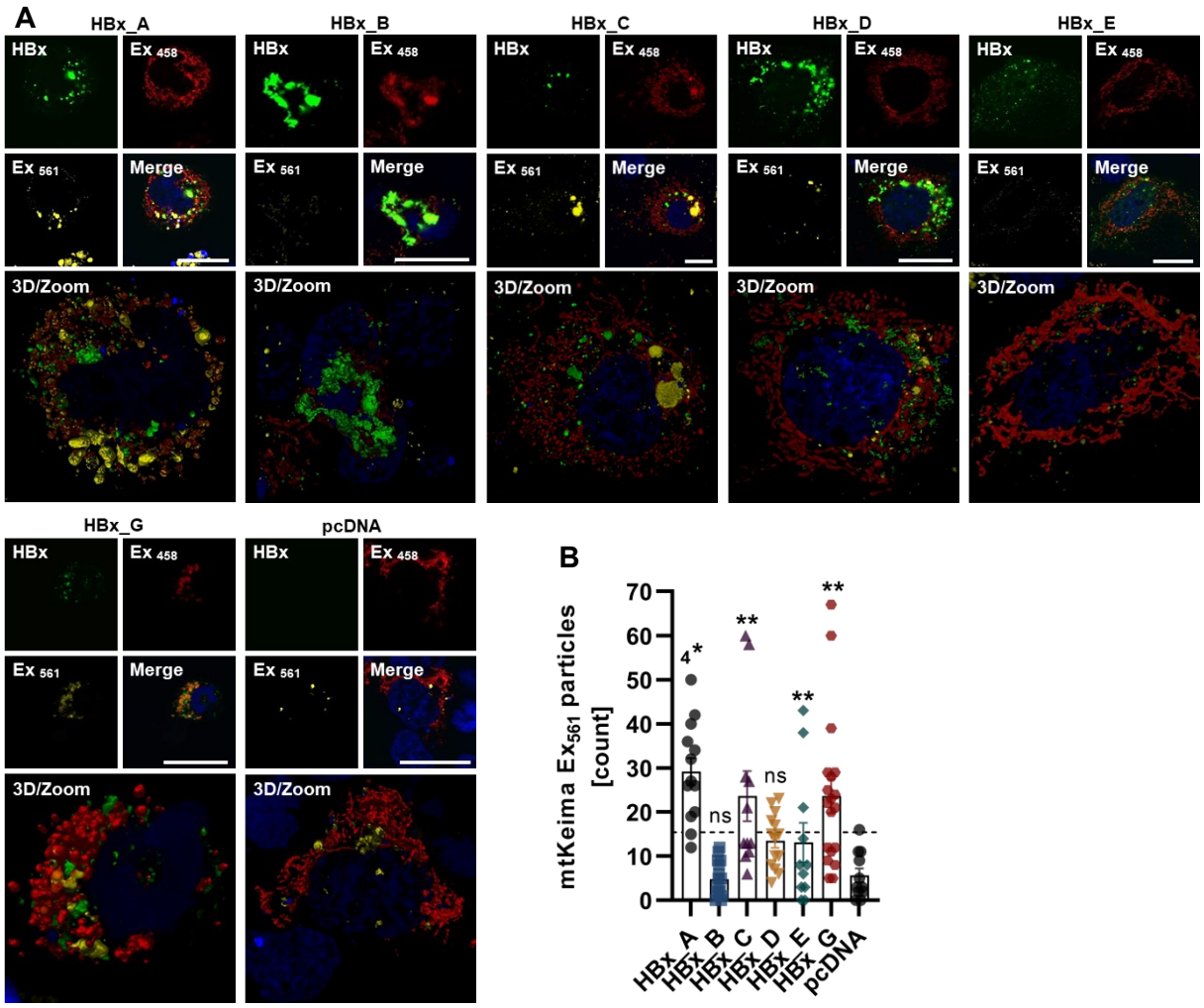

Figure 24: Mitophagy is mediated depending on the genetic variants of HBx. Huh7 cells were co-transfected with mtKeima-Red-Mito plasmid DNA (at pH ~7 red; at pH ~4 yellow) and eGFP-tagged HBx of different genotypes (green) and analyzed 72 h. p.t. by live cell imaging. Nuclei were counterstained with Hoechst 33342 immediately prior imaging. **(A)** Representative CLSM images. Dashed rectangles indicate the zoom section for 3D-high resolution images. Scale bar indicates 20 µm. **(B)** Quantification of the average number of acidic mitochondria particles per cell. For each condition between 11 and 19 cells were analyzed. Statistic is indicated as mean ± SEM with unpaired t-test related to pcDNA sample; ** $p < 0.01$, **** $p < 0.0001$.

Using the mitophagy specific assay, it was found that HBx causes a general induction of mitophagy (fig. 24A). However, based on the quantification of acidic mitochondria particles, there is no evidence of a significant influence through HBx Gt B and E. In contrast, the Gt A, C, D and G shown a clear shift of the mitochondrial balance towards mitophagy, evidenced by a dramatic shift in the mtKeima spectral features (fig. 24B).

4.6.2. Mitochondrial degradation is mediated by the host lysosomal system

To further confirm the engulfment of mitochondria in autophagosomal-vesicles, the interaction with host autophagy marker p62 or LC3 were examined by CLSM and Western blot analysis.

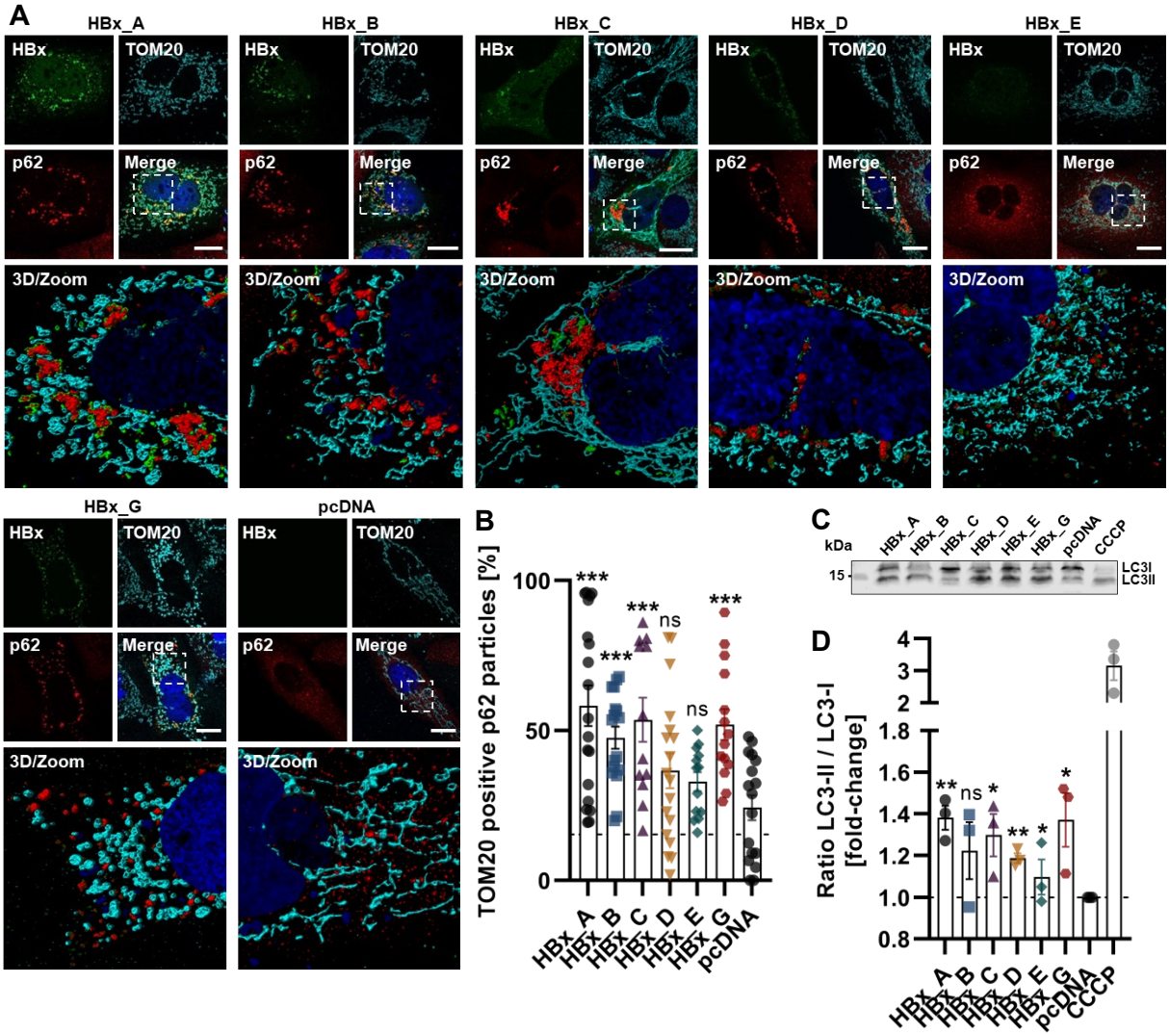

Figure 25: Genotype-specific, HBx-induced mitophagy is associated with host proteins of the endo-lysosomal system. (A) Representative CLSM images of HBx transfected Huh7 cells. Cells were fixed 72 h p.t. and immunostained for HBx via HA-specific antibody (green), p62 (red) and TOM20 (cyan), nuclei were counterstained with DAPI. Dashed rectangles indicate the zoom sections. Scale bar indicates 20 µm. **(B)** Quantification of the average number of TOM20 positive p62 particles per cell. More than 14 cells per condition were analyzed. **(C)** Representative Western blot of LC3 in total cell lysates. **(D)** Quantification of LC3II/LC3I ratio in (A) referred to pcDNA control. N=3 independent experiments. All data are indicated as mean ± SEM. Statistical analysis was performed by using unpaired t-test related to control cells. * $p < 0.05$; ** $p < 0.01$; *** $p<0.001$.

In accordance with previous observations, all genotypes demonstrated an increased amount of TOM20 containing p62 positive particles, however with of 50% Tom20 positive p62 particles compared to the control for the Gt A, C and G (fig. 25A) and was further coincide by the autophagic marker proteins LC3 (fig. 25B). The increase in the LC3I/II ratio validate the assumption of an elevated mitophagy and degradation of injured mitochondria through autophagosomal compartmentalization.

In summary, these data showed HBx-related, but importantly, genotype-dependent activation of mitophagy processes and moreover, inclusion in autophagosomal vesicles. A particularly prominent deregulation of these signaling pathways was examined for HBx Gt A, C and G.

4.7. HBx variants recruits the Pink1/Parkin signaling pathway to induce mitophagy

Upon loss of membrane potential and accumulation of fragmented and defective mitochondria, mitophagy is accounted as key mechanism for mitochondrial quality control, however is tightly regulated by post-translational modifications. One possible pathway to direct mitochondria towards lysosomal degradation is regulated by Pink1/Parkin. In this regard, defective mitochondria are ubiquitinated through a stepwise cascade and subsequently enable interaction with the host's lysosomal compartments. Furthermore, the PINK1/Parkin signaling pathway is the proposed pathway of HBx-mediated mitophagy [232], although the contribution based on the genetic variants of HBx remains unknown.

To improve the understanding of the mode of action of HBx-mediated PINK1/Parkin signaling, the different genetic variants of HBx were overexpressed in Huh7 cells, and the influence of the mitophagy-related contributors PINK1 and PARKIN were evaluated by Western blot analysis and RT- qPCR (fig. 26).

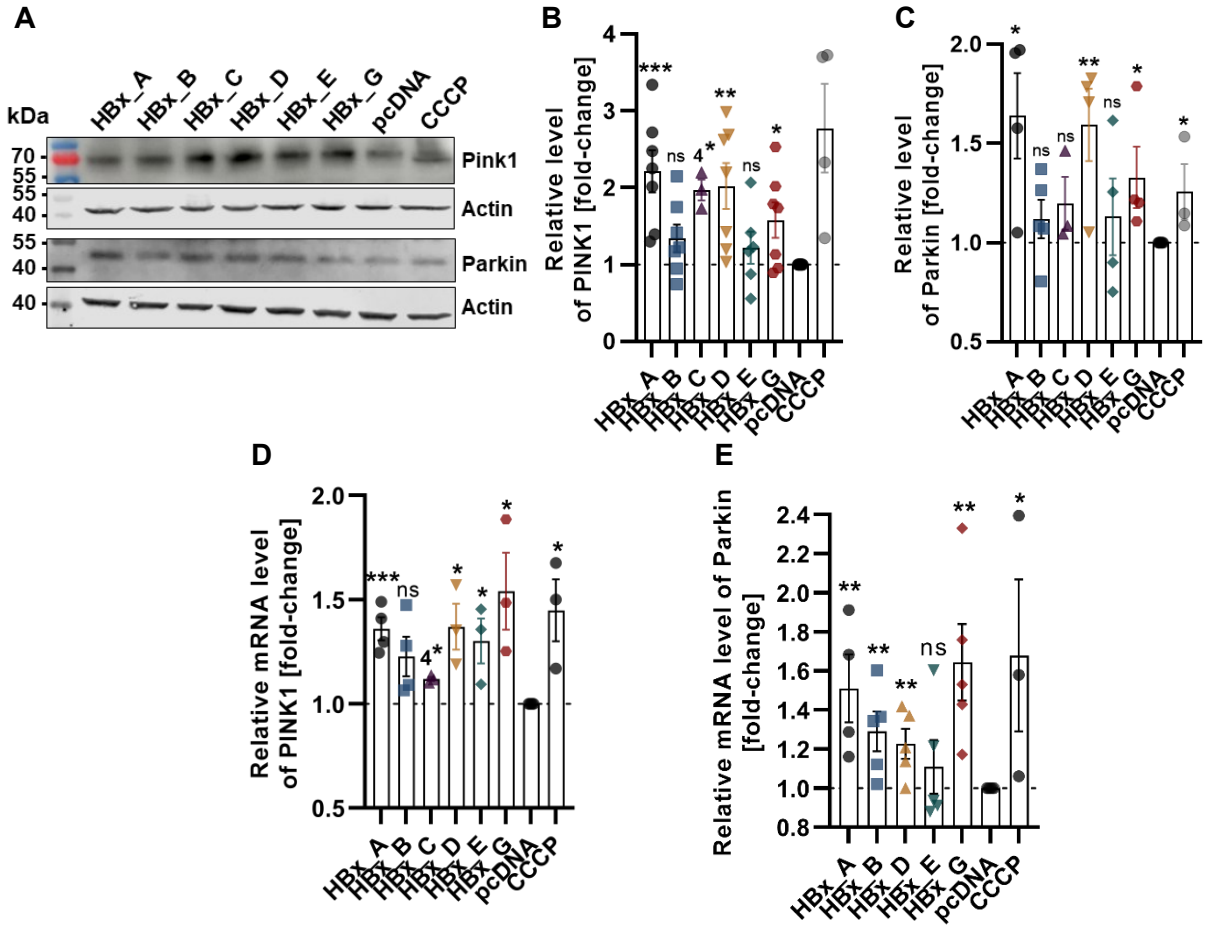

Figure 26: HBx leads to a genotype-dependent induction of intracellular Pink1 and Parkin levels. Huh7 cells were transiently transfected with HBx plasmid DNA (genotype A, B, C, D, E or G) or pcDNA (empty plasmid control) and harvested 72 h. p.t. **(A)** Representative Western blots of PINK1 and Parkin in total cell lysates. Actin was used as internal loading control. **(B-C)** Quantification of relative protein amounts in (A) referred to pcDNA control.

(D-E) Relative change in intracellular mRNA levels of PINK1 and Parkin assess by RT-qPCR analysis. Cells treated with Carbonyl cyanide m-chlorophenyl hydrazine (CCCP) were includes as positive control to induce mitochondrial damage. All data are indicated as mean ± SEM with unpaired t-test related to pcDNA sample with n ≥ 3. * p < 0.05; ** p < 0.01; *** p < 0.001.

Based on these results, HBx-dependent induction of PINK1 and Parkin can be observed at both transcriptional (fig. 26D-E) and translational levels. Focusing on the differences between the genotypes, only a moderate increase can be seen for HBx Gt B and E, particularly in the protein amounts of Pink1 and Parkin. In contrast, Gt A and G and, slightly behind, Gt C and D showed a strong upregulation of PINK1/Parkin. In this regard, an over 1.5-fold increase was detectable in the PINK1 and Parkin protein amount as compared to the control or HBx Gt B or D respectively (fig. 26A-C).

Since the detection of endogenous Parkin in cells was challenging due to the low basal expression level in Huh7 cells, genotype-dependent effects were further validated by using a reporter-tagged Parkin in an overexpressing system. Huh7 cells were therefore co-transfected with Parkin-YFP plasmid DNA, together with the HBx plasmid DNA of different genotypes and analyzed by CLSM (fig.27).

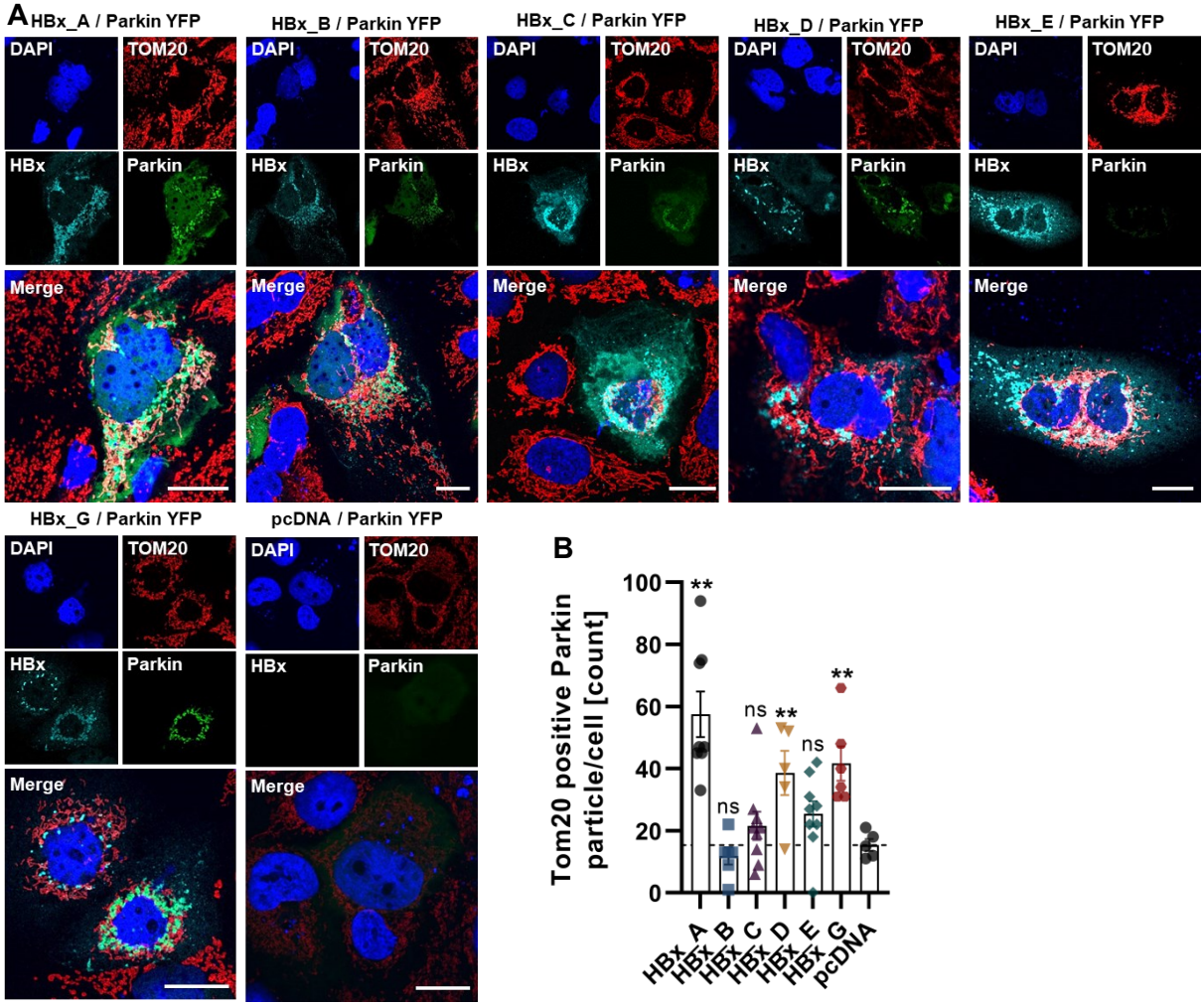

Figure 27: HBx lead to and genotype-dependent accumulation of Parkin. (A) Representative CLSM images of HBx and Parkin-YFP (green) co-transfected Huh7 cells. Cells were fixed 72 h p.t. and immunostained for HBx via HA-specific antibody (cyan) and TOM20 (red), nuclei were counterstained with DAPI. Scale bar indicates 20 µm. **(B)** Quantification of the average number of TOM20 positive parkin particles per cell. Between 5 and 10 cells per condition were analyzed and indicated as mean ± SEM. Statistical analysis was performed by using unpaired t-test related to control cells; ** $p < 0.01$.

The single-cell analysis revealed that the amount of Parkin is influenced by HBx, depending on the genetic variants of HBx. Notably, in this experiment, Parkin proteins were barely visible in the transfected control cells, reflecting a healthy mitochondrial phenotype. In contrast, together with HBx expression, a clear induction of YFP fluorescence signal intensity was observable and occurred together with an accumulation of Parkin at the outer mitochondrial membrane (fig. 27A). The quantification of Tom20 positive parkin particles confirms the observation and verify the previous results from Western blot and qPCR analysis with a clear effect for the Gt A, D and G (fig. 27B).

Taken together, these data reflect the relevance of the Pink1/Parkin pathway for HBx-mediated induction of mitophagy. However, major differences in the degree of PINK1/Parkin upregulation indicate a strong influence of the genetic variants of HBx and were especially observed for the Gt A, D and G.

5. Discussion

The influence of HBV genotypes has become more and more the focus of modern HBV research in recent decades. In particular, early detection and treatment are crucial for the course of the infection but are largely influenced by the heterogeneous behavior of the genotypes in terms of serological markers and treatment response [94, 233]. In addition to clinical factors, underlying molecular mechanisms and protein interactions, especially with host cell signaling pathways, are still largely unexplored. In particular, HBx have a decisive contribution to HBV-induced liver pathogenesis, but studies regarding the influence of genotypes are also scarce.

This study characterizes the intergenotypic differences of HBx in the context of host signaling pathways, with a particular focus on HBx-dependent effects on mitochondrial dynamics and function. In this regard, the construction of the mammalian expression vectors is based on the HBx protein sequence derived from genotyped wildtype HBV, and includes a C-terminal HA-tag. Hereby, the focus of this study was set on the HBx-sequence of the genotypes A, B, C, D, E and G. These genotypes represent the most common genotypes worldwide, but also in the European areas, and were accordingly selected for this study. Genotype G was included as an aberrant genotype, since it mainly occurs as co-infection and therefore has particular relevance. In addition, it must be considered that the genetic insertion of the artificial HA-tag can influence the protein synthesis and might also affect the solubility and structural properties. However, since no suitable antibody is available to recognize genotype-related sequence differences the viral HBx protein [229], this was accepted to ensure the detection of HBx in vitro. Additional experiments confirmed the expression of the HBx protein and the respective reporter tag, and also confirmed an equal localization compared to the reporter-free HBx.

The location and amount of the viral HBx protein synthesized in Huh7-transfected cells were found to reveal major differences between genotypes. Regarding cellular distribution, the majority of HBx was consistently localized in the cytoplasm for all genotypes. The time of fixation represents a late time point with an expected high expression level and is in accordance with previous studies that postulated a predominant cytoplasmic localization at high HBx levels [234]. Interestingly, however, a genotype-dependent distribution pattern can clearly be observed within the cytoplasm. One reason for this behavior could be a different solubility due to the sequence differences. This could also be explained by the only partial perinuclear aggregation of HBx in genotypes B, D and E, which occurs together with a

significantly higher variance in the quantification of HBx protein amount by Western blot analysis, possibly by the varying amount of soluble HBx protein in the independently conducted experiments. In this regard, a comparison of the three-dimensional structure of the genetic variants of HBx could provide further insights, but a complete structural model of HBx has not yet been established [229, 235].

A pathway enrichment analysis of genotype A indicated profound levels of deregulated kinase pathways due HBx and indicated a functional contribution to several host protein interactions. In particular, besides the regulation of central signaling pathways such as MAPK or Ras/Raf were altered by HBx Gt A, a remarkable number of upregulated kinases, associated with mitochondrial function and oxidative-stress pathways were identified to be upregulated. In order to follow this finding, a comparative analysis among the genetic variants of HBx was investigated and focused in particular on the impact on mitochondrial-associated kinases. Interestingly, several mitochondrial-specific kinases indicate distinct activation profiles among the HBx-genotypes. Notably, Scr family kinases (SFKs), which have an emerging role in modulating mitochondrial integrity, including respiratory function and mtROS-mediated induction of NF-κB [196, 236, 237], were differentially deregulated depending on the respective HBx genotype. Similar results were also obtained for other mitochondria-related kinases such as AKT, ErBB2 and JNK and therefore suggest, that the genetic variants of HBx have significantly different impact on mitochondrial-associated signal pathways and mechanisms in response to mitochondrial-related oxidative stress.

In fact, mitochondria represents a sophisticated dynamic in their morphology, further correlating with the function and overall cellular homeostasis [194]. Therefore, hijacking mitochondrial-associated proteins and altering the mitochondrial function is a common strategy of a variety of virus types [215, 238, 239]. By manipulating the “housekeeping” function of the cell and influencing the innate immune response, the virus promotes its own replication and evasion of the host's antiviral defense systems. Indeed, based on previous studies there is evidence that HBV, particular the HBx protein contributes to a profound mitochondrial turnover and damage accompanied by major consequences for the progression of hepatocarcinogeneses. An initial step in this process is given by the damage of the mitochondrial architecture up to complete fragmentation, followed by a cascade of further reactions and the emergence of a pathogenic cell-phenotype [203, 240, 241].

Investigation on the mitochondrial network reveals major differences in the mitochondrial network integrity between HBx expressing cells and the respective control sample, indicated by a decline in the mitochondrial footprint among all of the tested genotypes of HBx. In particular, the control sample represents a healthy phenotype of mitochondrial structure and overall cellular physiology, represented by large elongated and branched tubular structures. Apart from this, depending on the genotype, the mitochondrial dynamic is shifted with a certain degree towards fission. This is evident by moderate damage in genotype B and E, indicated by a slight decrease in the number of connected structures and branches, together with similar amounts of mitochondrial proteins compared to the control. Apart from this, tremendous changes in the mitochondrial network into small, round fragments and a clear reduction in the mitochondrial protein amount were observed for the genotypes A and G and suggest a major genotype-related impact on the mitochondrial structure. Overall, the midzonal division that occurred in the former genotypes (Gt B and E) could lead to mitochondrial proliferation and might also explain the slight increase in the amount of mitochondrial proteins in Gt B. In contrast, fragmentation beginning at the periphery of the tubular structures and observed in Gt A, C, D and G provides an indicator for dysfunctional mitochondria and enables rapid degradation. Similar results were also obtained in the HepG2 cell line, which represents another valuable cell culture system for HBx studies and indicates therefore a cell line independent effect by different HBx genotypes.

Additionally, based on this, it could be assumed, that the decline in the mitochondrial mass in these genotypes is due to an elevated removal process in response to nonfunctional mitochondria, particularly since the levels of TOM20 transcripts remain unchanged among all HBx genotypes. Loss of the mitochondrial membrane potential is accompanied with a severe impact in the mitochondrial physiology and with impact in the overall cellular function. Depolarized mitochondria are therefore a direct evidence for mitochondrial dysfunction and is mainly caused by a leak in the transition pores located at the outer mitochondrial membrane. In previous studies a direct interaction of HBx with the VDAC3 was described together with major impact in the mitochondrial function and elevated ROS levels [206]. In accordance to this, we could observe a clear co-localization between HBx and the VDAC3 in vitro, but importantly with clear differences between the genetic variants of HBx. In light of this only a moderate co-localization was detected for HBx Gt B and E together with a slight reduction in the mitochondrial membrane potential as compared to the control. In contrast, high levels of HBx-VDAC3 co-localization was observed mainly for the genotypes A and G but also for Gt C and D, accompanied with an elevated loss of the mitochondrial membrane potential and elevated cellular Ros levels.

In this regard, the cytochrome c oxidase provides a central part in the respiratory electron transport chain and is therefore essential for the maintenance of the mitochondrial membrane protentional and metabolic processes of the cell [242–244]. The activity of the cytochrome c oxidase represents thereby a further indicator for mitochondrial function and was based on this study generally reduced in presence of the HBx-protein. A significant decline was in particular observed for HBx of the genotypes C, D and G, but also in Gt B. Unfortunately, high standard deviations within the assay hamper a detailed, genotype-related investigation, despite the overall trend still corresponds with aforementioned observations (fig. 18).

Overall, these data first time evidence a genotype-dependent relation between HBx and mitochondria-dependent processes. Furthermore, tremendous alterations in the mitochondrial network in case of Gt A and G (partly Gt C and D) were directly correlated in response to profound HBx-mediated mitochondrial dysfunction. Apart from this HBx Gt B and E have apparently only minor impact in this context.

Manipulation of the overall redox metabolism as well as mitochondrial integrity is a common strategy of viruses to support their replication and escape from the immune system. In addition, these processes are associated with an elevated production and release of ROS into the cytoplasm. In fact, mitochondria are the main source of oxidative stress in cells, and on the one hand act as second messenger for a variety of signaling pathways, on the other hand when cellular ROS level are increased, they provide a feedback loop signal and enhance mitochondrial dysfunction. Therefore, a rapid detoxifying system is needed in order to prevent elevated cell damage and maintain cell survival [147, 189, 245].

In accordance to previous observations, the HBx-mediated induction in cellular ROS level is highly dependent on the genotype. According to a major impact in mitochondrial integrity and function, HBx Gt A, C and G (also slightly D) reveal a significant increase in the intracellular ROS level, which is further accompanied with an elevated expression of the NLRP3 inflammasome. The NLRP3 inflammasome is an important regulatory platform for mitochondrial related inflammatory processes and is mainly activated in case of mitochondrial instability and dysfunction [210]. In combination with the given increase in IL6, which was chosen as representative of pro-inflammatory mediators it could be speculated of an overall major inflammatory response process by these genotypes. Besides this, as the mitochondrial structure and function was only moderately affected in case of HBx Gt B and E, similar contributions were also suspected for the cellular ROS levels and related pathways. Interestingly, the data confirm this hypothesis only for Gt B but not for Gt E, which indicate noticeable higher amounts of intracellular ROS together with increased NLRP3 and IL6 expression levels. This discrepancy might be explained by the interplay of a numerous of

intracellular ROS mediated pathways. In this regard the mitochondrial-related and HBx-mediated ROS formation counteract with the modulation of ROS-detoxifying pathways as represented by the Nrf2/ARE-related activation of cytoprotective genes [101]. In addition, it has to be considered, that the analysis of intracellular oxidative radicals by using an oxyblot-detection assay reflects cumulative effects and might hamper to reflect the current ROS-level in the cell. Therefore, further studies in this context may be necessary to gain a more detailed understanding of the underlying mechanisms. Nonetheless, chronic hepatitis is often associated with and elevated damage of hepatocytes and is believed to be immune-mediated [246]. Therefore, an elevated immune-modulation as evident by NLRP3 and IL6 expression especially in genotype A and G might contribute the chronification of an HBV infection.

Elevated ROS levels, but also dysfunctional mitochondria itself trigger a organelle selective autophagy process called mitophagy [197]. Despite the elimination of non-functional mitochondria being an essential process for maintaining mitochondrial as well as cellular homeostasis and cell viability, several DNA and RNA viruses are generally believed to induce mitophagy and thus promote viral replication and proliferation [247, 248]. Although the contribution to HBV-related autophagy processes has long been controversial, it is known that the HBx-protein is involved in increased mitophagy and thus sustains infection persistence and hepatocyte survival by preventing cell death due to toxic levels by mtROS production [205].

In this process the transcription factor ATF4 is a key regulator in mitochondrial stress response. In response to elevated mitochondrial stress, ATF coordinate the expression of cytoprotective genes and initiate the reduction of mitochondrial activity and reprogram the cellular metabolism towards organelle repair and degradation mechanisms [230, 249]. Interestingly, in this study, ATF4 is activated on transcriptional levels for Gt A, C and G, in which also an elevated ROS level and induction of mitophagy and reduction in the mitochondrial mass was observable. This observations accounts therefore for a clear genotype-related degradation of mitochondria and is in addition supported by major functional alterations by these genotypes as evident by a major depolarization and mtROS production, which are the main targets for mitophagy.

The formation of mitophagosomes indicates in addition, the compartmentalization of dysfunctional mitochondria into the lysosomal system and correlates with an HBx-mediated mitophagy in a genotype-dependent manner, since these effects were only moderately regulated in the HBx-genotypes B and E. Accordingly, in these genotypes only a slight increase in the PINK1/Parkin protein levels were investigated, compared to the control. The PINK1/Parkin pathway is one possible route to induce mitophagy (also activated by ATF4) and remains therefore mainly unaffected since HBx Gt B and E revealed only moderate amounts of fragmented mitochondria and mitochondrial injury. In contrast, elevated mitophagy as

indicated by mainly Gt A and G, but also C and D is accompanied with major increase in the PINK1/Parkin protein as well as mRNA transcripts. This account the PINK1/Parkin pathways as the suggested route for HBx, genotype-dependent regulation of mitophagy. Furthermore, the increase in mitophagy-mediated genes suggested a feedback loop-signaling in response to a high need of mitochondrial deration due to major alterations in the mitochondrial dynamics.

By comparing the HBx-mediated but genotype-related impact on the mitochondrial dynamics and subsequent initiation of a sequential cascade of mitochondrial events along with the initial characterization of the cellular HBx-distribution, the perinuclear accumulation of HBx could be accounted as trigger for mitochondrial dysfunction. Importantly, since the overall impact on mitochondrial-associated pathways do not correlate with the different protein levels of the distinct HBx-genotypes, it is assumed, that the effect of HBx is caused by an intrinsic property, rather than an artifact related to the selected model-system and HBx-overexpression.

In summary this study provides unique insight into genotype-related contribution in host cellular signaling pathways and especially highlights fundamental impact into mitochondrial morphology and function. Especially, the HBx-protein related to genotype A and G, followed up by genotype C and D, heavily disrupts the overall mitochondrial network structure, accompanied with and clear impact in mitochondrial integrity, ROS production and related inflammatory response. On the other side, HBx Gt B and E cause only moderate impact and maintain most likely the mitochondrial and cellular physiology.

In the broader context, although HBV is considered a non-cytopathic virus, HBx-induced mitochondrial damage and serious impact in mitochondrial oxidative stress is known to promote the persistence of viral infection and contribute to the onset of liver pathogenesis. The findings of this study could therefore provide a hint of a genotype-dependent influence on chronification and the overall clinical course during HBV infection. Although the data do not allow a complete correlation between the altered mitochondrial dynamic of the respective HBx-genotypes and clinical data, it reflects the HBx-associated pathogenesis and the sophisticated impact in multifactorial processes of host factors. Additional factors, e.g. strong differences in the geographical distribution of HBV genotypes and thus in lifestyle and diet, could represent relevant variables for the course of chronic infections. It must also be considered that accumulating or synergistic effects of other viral proteins (e.g. preS2 activator) could also influence the overall mitochondrial system; but also, that the solubility behavior of HBx under physiological conditions and in the natural course of an HBV infection still is unknown. In this regard, infection experiments and the contribution of the other viral proteins might broaden the overall understanding of HBx-mediated mitochondrial-associated signaling pathways but

remain challenging due to several technical limitations in experimental implementation. Especially histopathological characterization of mitochondrial structures among the genetic variants of HBV might be valuable for clinical implications and genotype-related impact.

In addition, previous studies have demonstrated the release of mtDNA as a result of HBx-induced mitochondrial dysfunction in the blood serum of patients and speculated a connection with HCC progression [250]. Therefore, it would also be conceivable in the future, to investigate the release of mitochondrial metabolites such as mtDNA or cytochrome c as a result of the genotype-dependent alteration in the membrane permeability. Subsequently, circulation of mtDNA could therefore be used as an additional biological marker to determine oncogenicity in connection with HBV genotypes.

Returning to the main objective of this study, the data present in this work demonstrate significant intergenotypic differences in HBx-affected host signaling pathways and in particular in HBx-induced mitochondrial network fragmentation and function. The results are of particular importance as they demonstrate the profound contribution of HBV genotypes to host signaling pathways and highlight the role in HBx-induced liver pathogenesis.

With respect to the worldwide morbidity and mortality of HBV and without a complete cure and poor treatment options, sufficient knowledge of the distinct behavior of HBV genotypes is important in monitoring and diagnosing infections, but also highlights the need for either pan-genotypic or customized antiviral therapy options.

6. Summary

The hepatitis B virus is one of the most common causes of virus-related chronic liver disease and remains a major global health problem affecting 296 million people worldwide. Despite an available and highly effective vaccination, hepatitis B infections lead to an annual mortality rate of approximately 0.8 million people. The global prevalence is heterogeneously distributed and reflects a high infections and chronicity, particularly in low-income countries, due to a lack of vaccination strategies, underdiagnosis and low treatment rates. A complete cure remains undiscovered to this day. Based on their genetic makeup, the virus is categorized into nine genotypes with a genetic difference of more than 8% within the sequence. In addition to their geographical distribution, hepatitis B virus genotypes also differ in terms of their clinical outcome, pathogenesis and treatment response.

The viral protein HBx is known to interact with several cellular signaling pathways and is thereby accounted as the driving force in the development of hepatitis B virus-associated pathogenesis and progression of hepatocellular carcinoma. In particular, HBx interacts with mitochondria and induces profound alterations in the mitochondrial morphology and function with a severe impact on the liver's physiology and with an emerging role in liver-related disease progression.

This study aims to investigate the genotype-related impact of HBx with regard to their interaction with cellular signaling pathways. A particular focus was placed on mitochondria-dependent interactions and signaling pathways in order to broaden the understanding of the genetic diversity of the genotypes.

Differences between genotypes of HBx were examined and compared through in vitro experiments based on a cell culture-based system. Plasmid DNA encoding the HBx protein of the different genotypes was transiently transfected into Huh7 or HepG2 cells and examined for molecular and protein-biochemical effects on the host cell, usually 72 hours after transfection. This study focused on the most common genotypes A, B, C, D, E and G worldwide.

Based on initial kinome profiling analyses, it was found that HBx differs greatly within their genetic variants and suggests different effects on overall cell function and in particular on mitochondrial kinases. Furthermore, confocal laser scanning microscopy reveals profound HBx-mediated changes in the mitochondrial network structure, however with major differences among the different genotypes. In particular, HBx of genotypes A and G causes enormous fragmentation of mitochondrial structures, accompanied by emergent changes in mitochondrial function. Due to an increased interaction with the voltage-dependent anion channel 3, a

significant loss of mitochondrial membrane potential was also observed, together with an increased radial oxygen stress level and an induction of central mitochondria-dependent inflammatory mediators. In contrast, the contribution of HBx-genotype B and E reveals only moderate effects in these regards. Using a pH-sensitive reporter system, HBx genotypes which previously indicated a strong distribution in the mitochondrial morphology and function, also showed an elevated mitophagy through the PINK1/Parkin-mediated pathway.

This study provides direct evidence that HBx-mediated changes in host cell signaling pathways, especially in mitochondrial-associated pathways, fundamentally dependent on the different genotypes. In addition, the results also indicate an important role of HBx in the process of genotype-dependent liver pathogenesis and provide insight into the underlying cellular mechanisms and signaling pathways.

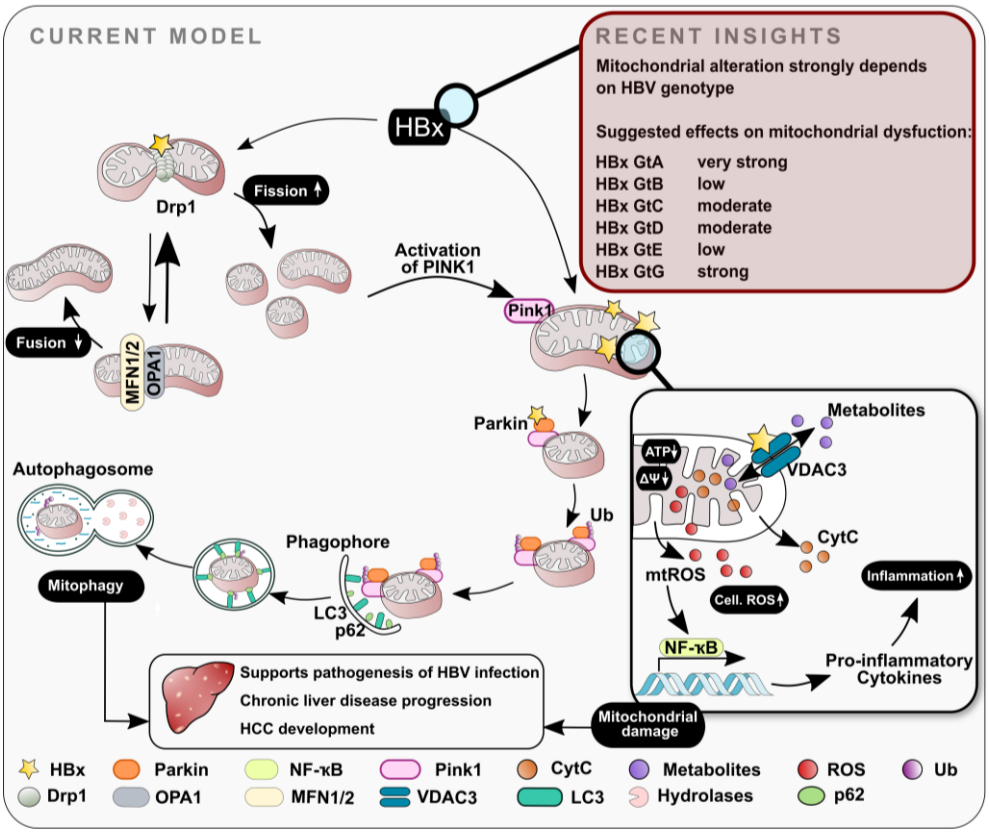

Figure 28: Schematic representation of the genotype-dependent impact on HBx-mediated changes in mitochondria morphology and function, discovered in this study. HBx of genotype A and G significantly shifts mitochondrial dynamic toward increased fission, which is accompanied with an elevated mitochondrial damage and dysfunction through the release of radical oxygen stress species and induction of inflammatory processes. Furthermore, prolonged mitophagy contributes to the progression of chronic liver disease. In contrast, HBx of genotype B and E indicated only low, genotype C and D have moderate impact in mitochondrial integrity and function.

7. Zusammenfassung

Das Hepatitis B Virus ist zusammen mit dem Hepatitis C Virus, die häufigste Ursache für eine virus-induzierte, chronische Lebererkrankung. Dabei geht die Weltgesundheitsorganisation davon aus, dass aktuell ca. 296 Millionen Menschen chronisch an Hepatitis B erkrankt sind und trotz einer verfügbaren und hoch wirksamen Impfung zu einer jährlichen Mortalitätsrate von ca. 0,8 Millionen Menschen führt. Hierbei ist die weltweite Prävalenz heterogen verteilt und reflektiert insbesondere in Entwicklungsländern durch fehlende Impfstrategien, unzureichenden Diagnosen und geringen Behandlungsraten eine hohe Infektions-, und Chronifizierungsrate. Insgesamt spielen aber auch sozioökonomische Parameter eine entscheidende Rolle für die viral Endemizität.

Eine Übertragung des Viruses erfolgt primär durch kontaminiertes Blut oder Blutprodukte, kann jedoch auch durch andere Körperflüssigkeiten übertragen werden. Insbesondere ist eine perinatale Übertragung gravierend, da das Übertragungsrisiko bei der Geburt auf das Neugeborene bei bis zu 90% liegt und eine ebenso hohe Rate der Chronifizierung während der ersten Lebensjahre besteht.
Hepatitis B Viren haben einen strikten Gewebetropismus und replizieren somit nahezu ausschließlich in Leberzellen. Der klinische Verlauf beginnt mit einer akuten Phase, die meist asymptomatisch und somit nur über serologische Marker nachzuweisen ist. Möglich sind auch unspezifische Symptome einer ikterischen Hepatitis und innerhalb von 6 Monaten selbstständig ausheilt. In seltenen Fällen jedoch kann es durch eine verstärkte Immunantwort zu einer gravierenden Schädigung der Hepatozyten kommen und eine fulminante Hepatitis mit schlussendlichem Leberversagen induzieren. Persistiert die Infektion mehr als 6 Monate, liegt eine chronische Erkrankung vor. Dies ist charakterisiert durch verschiedene Infektionsstadien und impliziert unterschiedliche Level der serologischen Marker. Neben einem nahezu symptomfreien Verlauf, kann es infolge der chronischen Infektion zur Entstehung von Fibrosen Leberzirrhose, und hepatozellulären Karzinom kommen. Aufgrund der Persistenz des viralen Genoms in der Wirtszelle und einer bis heute nicht vorhandenen Heilungsmöglichkeit sind eine medikamentöse Eindämmung der Symptome und Reduzierung der Viruslast die einzigen Behandlungsmöglichkeiten.

Das Hepatitis B Virus ist ein kleines umhülltes DNA-Virus, zugehörig zur Familie der Hepadnaviridae. Charakteristisch ist dabei das Virusgenom, dass aus einer zirkulären, partiell doppelsträngigen DNA besteht und mithilfe eines RNA-Intermediates repliziert wird. Das Genom enthält vier offene Leseraster, codierend für sieben virale Proteine und klassifiziert

sich anhand eine Sequenz-differenz von mehr als 8% in neun verschiedene Genotypen. Hierbei ist in den letzten Jahrzehnten Forschunge, nicht nur die geographische Heterogenität der Genotypen, sondern insbesondere gravierende Unterschiede im klinischen Verlauf, Therapiemöglichkeiten und Kanzerogenität präsent geworden. Die molekularen Zusammenhänge der Genotypen mit der Wirtszelle sind jedoch nach wie vor größtenteils unbekannt.

Das infektiöse Virion ist ein sphärischeres Partikel mit 42 nm im Durchmesser und besteht aus Kapsid-proteinen, die einen Ikosaeder-förmige Kernhülle um das virale Genom bilden. Die Oberflächenproteine LHBs, MHBs und SHBs sind eingebettet in einer Doppellipidmembran und umschließen das Kapsid. Der Anteil der Oberflächenproteine variiert dabei zwischen Virionen und sogenannten subviralen Partikeln, die im hohen Überschuss produziert werden, jedoch nicht infektiös sind und vermutlich eine neutralisierende Wirkung auf das Immunsystem haben. Neben den Strukturproteinen werden weitere virale Proteine synthetisiert: Die Polymerase ist essentiell für die Replikation des Viruses und ist zusammen mit der viralen DNA im Kern verpackt. Das HBeAg ist ein Spleiß-Produkt des Core-Leserasters und wird nach Synthese aus der Zelle sezerniert. Eine wichtige Rolle übernimmt schlussendlich das HBx-Protein.

Das HBx-Protein ist ein multifunktionales Protein mit einer Vielzahl an zellulären Interaktionspartnern und ist somit treibende Kraft für die Hepatitis B initiierte Tumorprogression. Das Protein umfasst 145 Aminosäuren, verbleibt jedoch bis heute ohne klare Strukturdarstellung. Dabei sind insbesondere die geringe Löslichkeit und das flexible Verhalten, sowie ein geringes Vorkommen während des natürlichen Infektionsverlaufs ausschlaggebend für die fehlenden strukturellen Informationen. Dies bedingt aber auch, dass die genaue Funktion des Proteins bis heute noch nicht vollständig verstanden ist. Dennoch sind verschiedene funktionale und regulatorische Domänen innerhalb von HBx bekannt, die mit viralen aber insbesondere auch zelluläre Promotoren interagieren und eine transaktivierende Wirkung, ohne direkte DNA-Bindung verursachen. Je nach Lokalisation von HBx, die je nach Abundanz entweder nuklear oder zytoplasmatisch vorliegt, werden dadurch eine Vielzahl an zellulären Signalwegen moduliert und haben dadurch immense Auswirkungen auf den Zell-Zyklus, Apoptose, Calcium-abhängige Signalwege, Zell-Progression und Weitere. Folgend kommt es zu einer Veränderung der gesamten Zell-Homöostasis und Proliferation, Induktion von Inflammationswegen, genomischer Instabilität und final zur Initiation von Metastasen und Tumorgenese. Aufgrund der pleiotropen Regulierung von unterschiedlichsten hepatozellulären Karzinom Merkmalen wird das HBx-Protein auch als vielversprechendes Ziel für therapeutische Strategien, insbesondere zur Intervention der Tumorentstehung, angesehen.

In diesem Zusammenhang ist zudem auch die Interaktion von HBx mit mitochondrien-assoziierten Proteinen und Signalwegen von zentraler Bedeutung. Mitochondrien haben insbesondere durch die Generierung von Adenosintriphosphat über die Atmungskette eine zentrale Funktion für die Zelle. Darüber hinaus spielen Mitochondrien aber auch eine wichtige Rolle bei der Apoptose, der Immunantwort und als Calcium Speicher. Ebenso sind sie die größte Quelle an oxidativen Radikalen als Nebenprodukt der Atmungskette. Mitochondrien sind hoch dynamische Organellen, die ihre Form der jeweiligen Funktion und äußeren Einflüssen anpassen. Je nach Situation liegen die Organellen entweder separat oder verschmolzen, als einziges Netzwerk aus tubulären und verzweigten Strukturen vor. Eine Fragmentierung und anschließendem selektivem Abbau im Lysosomalen System (Mitophagie) dient einerseits dem Abbau von nichtfunktionalen Mitochondrien und andererseits dem Überleben der Zelle und Schutz vor oxidativem Stress und Fehlfunktionen innerhalb der Zelle.

Die Interaktion des viralen HBx-Proteins mit mitochondrien-assoziierten Proteinen ist dabei mit einer Deregulation verschiedenster mitochondrialer Funktionen begleitet und hat darüber hinaus enormen Einfluss auf die Induktion von Leberschädigungen und insbesondere Auswirkungen auf die Regulation der angeborenen Immunantwort. Bisherige Studien konnten in diesem Zusammenhang, einerseits einen HBx-induzierten Einfluss auf die Morphologie und Dynamik der mitochondrialen Struktur beobachten. Andererseits wurde eine durch HBx bedingte Änderung des Membranpotenzials und damit verbundenen verstärkten Freisetzung von mitochondrialem, oxidativem Stress und Induktion der Mitophagie beobachtet. Die exzessive Änderung mitochondrialer Dynamik und Funktion steht dabei auch im direkten Zusammenhand mit der Leberpathophysiologie und Entwicklung folgeschwerer Leberschädigungen. Obwohl die Zusammenhänge zwischen HBx und Mitochondrien bereits bekannt sind, ist der Beitrag der genetischen Varianten (Genotypen) von HBx bisher nicht bekannt.

Das Ziel dieser Arbeit war es, den Beitrag von HBx basierend auf den unterschiedlichen Varianten der Genotypen hinsichtlich ihrer Interaktion mit zellulären Signalwegen zu untersuchen. Ein besonderer Fokus wurde dabei auf die mitochondrien-abhängigen Interaktionen gelegt. Unterschiede zwischen den Genotypen von HBx wurden durch *in vitro* Experimente untersucht und miteinander verglichen. Hierbei wurden Huh7, eine humane Leberzelllinie als Modellsystem gewählt. Mittels transienter Transfektion wurde Plasmid-DNA, codierend für das HBx-Protein der unterschiedlichen Genotypen, temporär in die Zelle eingebracht und in der Regel 72 Stunden nach Transfektion hinsichtlich molekularer und Protein-biochemischer Auswirkungen auf die Wirtszelle untersucht. Diese Studie fokussiert dabei auf die weltweit häufigsten Genotypen A, B, C, D, E und G.

Initial konnte anhand von vergleichenden Kinomprofilen der verschiedenen Varianten von HBx bereits deutlichen Unterschiede in der Aktivierung bestimmter Kinasen beobachtet werden. Basierend auf einer bioinformatischen Analyse signifikant aktivierter Signalwege des HBx Genotyp A konnte eine deutliche Aktivierung mitochondrialer und mitochondrien-assoziierten Signalwege beobachtet werden. Im weiteren Verlauf zeigte ein Vergleich der anderen Genotypen, mit spezifischem Fokus auf Kinasen die mit mitochondrialer Funktion assoziiert sind, eine heterogene Aktivierung. Somit wurde anhand der Kinomprofile vermutet, dass sich je nach Genotyp die HBx-abhängige Wirkung auf Mitochondrien stark unterscheidet. Um diese Effekte weiter zu untersuchen wurde im Folgenden die Morphologie und Funktion der Mitochondrien in Abhängigkeit der verschiedenen HBx Genotypen genauer untersucht.

Insbesondere wurde die Struktur der Mitochondrien nach Expression der genetischen Varianten von HBx mittels Konfokaler Laser Scanning Mikroskopie zusammen mit einem dreidimensionalen, computerbasierten Superauflösungsmodul (Lightning) untersucht und mit einer Kontrollgruppe aus HBx-negativen Zellen verglichen. Hierbei konnte insbesondere für HBx Genotypen A und G eine drastische Fragmentierung der Mitochondrien beobachtet werden, die Änderung der tubulären Mitochondrien Strukturen innerhalb der Genotypen B und E zeigten hingegen nur marginale Unterschiede im Vergleich zur Kontrolle. Diese Ergebnisse konnten ebenfalls anhand einer Einzel-Zell Quantifizierung mittels eines Mitochondrien-Netzwerk Analyse Programm verifiziert werden.

Durch die enge Korrelation zwischen Struktur und Form der Mitochondrien wurde folglich vermutet, dass insbesondre bei den beobachteten fragmentierten Phänotypen ebenso eine Einschränkung in der mitochondrialen Funktion auftritt. Eine bisher intensiv erforschte Interaktion von HBx ist in diesem Zusammenhang die Bindung des Spannungs-abhängigen Anionen Kanal. Dieser ist an der äußeren Mitochondrienmembran lokalisiert und reguliert, spannungs-abhängig, die Freisetzung von Ionen und anderen Metaboliten. Insbesondere führt eine Deregulation des Kanals zu einem Verlust des mitochondrialen Membranpotenziales mit fatalen Folgen für die Funktionalität der Atmungskette und der Generierung des Adenosintriphosphates.

Interessanterweise konnte für alle getesteten Varianten des HBx-Proteins eine Co-Lokalisation mit dem Spannungs-abhängigen Anionen Kanal 3 beobachtet werden, die Quantität variierte jedoch stark abhängig von den jeweiligen Genotypen. Insbesondere konnten die Genotypen von HBx mit vorheriger starker Fragmentierung der Mitochondrien mit einem signifikant höheren Level an Co-Lokalisation korreliert werden und weiterhin mit einer deutlichen Verminderung des mitochondrialen Membranpotenziales. Diese Effekte waren insbesondere für die HBx-Genotypen B und E deutlich moderater, Genotyp C und D zeigt sich mit leicht verstärkten Effekten als Intermediate zwischen A und G beziehungsweise B und E.

Die Freisetzung von mitochondrialem, oxidativem Stress in das Zytosol steht ebenfalls zentral in Verbindung mit einer HBx-induzieren Änderung des Anionen-Kanals und hat weitreichende Auswirkungen auf den zellulären Metabolismus und der Immunmodulation. Entsprechend zu den vorherigen Daten konnten auch hierbei deutliche, Genotypen-spezifische Unterschiede im zellulären Radikal-Spiegel, aber auch in der Induktion zytoprotektiver Gene und inflammatorische Mediatoren beobachtet werden. Anhand dieser Daten konnte neben einer HBx-spezifischen und insbesondere Genotypen-abhängigen Änderung der Mitochondrien-struktur, auch ein differenzierter Einfluss auf die mitochondriale Funktion bewiesen werden.

Als Konsequenz für deutliche Änderungen in der mitochondrialen Physiologie wurde final eine mögliche Degradation dysfunktionaler Mitochondrien durch einen selektiven Autophagie-mechanismus (Mitophagie) vermutet. Anhand eines pH-sensitiven und mitochondrien-assoziierten Reporter-Plasmides konnte mittels Konfokaler Laser Scanning Mikroskopie eine Genotypen-abhängige Wirkung durch HBx beobachtet werden. Auch hier korrelierten verstärkte Mengen azider Mitochondrien (Lysosomen-assoziiert) mit den vorherigen Beobachtungen und ergaben insbesondere für HBx-Genotyp A, D und G eine deutlich stärkere Induktion der Mitophagie im Vergleich zur Kontrollgruppe, die vermutlich über den PINK1/Parkin abhängigen Signalweg reguliert wird. Entsprechend zu einer moderaten Änderung in der Mitochondrialen Funktion, scheint entsprechend auch nur ein geringer Anteil der Mitochondrien durch HBx moduliert zu seine und bedarf keiner größeren Notwendigkeit, dysfunktionale Mitochondrien abzubauen um somit das Überleben der Zelle zu sichern.

Schließlich konnte, basierend auf den in dieser Arbeit beschriebenen Daten, ein gravierender Einfluss der Genotypen auf die HBx-abhängige Mitochondrien-modulation bewiesen werden. Als zentrale Organellen in der gesamten Zellhomöostase und auch für die Regulation der Immunantwort, ist eine Fehlregulation der Mitochondrien mit entscheidenden pathophysiologischen Konsequenzen verbunden. Dabei könnten insbesondere die HBx Genotypen A und G einen entscheidenden Beitrag an einer Leberschädigung und Tumorprogression leisten. Jedoch muss berücksichtigt werden, dass die vorliegenden Daten ausschließlich auf Zellkultur basierten Ergebnissen beruhen. Insbesondere klinische Daten im Verlauf einer natürlichen Infektion sind bisher nicht verfügbar könnten jedoch weitere, wichtige Kenntnisse in diesem Zusammenhang liefern.

Insgesamt sind die gewonnenen Erkenntnisse jedoch von zentraler Bedeutung, um das Verständnis der unterschiedlichen Genotypen insbesondere auf zellulärer Ebene und in Interaktion mit Signalwegen des Wirtsystems besser zu verstehen. Aber auch um das Wissen spezifisch auf HBx zu erweitern und mögliche, zielgerichtete und Genotypen-angepasste Therapieoptionen zu ermöglichen.

8. References

[1] Thomas E, Yoneda M, Schiff ER. Viral hepatitis: past and future of HBV and HDV. Cold Spring Harbor Perspectives in Medicine 2015;5(2):a021345.

[2] Papavramidou N, Fee E, Christopoulou-Aletra H. Jaundice in the Hippocratic Corpus. Journal of gastrointestinal surgery official journal of the Society for Surgery of the Alimentary Tract 2007;11(12):1728–31.

[3] Gruber W, Virchow R. Ueber das Vorkommen und den Nachweis des hepatogenen, insbesondere des katarrhalischen Icterus. Archiv f. pathol. Anat. 1865;32(1):117–25.

[4] Roholm K, Iversen P. CHANGES IN THE LIVER IN ACUTE EPIDEMIC HEPATITIS (CATARRHAL JAUNDICE) BASED ON 38 ASPIRATION BIOPSIES*. Acta Pathologica Microbiologica Scandinavica 1939;16(4):427–42.

[5] BLUMBERG BS, ALTER HJ, VISNICH S. A "NEW" ANTIGEN IN LEUKEMIA SERA. JAMA 1965;191:541–6.

[6] Gerlich WH. Medical virology of hepatitis B: how it began and where we are now. Virology journal 2013;10:239.

[7] Al-Mahtab M, Roy PP, Khan MSI, Akbar SM. Nobel Prize for the Discovery of Hepatitis B and C: A Brief History in Time. Euroasian journal of hepato-gastroenterology 2020;10(2):98–100.

[8] Dane DS, Cameron CH, Briggs M. Virus-like particles in serum of patients with Australia-antigen-associated hepatitis. Lancet (London, England) 1970;1(7649):695–8.

[9] Krugman S. Viral Hepatitis, Type B (MS-2 Strain). JAMA 1971;217(1):41.

[10] Lavanchy D. Viral hepatitis: global goals for vaccination. Journal of clinical virology the official publication of the Pan American Society for Clinical Virology 2012;55(4):296–302.

[11] Yan H, Zhong G, Xu G, He W, Jing Z, Gao Z et al. Sodium taurocholate cotransporting polypeptide is a functional receptor for human hepatitis B and D virus. eLife 2012;1.

[12] Verrier ER, Colpitts CC, Schuster C, Zeisel MB, Baumert TF. Cell Culture Models for the Investigation of Hepatitis B and D Virus Infection. Viruses 2016;8(9).

[13] WORLD HEALTH ORGANIZATION, et al. Global hepatitis report 2017. World Health Organization;2017.

[14] Bender D, Glitscher M, Hildt E. Die Virushepatitiden A bis E: Prävalenz, Erregermerkmale und Pathogenese. Bundesgesundheitsblatt, Gesundheitsforschung, Gesundheitsschutz 2022;65(2):139–48.

[15] Malik GF, Zakaria N, Majeed MI, Ismail FW. Viral Hepatitis - The Road Traveled and the Journey Remaining. Hepatic medicine evidence and research 2022;14:13–26.

[16] Zeng D-Y, Li J-M, Lin S, Dong X, You J, Xing Q-Q et al. Global burden of acute viral hepatitis and its association with socioeconomic development status, 1990-2019. Journal of hepatology 2021;75(3):547–56.

[17] Waheed Y, Siddiq M, Jamil Z, Najmi MH. Hepatitis elimination by 2030: Progress and challenges. World journal of gastroenterology 2018;24(44):4959–61.

[18] Hsu Y-C, Huang DQ, Nguyen MH. Global burden of hepatitis B virus: current status, missed opportunities and a call for action. Nature reviews. Gastroenterology & hepatology 2023;20(8):524–37.

[19] Gust ID, Burrell CJ, Coulepis AG, Robinson WS, Zuckerman AJ. Taxonomic classification of human hepatitis B virus. Intervirology 1986;25(1):14–29.

[20] Schaefer S. Hepatitis B virus taxonomy and hepatitis B virus genotypes. World journal of gastroenterology 2007;13(1):14–21.

[21] Datta S, Chatterjee S, Veer V, Chakravarty R. Molecular biology of the hepatitis B virus for clinicians. Journal of clinical and experimental hepatology 2012;2(4):353–65.

[22] World Health Organization. Global progress report on HIV, viral hepatitis and sexually transmitted infections, 2021;2021(ISBN 978-92-4-002707-7).

[23] MacLachlan JH, Cowie BC. Hepatitis B virus epidemiology. Cold Spring Harbor Perspectives in Medicine 2015;5(5):a021410.

[24] Nelson NP, Easterbrook PJ, McMahon BJ. Epidemiology of Hepatitis B Virus Infection and Impact of Vaccination on Disease. Clinics in liver disease 2016;20(4):607–28.

[25] Schweitzer A, Horn J, Mikolajczyk RT, Krause G, Ott JJ. Estimations of worldwide prevalence of chronic hepatitis B virus infection: a systematic review of data published between 1965 and 2013. Lancet (London, England) 2015;386(10003):1546–55.

[26] Ahmad AA, Falla AM, Duffell E, Noori T, Bechini A, Reintjes R et al. Estimating the scale of chronic hepatitis B virus infection among migrants in EU/EEA countries. BMC infectious diseases 2018;18(1):34.

[27] Rossi C, Shrier I, Marshall L, Cnossen S, Schwartzman K, Klein MB et al. Seroprevalence of chronic hepatitis B virus infection and prior immunity in immigrants and refugees: a systematic review and meta-analysis. PloS one 2012;7(9):e44611.

[28] Pedersini R, Marano C, Moerlooze L de, Chen L, Vietri J. HAV & HBV vaccination among travellers participating in the National Health and Wellness Survey in five European countries. Travel medicine and infectious disease 2016;14(3):221–32.

[29] Sabeena S, Ravishankar N. Horizontal Modes of Transmission of Hepatitis B Virus (HBV): A Systematic Review and Meta-Analysis. Iranian journal of public health 2022;51(10):2181–93.

[30] Komatsu H, Inui A, Sogo T, Tateno A, Shimokawa R, Fujisawa T. Tears from children with chronic hepatitis B virus (HBV) infection are infectious vehicles of HBV transmission:

experimental transmission of HBV by tears, using mice with chimeric human livers. The Journal of infectious diseases 2012;206(4):478–85.

[31] Di Filippo Villa D, Navas M-C. Vertical Transmission of Hepatitis B Virus-An Update. Microorganisms 2023;11(5).

[32] Than TT, Jo E, Todt D, Nguyen PH, Steinmann J, Steinmann E et al. High Environmental Stability of Hepatitis B Virus and Inactivation Requirements for Chemical Biocides. The Journal of infectious diseases 2019;219(7):1044–8.

[33] Zhang Z-H, Wu C-C, Chen X-W, Li X, Li J, Lu M-J. Genetic variation of hepatitis B virus and its significance for pathogenesis. World journal of gastroenterology 2016;22(1):126–44.

[34] Girones R, Miller RH. Mutation rate of the hepadnavirus genome. Virology 1989;170(2):595–7.

[35] Chotiyaputta W, Lok ASF. Hepatitis B virus variants. Nature reviews. Gastroenterology & hepatology 2009;6(8):453–62.

[36] Torres C, Fernández MDB, Flichman DM, Campos RH, Mbayed VA. Influence of overlapping genes on the evolution of human hepatitis B virus. Virology 2013;441(1):40–8.

[37] Kramvis A. Genotypes and genetic variability of hepatitis B virus. Intervirology 2014;57(3-4):141–50.

[38] Bancroft WH, Mundon FK, Russell PK. Detection of Additional Antigenic Determinants of Hepatitis B Antigen. The Journal of Immunology 1972;109(4):842–8.

[39] Kidd-Ljunggren K, Miyakawa Y, Kidd AH. Genetic variability in hepatitis B viruses. The Journal of general virology 2002;83(Pt 6):1267–80.

[40] Okamoto H, Tsuda F, Sakugawa H, Sastrosoewignjo RI, Imai M, Miyakawa Y et al. Typing hepatitis B virus by homology in nucleotide sequence: comparison of surface antigen subtypes. The Journal of general virology 1988;69 (Pt 10):2575–83.

[41] Tatematsu K, Tanaka Y, Kurbanov F, Sugauchi F, Mano S, Maeshiro T et al. A genetic variant of hepatitis B virus divergent from known human and ape genotypes isolated from a Japanese patient and provisionally assigned to new genotype J. Journal of virology 2009;83(20):10538–47.

[42] Cao G-W. Clinical relevance and public health significance of hepatitis B virus genomic variations. World journal of gastroenterology 2009;15(46):5761–9.

[43] Jefferies M, Rauff B, Rashid H, Lam T, Rafiq S. Update on global epidemiology of viral hepatitis and preventive strategies. World journal of clinical cases 2018;6(13):589–99.

[44] Velkov S, Ott JJ, Protzer U, Michler T. The Global Hepatitis B Virus Genotype Distribution Approximated from Available Genotyping Data. Genes 2018;9(10).

[45] Pourkarim MR, Amini-Bavil-Olyaee S, Lemey P, Maes P, van Ranst M. Are hepatitis B virus "subgenotypes" defined accurately? Journal of clinical virology the official publication of the Pan American Society for Clinical Virology 2010;47(4):356–60.

[46] Yousif M, Kramvis A. Genotype D of hepatitis B virus and its subgenotypes: An update. Hepatology research the official journal of the Japan Society of Hepatology 2013;43(4):355–64.

[47] Norder H, Couroucé A-M, Coursaget P, Echevarria JM, Lee S-D, Mushahwar IK et al. Genetic diversity of hepatitis B virus strains derived worldwide: genotypes, subgenotypes, and HBsAg subtypes. Intervirology 2004;47(6):289–309.

[48] Malagnino V, Bottero J, Miailhes P, Lascoux-Combe C, Girard P-M, Zoulim F et al. Hepatitis B virus genotype G and liver fibrosis progression in chronic hepatitis B and human immunodeficiency virus coinfection. Journal of medical virology 2019;91(4):630–41.

[49] Olinger CM, Jutavijittum P, Hübschen JM, Yousukh A, Samountry B, Thammavong T et al. Possible new hepatitis B virus genotype, southeast Asia. Emerging infectious diseases 2008;14(11):1777–80.

[50] Yu H, Yuan Q, Ge S-X, Wang H-Y, Zhang Y-L, Chen Q-R et al. Molecular and phylogenetic analyses suggest an additional hepatitis B virus genotype "I". PloS one 2010;5(2):e9297.

[51] Simmonds P, Midgley S. Recombination in the genesis and evolution of hepatitis B virus genotypes. Journal of virology 2005;79(24):15467–76.

[52] Günther S. Genetic variation in HBV infection: genotypes and mutants. Journal of clinical virology the official publication of the Pan American Society for Clinical Virology 2006;36 Suppl 1:S3-S11.

[53] Kamijo N, Matsumoto A, Umemura T, Shibata S, Ichikawa Y, Kimura T et al. Mutations of pre-core and basal core promoter before and after hepatitis B e antigen seroconversion. World journal of gastroenterology 2015;21(2):541–8.

[54] Peiffer K-H, Spengler C, Basic M, Jiang B, Kuhnhenn L, Obermann W et al. Quadruple mutation GCAC1809-1812TTCT acts as a biomarker in healthy European HBV carriers. JCI insight 2020;5(22).

[55] Ali A, Abdel-Hafiz H, Suhail M, Al-Mars A, Zakaria MK, Fatima K et al. Hepatitis B virus, HBx mutants and their role in hepatocellular carcinoma. World journal of gastroenterology 2014;20(30):10238–48.

[56] Datta S, Banerjee A, Chandra PK, Biswas A, Panigrahi R, Mahapatra PK et al. Analysis of hepatitis B virus X gene phylogeny, genetic variability and its impact on pathogenesis: implications in Eastern Indian HBV carriers. Virology 2008;382(2):190–8.

[57] Zhou B, He W, Hou J. HBx mutations emerged during antiviral therapy: a new face of a multifaceted HBV protein? Hepatology international 2020;14(6):944–6.

[58] Liang TJ. Hepatitis B: the virus and disease. Hepatology (Baltimore, Md.) 2009;49(5 Suppl):S13-21.

[59] Shepard CW, Simard EP, Finelli L, Fiore AE, Bell BP. Hepatitis B virus infection: epidemiology and vaccination. Epidemiologic reviews 2006;28:112–25.

[60] Burns GS, Thompson AJ. Viral hepatitis B: clinical and epidemiological characteristics. Cold Spring Harbor Perspectives in Medicine 2014;4(12):a024935.

[61] Tsai K-N, Kuo C-F, Ou J-HJ. Mechanisms of Hepatitis B Virus Persistence. Trends in microbiology 2018;26(1):33–42.

[62] Kramvis A, Chang K-M, Dandri M, Farci P, Glebe D, Hu J et al. A roadmap for serum biomarkers for hepatitis B virus: current status and future outlook. Nature reviews. Gastroenterology & hepatology 2022;19(11):727–45.

[63] Krugman S, Overby LR, Mushahwar IK, Ling CM, Frösner GG, Deinhardt F. Viral hepatitis, type B. Studies on natural history and prevention re-examined. The New England journal of medicine 1979;300(3):101–6.

[64] Lavanchy D. Hepatitis B virus epidemiology, disease burden, treatment, and current and emerging prevention and control measures. Journal of viral hepatitis 2004;11(2):97–107.

[65] EASL 2017 Clinical Practice Guidelines on the management of hepatitis B virus infection. Journal of hepatology 2017;67(2):370–98.

[66] Bousali M, Papatheodoridis G, Paraskevis D, Karamitros T. Hepatitis B Virus DNA Integration, Chronic Infections and Hepatocellular Carcinoma. Microorganisms 2021;9(8).

[67] Lok AS, Lai CL, Wu PC, Leung EK, Lam TS. Spontaneous hepatitis B e antigen to antibody seroconversion and reversion in Chinese patients with chronic hepatitis B virus infection. Gastroenterology 1987;92(6):1839–43.

[68] McMahon BJ. Epidemiology and natural history of hepatitis B. Seminars in liver disease 2005;25 Suppl 1:3–8.

[69] Lok ASF, McMahon BJ. Chronic hepatitis B. Hepatology (Baltimore, Md.) 2007;45(2):507–39.

[70] Bonino F, Colombatto P, Brunetto MR. HBeAg-Negative/Anti-HBe-Positive Chronic Hepatitis B: A 40-Year-Old History. Viruses 2022;14(8).

[71] Mak L-Y, Wong DK-H, Pollicino T, Raimondo G, Hollinger FB, Yuen M-F. Occult hepatitis B infection and hepatocellular carcinoma: Epidemiology, virology, hepatocarcinogenesis and clinical significance. Journal of hepatology 2020;73(4):952–64.

[72] Raimondo G, Pollicino T, Cacciola I, Squadrito G. Occult hepatitis B virus infection. Journal of hepatology 2007;46(1):160–70.

[73] Liang J, Liu L, Cao Y, Zhang Q, Liu F, Chen Y et al. Hepatitis B-related acute-on-chronic liver failure induced by hepatotropic viral insult is associated with worse prognosis than that induced by non-virus insult. BMC infectious diseases 2021;21(1):1273.

[74] Chen C-J, Yang H-I, Su J, Jen C-L, You S-L, Lu S-N et al. Risk of hepatocellular carcinoma across a biological gradient of serum hepatitis B virus DNA level. JAMA 2006;295(1):65–73.

[75] Gustot T, Stadlbauer V, Laleman W, Alessandria C, Thursz M. Transition to decompensation and acute-on-chronic liver failure: Role of predisposing factors and precipitating events. Journal of hepatology 2021;75 Suppl 1:S36-S48.

[76] Kappus MR, Sterling RK. Extrahepatic manifestations of acute hepatitis B virus infection. Gastroenterology & hepatology 2013;9(2):123–6.

[77] Liu J, Yang H-I, Lee M-H, Lu S-N, Jen C-L, Wang L-Y et al. Incidence and determinants of spontaneous hepatitis B surface antigen seroclearance: a community-based follow-up study. Gastroenterology 2010;139(2):474–82.

[78] Beasley RP, Hwang LY, Lee GC, Lan CC, Roan CH, Huang FY et al. Prevention of perinatally transmitted hepatitis B virus infections with hepatitis B immune globulin and hepatitis B vaccine. Lancet (London, England) 1983;2(8359):1099–102.

[79] Walayat S, Ahmed Z, Martin D, Puli S, Cashman M, Dhillon S. Recent advances in vaccination of non-responders to standard dose hepatitis B virus vaccine. World journal of hepatology 2015;7(24):2503–9.

[80] Yanny B, Konyn P, Najarian LM, Mitry A, Saab S. Management Approaches to Hepatitis B Virus Vaccination Nonresponse. Gastroenterology & hepatology 2019;15(2):93–9.

[81] Chang M-H, Chen D-S. Prevention of hepatitis B. Cold Spring Harbor Perspectives in Medicine 2015;5(3):a021493.

[82] World Health Organization. Fact-sheet HepatitisB. [August 12, 2023]; Available from: https://www.who.int/news-room/fact-sheets/detail/hepatitis-b.

[83] Fang CT. Blood screening for HBV DNA. Journal of clinical virology the official publication of the Pan American Society for Clinical Virology 2006;36 Suppl 1:S30-2.

[84] Aspinall EJ, Hawkins G, Fraser A, Hutchinson SJ, Goldberg D. Hepatitis B prevention, diagnosis, treatment and care: a review. Occupational medicine (Oxford, England) 2011;61(8):531–40.

[85] Carey I, Harrison PM. Monotherapy versus combination therapy for the treatment of chronic hepatitis B. Expert opinion on investigational drugs 2009;18(11):1655–66.

[86] Di Marco V, Craxì A. Chronic hepatitis B: who to treat and which choice of treatment? Expert review of anti-infective therapy 2009;7(3):281–91.

[87] Soriano V, Barreiro P, Cachay E, Kottilil S, Fernandez-Montero JV, Mendoza C de. Advances in hepatitis B therapeutics. Therapeutic advances in infectious disease 2020;7:2049936120965027.

[88] Lin C-L, Kao J-H. The clinical implications of hepatitis B virus genotype: Recent advances. Journal of gastroenterology and hepatology 2011;26 Suppl 1:123–30.

[89] Liu Y, Park D, Cafiero TR, Bram Y, Chandar V, Tseng A et al. Molecular clones of genetically distinct hepatitis B virus genotypes reveal distinct host and drug treatment responses. JHEP reports innovation in hepatology 2022;4(9):100535.

[90] Wiegand J, Hasenclever D, Tillmann HL. Should treatment of hepatitis B depend on hepatitis B virus genotypes? A hypothesis generated from an explorative analysis of published evidence. Antiviral therapy 2008;13(2):211–20.

[91] Erhardt A, Göbel T, Ludwig A, Lau GKK, Marcellin P, van Bömmel F et al. Response to antiviral treatment in patients infected with hepatitis B virus genotypes E-H. Journal of medical virology 2009;81(10):1716–20.

[92] Mu S-C, Lin Y-M, Jow G-M, Chen B-F. Occult hepatitis B virus infection in hepatitis B vaccinated children in Taiwan. Journal of hepatology 2009;50(2):264–72.

[93] Elizalde MM, Tadey L, Mammana L, Quarleri JF, Campos RH, Flichman DM. Biological Characterization of Hepatitis B virus Genotypes: Their Role in Viral Replication and Antigen Expression. Frontiers in microbiology 2021;12:758613.

[94] Hassemer M, Finkernagel M, Peiffer K-H, Glebe D, Akhras S, Reuter A et al. Comparative characterization of hepatitis B virus surface antigen derived from different hepatitis B virus genotypes. Virology 2017;502:1–12.

[95] Shih Y-F, Liu C-J. Hepatitis C Virus and Hepatitis B Virus Co-Infection. Viruses 2020;12(7).

[96] Thio CL. Hepatitis B and human immunodeficiency virus coinfection. Hepatology (Baltimore, Md.) 2009;49(5 Suppl):S138-45.

[97] Urban S, Neumann-Haefelin C, Lampertico P. Hepatitis D virus in 2021: virology, immunology and new treatment approaches for a difficult-to-treat disease. Gut 2021;70(9):1782–94.

[98] Lin Y, Yuan J, Long Q, Hu J, Deng H, Zhao Z et al. Patients with SARS-CoV-2 and HBV co-infection are at risk of greater liver injury. Genes & diseases 2021;8(4):484–92.

[99] Liu J, Wang T, Cai Q, Sun L, Huang D, Zhou G et al. Longitudinal changes of liver function and hepatitis B reactivation in COVID-19 patients with pre-existing chronic hepatitis B virus infection. Hepatology research the official journal of the Japan Society of Hepatology 2020;50(11):1211–21.

[100] Hu J, Liu K. Complete and Incomplete Hepatitis B Virus Particles: Formation, Function, and Application. Viruses 2017;9(3).

[101] Schädler S, Hildt E. HBV life cycle: entry and morphogenesis. Viruses 2009;1(2):185–209.

[102] Bruss V. Hepatitis B virus morphogenesis. World journal of gastroenterology 2007;13(1):65–73.

[103] Crowther RA, Kiselev NA, Böttcher B, Berriman JA, Borisova GP, Ose V et al. Three-dimensional structure of hepatitis B virus core particles determined by electron cryomicroscopy. Cell 1994;77(6):943–50.

[104] Dryden KA, Wieland SF, Whitten-Bauer C, Gerin JL, Chisari FV, Yeager M. Native hepatitis B virions and capsids visualized by electron cryomicroscopy. Molecular cell 2006;22(6):843–50.

[105] Sakamoto Y, Yamada G, Mizuno M, Nishihara T, Kinoyama S, Kobayashi T et al. Full and empty particles of hepatitis B virus in hepatocytes from patients with HBsAg-positive chronic active hepatitis. Laboratory investigation; a journal of technical methods and pathology 1983;48(6):678–82.

[106] Tsukuda S, Watashi K. Hepatitis B virus biology and life cycle. Antiviral research 2020;182:104925.

[107] Iannacone M, Guidotti LG. Immunobiology and pathogenesis of hepatitis B virus infection. Nature reviews. Immunology 2022;22(1):19–32.

[108] Miller RH, Kaneko S, Chung CT, Girones R, Purcell RH. Compact organization of the hepatitis B virus genome. Hepatology (Baltimore, Md.) 1989;9(2):322–7.

[109] Beck J, Nassal M. Hepatitis B virus replication. World journal of gastroenterology 2007;13(1):48–64.

[110] Tong S, Revill P. Overview of hepatitis B viral replication and genetic variability. Journal of hepatology 2016;64(1 Suppl):S4-S16.

[111] Seeger C, Ganem D, Varmus HE. Biochemical and genetic evidence for the hepatitis B virus replication strategy. Science (New York, N.Y.) 1986;232(4749):477–84.

[112] Haines KM, Loeb DD. The sequence of the RNA primer and the DNA template influence the initiation of plus-strand DNA synthesis in hepatitis B virus. Journal of molecular biology 2007;370(3):471–80.

[113] Lamontagne RJ, Bagga S, Bouchard MJ. Hepatitis B virus molecular biology and pathogenesis. Hepatoma research 2016;2:163–86.

[114] Lupberger J, Schaedler S, Peiran A, Hildt E. Identification and characterization of a novel bipartite nuclear localization signal in the hepatitis B virus polymerase. World journal of gastroenterology 2013;19(44):8000–10.

[115] Glebe D, Bremer CM. The molecular virology of hepatitis B virus. Seminars in liver disease 2013;33(2):103–12.

[116] Nassal M. HBV cccDNA: viral persistence reservoir and key obstacle for a cure of chronic hepatitis B. Gut 2015;64(12):1972–84.

[117] Huovila AP, Eder AM, Fuller SD. Hepatitis B surface antigen assembles in a post-ER, pre-Golgi compartment. The Journal of cell biology 1992;118(6):1305–20.

[118] Mangold CM, Streeck RE. Mutational analysis of the cysteine residues in the hepatitis B virus small envelope protein. Journal of virology 1993;67(8):4588–97.

[119] Eble BE, MacRae DR, Lingappa VR, Ganem D. Multiple topogenic sequences determine the transmembrane orientation of the hepatitis B surface antigen. Molecular and cellular biology 1987;7(10):3591–601.

[120] Zhao F, Xie X, Tan X, Yu H, Tian M, Lv H et al. The Functions of Hepatitis B Virus Encoding Proteins: Viral Persistence and Liver Pathogenesis. Frontiers in immunology 2021;12:691766.

[121] Hildt E, Hofschneider PH. The PreS2 activators of the hepatitis B virus: activators of tumour promoter pathways. Recent results in cancer research. Fortschritte der Krebsforschung. Progres dans les recherches sur le cancer 1998;154:315–29.

[122] Bruss V. Envelopment of the hepatitis B virus nucleocapsid. Virus research 2004;106(2):199–209.

[123] Wynne SA, Crowther RA, Leslie AG. The crystal structure of the human hepatitis B virus capsid. Molecular cell 1999;3(6):771–80.

[124] Bock CT, Schwinn S, Locarnini S, Fyfe J, Manns MP, Trautwein C et al. Structural organization of the hepatitis B virus minichromosome. Journal of molecular biology 2001;307(1):183–96.

[125] Tajwar R, Bradley DP, Ponzar NL, Tavis JE. Predicted structure of the hepatitis B virus polymerase reveals an ancient conserved protein fold. Protein science a publication of the Protein Society 2022;31(10):e4421.

[126] Edwards TC, Ponzar NL, Tavis JE. Shedding light on RNaseH: a promising target for hepatitis B virus (HBV). Expert opinion on therapeutic targets 2019;23(7):559–63.

[127] Milich DR, McLachlan A, Stahl S, Wingfield P, Thornton GB, Hughes JL et al. Comparative immunogenicity of hepatitis B virus core and E antigens. The Journal of Immunology 1988;141(10):3617–24.

[128] Milich D, Liang TJ. Exploring the biological basis of hepatitis B e antigen in hepatitis B virus infection. Hepatology (Baltimore, Md.) 2003;38(5):1075–86.

[129] Hadziyannis E, Laras A. Viral Biomarkers in Chronic HBeAg Negative HBV Infection. Genes 2018;9(10).

[130] Song H, Xu F, Xiao Q, Tan G. Hepatitis B virus X protein and its host partners. Cellular & molecular immunology 2021;18(5):1345–6.

[131] Jung S-Y, Kim Y-J. C-terminal region of HBx is crucial for mitochondrial DNA damage. Cancer letters 2013;331(1):76–83.

[132] Chuang Y-C, Tsai K-N, Ou J-HJ. Pathogenicity and virulence of Hepatitis B virus. Virulence 2022;13(1):258–96.

[133] Urban S, Hildt E, Eckerskorn C, Sirma H, Kekulé A, Hofschneider PH. Isolation and molecular characterization of hepatitis B virus X-protein from a baculovirus expression system. Hepatology (Baltimore, Md.) 1997;26(4):1045–53.

[134] Rivière L, Ducroux A, Buendia MA. The oncogenic role of hepatitis B virus. Recent results in cancer research. Fortschritte der Krebsforschung. Progres dans les recherches sur le cancer 2014;193:59–74.

[135] Hafner A, Brandenburg B, Hildt E. Reconstitution of gene expression from a regulatory-protein-deficient hepatitis B virus genome by cell-permeable HBx protein. EMBO reports 2003;4(8):767–73.

[136] Cha M-Y, Ryu D-K, Jung H-S, Chang H-E, Ryu W-S. Stimulation of hepatitis B virus genome replication by HBx is linked to both nuclear and cytoplasmic HBx expression. The Journal of general virology 2009;90(Pt 4):978–86.

[137] Sivasudhan E, Blake N, Lu Z, Meng J, Rong R. Hepatitis B Viral Protein HBx and the Molecular Mechanisms Modulating the Hallmarks of Hepatocellular Carcinoma: A Comprehensive Review. Cells 2022;11(4).

[138] Zhou Q, Yan L, Xu B, Wang X, Sun X, Han N et al. Screening of the HBx transactivation domain interacting proteins and the function of interactor Pin1 in HBV replication. Scientific reports 2021;11(1):14176.

[139] Schollmeier A, Glitscher M, Hildt E. Relevance of HBx for Hepatitis B Virus-Associated Pathogenesis. International journal of molecular sciences 2023;24(5).

[140] Zeisel MB, Guerrieri F, Levrero M. Host Epigenetic Alterations and Hepatitis B Virus-Associated Hepatocellular Carcinoma. Journal of clinical medicine 2021;10(8).

[141] Park IY, Sohn BH, Yu E, Suh DJ, Chung Y-H, Lee J-H et al. Aberrant epigenetic modifications in hepatocarcinogenesis induced by hepatitis B virus X protein. Gastroenterology 2007;132(4):1476–94.

[142] Lee S-M, Lee Y, Bae J-B, Choi JK, Tayama C, Hata K et al. HBx induces hypomethylation of distal intragenic CpG islands required for active expression of developmental regulators. Proc. Natl. Acad. Sci. U.S.A. 2014;111(26):9555–60.

[143] Tricoli L, Niture S, Chimeh U, Ressom H, Kumar D. Role of microRNAs in the development of hepatocellular carcinoma and drug resistance. Frontiers in bioscience (Landmark edition) 2019;24(2):382–91.

[144] Pfister SX, Ashworth A. Marked for death: targeting epigenetic changes in cancer. Nature reviews. Drug discovery 2017;16(4):241–63.

[145] Kanda T, Goto T, Hirotsu Y, Moriyama M, Omata M. Molecular Mechanisms Driving Progression of Liver Cirrhosis towards Hepatocellular Carcinoma in Chronic Hepatitis B and C Infections: A Review. International journal of molecular sciences 2019;20(6).

[146] Sekiba K, Otsuka M, Funato K, Miyakawa Y, Tanaka E, Seimiya T et al. HBx-induced degradation of Smc5/6 complex impairs homologous recombination-mediated repair of damaged DNA. Journal of hepatology 2022;76(1):53–62.

[147] Ling L-R, Zheng D-H, Zhang Z-Y, Xie W-H, Huang Y-H, Chen Z-X et al. Effect of HBx on inflammation and mitochondrial oxidative stress in mouse hepatocytes. Oncology letters 2020;19(4):2861–9.

[148] Yu D-Y. Relevance of reactive oxygen species in liver disease observed in transgenic mice expressing the hepatitis B virus X protein. Laboratory animal research 2020;36:6.

[149] Xie W-H, Ding J, Xie X-X, Yang X-H, Wu X-F, Chen Z-X et al. Hepatitis B virus X protein promotes liver cell pyroptosis under oxidative stress through NLRP3 inflammasome activation. Inflammation research official journal of the European Histamine Research Society … [et al.] 2020;69(7):683–96.

[150] Zhou X, Liu D, Li Z, Zhao J, Cai S, Cao G. The Mechanism of Hepatitis B Virus X Gene in Promoting Hepatocellular Carcinoma. J Cancer Sci Clin Ther 2022;06(02).

[151] Schaedler S, Krause J, Himmelsbach K, Carvajal-Yepes M, Lieder F, Klingel K et al. Hepatitis B virus induces expression of antioxidant response element-regulated genes by activation of Nrf2. The Journal of biological chemistry 2010;285(52):41074–86.

[152] Ariffianto A, Deng L, Abe T, Matsui C, Ito M, Ryo A et al. Oxidative stress sensor Keap1 recognizes HBx protein to activate the Nrf2/ARE signaling pathway, thereby inhibiting hepatitis B virus replication. Journal of virology 2023;97(10):e0128723.

[153] Hossain MG, Akter S, Ohsaki E, Ueda K. Impact of the Interaction of Hepatitis B Virus with Mitochondria and Associated Proteins. Viruses 2020;12(2).

[154] Esser K, Cheng X, Wettengel JM, Lucifora J, Hansen-Palmus L, Austen K et al. Hepatitis B Virus Targets Lipid Transport Pathways to Infect Hepatocytes. Cellular and molecular gastroenterology and hepatology 2023;16(2):201–21.

[155] Protzer U, Maini MK, Knolle PA. Living in the liver: hepatic infections. Nature reviews. Immunology 2012;12(3):201–13.

[156] Ni Y, Li J-M, Liu M-K, Zhang T-T, Wang D-P, Zhou W-H et al. Pathological process of liver sinusoidal endothelial cells in liver diseases. World journal of gastroenterology 2017;23(43):7666–77.

[157] Wisse E, Zanger RB de, Charels K, van der Smissen P, McCuskey RS. The liver sieve: considerations concerning the structure and function of endothelial fenestrae, the sinusoidal wall and the space of Disse. Hepatology (Baltimore, Md.) 1985;5(4):683–92.

[158] Schulze A, Gripon P, Urban S. Hepatitis B virus infection initiates with a large surface protein-dependent binding to heparan sulfate proteoglycans. Hepatology (Baltimore, Md.) 2007;46(6):1759–68.

[159] Gripon P, Le Seyec J, Rumin S, Guguen-Guillouzo C. Myristylation of the hepatitis B virus large surface protein is essential for viral infectivity. Virology 1995;213(2):292–9.

[160] Iwamoto M, Saso W, Sugiyama R, Ishii K, Ohki M, Nagamori S et al. Epidermal growth factor receptor is a host-entry cofactor triggering hepatitis B virus internalization. Proc. Natl. Acad. Sci. U.S.A. 2019;116(17):8487–92.

[161] Jiang B, Hildt E. Intracellular Trafficking of HBV Particles. Cells 2020;9(9).

[162] Rabe B, Vlachou A, Panté N, Helenius A, Kann M. Nuclear import of hepatitis B virus capsids and release of the viral genome. Proc. Natl. Acad. Sci. U.S.A. 2003;100(17):9849–54.

[163] Diogo Dias J, Sarica N, Neuveut C. Early Steps of Hepatitis B Life Cycle: From Capsid Nuclear Import to cccDNA Formation. Viruses 2021;13(5).

[164] Hofmann S, Plank V, Groitl P, Skvorc N, Hofmann K, Luther J et al. SUMO Modification of Hepatitis B Virus Core Mediates Nuclear Entry, Promyelocytic Leukemia Nuclear Body Association, and Efficient Formation of Covalently Closed Circular DNA. Microbiology spectrum 2023;11(3):e0044623.

[165] Tang L, Sheraz M, McGrane M, Chang J, Guo J-T. DNA Polymerase alpha is essential for intracellular amplification of hepatitis B virus covalently closed circular DNA. PLoS pathogens 2019;15(4):e1007742.

[166] Long Q, Yan R, Hu J, Cai D, Mitra B, Kim ES et al. The role of host DNA ligases in hepadnavirus covalently closed circular DNA formation. PLoS pathogens 2017;13(12):e1006784.

[167] Sheraz M, Cheng J, Tang L, Chang J, Guo J-T. Cellular DNA Topoisomerases Are Required for the Synthesis of Hepatitis B Virus Covalently Closed Circular DNA. Journal of virology 2019;93(11).

[168] Pollicino T, Belloni L, Raffa G, Pediconi N, Squadrito G, Raimondo G et al. Hepatitis B virus replication is regulated by the acetylation status of hepatitis B virus cccDNA-bound H3 and H4 histones. Gastroenterology 2006;130(3):823–37.

[169] Urban S, Schulze A, Dandri M, Petersen J. The replication cycle of hepatitis B virus. Journal of hepatology 2010;52(2):282–4.

[170] Kramvis A, Kew MC. Structure and function of the encapsidation signal of hepadnaviridae. Journal of viral hepatitis 1998;5(6):357–67.

[171] Budzinska MA, Shackel NA, Urban S, Tu T. Cellular Genomic Sites of Hepatitis B Virus DNA Integration. Genes 2018;9(7).

[172] Zhao K, Liu A, Xia Y. Insights into Hepatitis B Virus DNA Integration-55 Years after Virus Discovery. Innovation (Cambridge (Mass.)) 2020;1(2):100034.

[173] Hoffmann J, Boehm C, Himmelsbach K, Donnerhak C, Roettger H, Weiss TS et al. Identification of α-taxilin as an essential factor for the life cycle of hepatitis B virus. Journal of hepatology 2013;59(5):934–41.

[174] Watanabe T, Sorensen EM, Naito A, Schott M, Kim S, Ahlquist P. Involvement of host cellular multivesicular body functions in hepatitis B virus budding. Proc. Natl. Acad. Sci. U.S.A. 2007;104(24):10205–10.

[175] Lambert C, Döring T, Prange R. Hepatitis B virus maturation is sensitive to functional inhibition of ESCRT-III, Vps4, and gamma 2-adaptin. Journal of virology 2007;81(17):9050–60.

[176] Wu Q, Glitscher M, Tonnemacher S, Schollmeier A, Raupach J, Zahn T et al. Presence of Intact Hepatitis B Virions in Exosomes. Cellular and molecular gastroenterology and hepatology 2022;15(1):237–59.

[177] Jiang B, Himmelsbach K, Ren H, Boller K, Hildt E. Subviral Hepatitis B Virus Filaments, like Infectious Viral Particles, Are Released via Multivesicular Bodies. Journal of virology 2015;90(7):3330–41.

[178] Patient R, Hourioux C, Roingeard P. Morphogenesis of hepatitis B virus and its subviral envelope particles. Cellular microbiology 2009;11(11):1561–70.

[179] Chou S-F, Tsai M-L, Huang J-Y, Chang Y-S, Shih C. The Dual Role of an ESCRT-0 Component HGS in HBV Transcription and Naked Capsid Secretion. PLoS pathogens 2015;11(10):e1005123.

[180] Bardens A, Döring T, Stieler J, Prange R. Alix regulates egress of hepatitis B virus naked capsid particles in an ESCRT-independent manner. Cellular microbiology 2011;13(4):602–19.

[181] Ma X, McKeen T, Zhang J, Ding W-X. Role and Mechanisms of Mitophagy in Liver Diseases. Cells 2020;9(4).

[182] Dan Dunn J, Alvarez LA, Zhang X, Soldati T. Reactive oxygen species and mitochondria: A nexus of cellular homeostasis. Redox biology 2015;6:472–85.

[183] Sorouri M, Chang T, Hancks DC. Mitochondria and Viral Infection: Advances and Emerging Battlefronts. mBio 2022;13(1):e0209621.

[184] Anderson S, Bankier AT, Barrell BG, Bruijn MH de, Coulson AR, Drouin J et al. Sequence and organization of the human mitochondrial genome. Nature 1981;290(5806):457–65.

[185] Kühlbrandt W. Structure and function of mitochondrial membrane protein complexes. BMC biology 2015;13:89.

[186] Wang Y, Palmfeldt J, Gregersen N, Makhov AM, Conway JF, Wang M et al. Mitochondrial fatty acid oxidation and the electron transport chain comprise a multifunctional mitochondrial protein complex. The Journal of biological chemistry 2019;294(33):12380–91.

[187] Foo J, Bellot G, Pervaiz S, Alonso S. Mitochondria-mediated oxidative stress during viral infection. Trends in microbiology 2022;30(7):679–92.

[188] Osellame LD, Blacker TS, Duchen MR. Cellular and molecular mechanisms of mitochondrial function. Best practice & research. Clinical endocrinology & metabolism 2012;26(6):711–23.

[189] Nolfi-Donegan D, Braganza A, Shiva S. Mitochondrial electron transport chain: Oxidative phosphorylation, oxidant production, and methods of measurement. Redox biology 2020;37:101674.

[190] Becker T, Wagner R. Mitochondrial Outer Membrane Channels: Emerging Diversity in Transport Processes. BioEssays news and reviews in molecular, cellular and developmental biology 2018;40(7):e1800013.

[191] Mannella CA. VDAC-A Primal Perspective. International journal of molecular sciences 2021;22(4).

[192] Lee S, Min K-T. The Interface Between ER and Mitochondria: Molecular Compositions and Functions. Molecules and cells 2018;41(12):1000–7.

[193] Feng S-T, Wang Z-Z, Yuan Y-H, Wang X-L, Sun H-M, Chen N-H et al. Dynamin-related protein 1: A protein critical for mitochondrial fission, mitophagy, and neuronal death in Parkinson's disease. Pharmacological research 2020;151:104553.

[194] Meyer JN, Leuthner TC, Luz AL. Mitochondrial fusion, fission, and mitochondrial toxicity. Toxicology 2017;391:42–53.

[195] Yoo S-M, Jung Y-K. A Molecular Approach to Mitophagy and Mitochondrial Dynamics. Molecules and cells 2018;41(1):18–26.

[196] Lim S, Smith KR, Lim S-TS, Tian R, Lu J, Tan M. Regulation of mitochondrial functions by protein phosphorylation and dephosphorylation. Cell & bioscience 2016;6:25.

[197] Zorov DB, Vorobjev IA, Popkov VA, Babenko VA, Zorova LD, Pevzner IB et al. Lessons from the Discovery of Mitochondrial Fragmentation (Fission): A Review and Update. Cells 2019;8(2).

[198] Zuo Z, Jing K, Wu H, Wang S, Ye L, Li Z et al. Mechanisms and Functions of Mitophagy and Potential Roles in Renal Disease. Frontiers in physiology 2020;11:935.

[199] Gkikas I, Palikaras K, Tavernarakis N. The Role of Mitophagy in Innate Immunity. Frontiers in immunology 2018;9:1283.

[200] Durcan TM, Fon EA. The three 'P's of mitophagy: PARKIN, PINK1, and post-translational modifications. Genes & development 2015;29(10):989–99.

[201] Onishi M, Yamano K, Sato M, Matsuda N, Okamoto K. Molecular mechanisms and physiological functions of mitophagy. The EMBO journal 2021;40(3):e104705.

[202] Elesela S, Lukacs NW. Role of Mitochondria in Viral Infections. Life (Basel, Switzerland) 2021;11(3).

[203] Huh K-W, Siddiqui A. Characterization of the mitochondrial association of hepatitis B virus X protein, HBx. Mitochondrion 2002;1(4):349–59.

[204] Li SK, Ho SF, Tsui KW, Fung KP, Waye MYM. Identification of functionally important amino acid residues in the mitochondria targeting sequence of hepatitis B virus X protein. Virology 2008;381(1):81–8.

[205] Kim S-J, Khan M, Quan J, Till A, Subramani S, Siddiqui A. Hepatitis B virus disrupts mitochondrial dynamics: induces fission and mitophagy to attenuate apoptosis. PLoS pathogens 2013;9(12):e1003722.

[206] Rahmani Z, Huh KW, Lasher R, Siddiqui A. Hepatitis B virus X protein colocalizes to mitochondria with a human voltage-dependent anion channel, HVDAC3, and alters its transmembrane potential. Journal of virology 2000;74(6):2840–6.

[207] Xuan W, Song D, Yan Y, Yang M, Sun Y. A Potential Role for Mitochondrial DNA in the Activation of Oxidative Stress and Inflammation in Liver Disease. Oxidative medicine and cellular longevity 2020;2020:1–10.

[208] Waris G, Huh KW, Siddiqui A. Mitochondrially associated hepatitis B virus X protein constitutively activates transcription factors STAT-3 and NF-kappa B via oxidative stress. Molecular and cellular biology 2001;21(22):7721–30.

[209] Liu Q, Zhang D, Hu D, Zhou X, Zhou Y. The role of mitochondria in NLRP3 inflammasome activation. Molecular immunology 2018;103:115–24.

[210] Yabal M, Calleja DJ, Simpson DS, Lawlor KE. Stressing out the mitochondria: Mechanistic insights into NLRP3 inflammasome activation. Journal of leukocyte biology 2019;105(2):377–99.

[211] Wang F, Shen F, Wang Y, Li Z, Chen J, Yuan Z. Residues Asn118 and Glu119 of hepatitis B virus X protein are critical for HBx-mediated inhibition of RIG-I-MAVS signaling. Virology 2020;539:92–103.

[212] Yin C, Li DY, Guo X, Cao HY, Chen YB, Zhou F et al. NGS-based profiling reveals a critical contributing role of somatic D-loop mtDNA mutations in HBV-related hepatocarcinogenesis. Annals of oncology official journal of the European Society for Medical Oncology 2019;30(6):953–62.

[213] Nakabayashi H, Taketa K, Miyano K, Yamane T, Sato J. Growth of human hepatoma cells lines with differentiated functions in chemically defined medium. Cancer research 1982;42(9):3858–63.

[214] Narendra D, Tanaka A, Suen D-F, Youle RJ. Parkin is recruited selectively to impaired mitochondria and promotes their autophagy. The Journal of cell biology 2008;183(5):795–803.

[215] Singh B, Avula K, Sufi SA, Parwin N, Das S, Alam MF et al. Defective Mitochondrial Quality Control during Dengue Infection Contributes to Disease Pathogenesis. Journal of virology 2022;96(20):e0082822.

[216] Zhou B, Zhang J-Y, Liu X-S, Chen H-Z, Ai Y-L, Cheng K et al. Tom20 senses iron-activated ROS signaling to promote melanoma cell pyroptosis. Cell research 2018;28(12):1171–85.

[217] Bouman L, Schlierf A, Lutz AK, Shan J, Deinlein A, Kast J et al. Parkin is transcriptionally regulated by ATF4: evidence for an interconnection between mitochondrial stress and ER stress. Cell death and differentiation 2011;18(5):769–82.

[218] Livak KJ, Schmittgen TD. Analysis of relative gene expression data using real-time quantitative PCR and the 2(-Delta Delta C(T)) Method. Methods (San Diego, Calif.) 2001;25(4):402–8.

[219] Bradford MM. A rapid and sensitive method for the quantitation of microgram quantities of protein utilizing the principle of protein-dye binding. Analytical biochemistry 1976;72:248–54.

[220] Laemmli UK. Cleavage of structural proteins during the assembly of the head of bacteriophage T4. Nature 1970;227(5259):680–5.

[221] Sivandzade F, Bhalerao A, Cucullo L. Analysis of the Mitochondrial Membrane Potential Using the Cationic JC-1 Dye as a Sensitive Fluorescent Probe. Bio-protocol 2019;9(1).

[222] Hurkmans DP, Verdegaal EME, Hogan SA, Wijn R de, Hovestad L, van den Heuvel DMA et al. Blood-based kinase activity profiling: a potential predictor of response to immune checkpoint inhibition in metastatic cancer. Journal for immunotherapy of cancer 2020;8(2).

[223] Bu D, Luo H, Huo P, Wang Z, Zhang S, He Z et al. KOBAS-i: intelligent prioritization and exploratory visualization of biological functions for gene enrichment analysis. Nucleic acids research 2021;49(W1):W317-W325.

[224] Center for Bioinformatics Peking University & Institute of Computing Technology, Chinese Academy of Sciences. KOBAS-intelligence. [August 21, 2023]; Available from: http://kobas.cbi.pku.edu.cn/.

[225] Brunelle JL, Green R. One-dimensional SDS-polyacrylamide gel electrophoresis (1D SDS-PAGE). Methods in enzymology 2014;541:151–9.

[226] Goldman A, Ursitti JA, Mozdzanowski J, Speicher DW. Electroblotting from Polyacrylamide Gels. Current protocols in protein science 2015;82:10.7.1-10.7.16.

[227] Valente AJ, Maddalena LA, Robb EL, Moradi F, Stuart JA. A simple ImageJ macro tool for analyzing mitochondrial network morphology in mammalian cell culture. Acta histochemica 2017;119(3):315–26.

[228] Dr. Jeff Stuart. MiNA - ImageJ Tools for Mitochondrial Morphology Research. [August 17, 2023]; Available from: https://github.com/StuartLab/MiNA.

[229] Slagle BL, Andrisani OM, Bouchard MJ, Lee CGL, Ou J-HJ, Siddiqui A. Technical standards for hepatitis B virus X protein (HBx) research. Hepatology (Baltimore, Md.) 2015;61(4):1416–24.

[230] Quirós PM, Prado MA, Zamboni N, D'Amico D, Williams RW, Finley D et al. Multi-omics analysis identifies ATF4 as a key regulator of the mitochondrial stress response in mammals. The Journal of cell biology 2017;216(7):2027–45.

[231] Mansouri A, Gattolliat C-H, Asselah T. Mitochondrial Dysfunction and Signaling in Chronic Liver Diseases. Gastroenterology 2018;155(3):629–47.

[232] Huang X-Y, Li D, Chen Z-X, Huang Y-H, Gao W-Y, Zheng B-Y et al. Hepatitis B Virus X protein elevates Parkin-mediated mitophagy through Lon Peptidase in starvation. Experimental cell research 2018;368(1):75–83.

[233] Wose Kinge CN, Bhoola NH, Kramvis A. In Vitro Systems for Studying Different Genotypes/Sub-Genotypes of Hepatitis B Virus: Strengths and Limitations. Viruses 2020;12(3).

[234] Henkler F, Hoare J, Waseem N, Goldin RD, McGarvey MJ, Koshy R et al. Intracellular localization of the hepatitis B virus HBx protein. The Journal of general virology 2001;82(Pt 4):871–82.

[235] Zhang T-Y, Chen H-Y, Cao J-L, Xiong H-L, Mo X-B, Li T-L et al. Structural and functional analyses of hepatitis B virus X protein BH3-like domain and Bcl-xL interaction. Nature communications 2019;10(1):3192.

[236] Hunter CA, Koc H, Koc EC. c-Src kinase impairs the expression of mitochondrial OXPHOS complexes in liver cancer. Cellular signalling 2020;72:109651.

[237] Ogura M, Yamaki J, Homma MK, Homma Y. Mitochondrial c-Src regulates cell survival through phosphorylation of respiratory chain components. The Biochemical journal 2012;447(2):281–9.

[238] Khan M, Syed GH, Kim S-J, Siddiqui A. Mitochondrial dynamics and viral infections: A close nexus. Biochimica et biophysica acta 2015;1853(10 Pt B):2822–33.

[239] Jassey A, Liu C-H, Changou CA, Richardson CD, Hsu H-Y, Lin L-T. Hepatitis C Virus Non-Structural Protein 5A (NS5A) Disrupts Mitochondrial Dynamics and Induces Mitophagy. Cells 2019;8(4).

[240] Kim S, Kim H-Y, Lee S, Kim SW, Sohn S, Kim K et al. Hepatitis B virus x protein induces perinuclear mitochondrial clustering in microtubule- and Dynein-dependent manners. Journal of virology 2007;81(4):1714–26.

[241] Lin C, Ou Q. Emerging role of mitochondria in response to HBV infection. Journal of clinical laboratory analysis 2022;36(10):e24704.

[242] Shirakata Y, Koike K. Hepatitis B virus X protein induces cell death by causing loss of mitochondrial membrane potential. The Journal of biological chemistry 2003;278(24):22071–8.

[243] Zou L-Y, Zheng B-Y, Fang X-F, Li D, Huang Y-H, Chen Z-X et al. HBx co-localizes with COXIII in HL-7702 cells to upregulate mitochondrial function and ROS generation. Oncology reports 2015;33(5):2461–7.

[244] Garrido C, Galluzzi L, Brunet M, Puig PE, Didelot C, Kroemer G. Mechanisms of cytochrome c release from mitochondria. Cell death and differentiation 2006;13(9):1423–33.

[245] Choi YB, Harhaj EW. Functional implications of mitochondrial reactive oxygen species generated by oncogenic viruses. Frontiers in biology 2014;9(6):423–36.

[246] Khanam A, Chua JV, Kottilil S. Immunopathology of Chronic Hepatitis B Infection: Role of Innate and Adaptive Immune Response in Disease Progression. International journal of molecular sciences 2021;22(11).

[247] Yang Y, Shi R, Soomro MH, Hu F, Du F, She R. Hepatitis E Virus Induces Hepatocyte Apoptosis via Mitochondrial Pathway in Mongolian Gerbils. Frontiers in microbiology 2018;9:460.

[248] Ruggieri V, Mazzoccoli C, Pazienza V, Andriulli A, Capitanio N, Piccoli C. Hepatitis C virus, mitochondria and auto/mitophagy: exploiting a host defense mechanism. World journal of gastroenterology 2014;20(10):2624–33.

[249] Li TY, Wang Q, Gao AW, Li X, Sun Y, Mottis A et al. Lysosomes mediate the mitochondrial UPR via mTORC1-dependent ATF4 phosphorylation. Cell discovery 2023;9(1):92.

[250] Campo DS, Nayak V, Srinivasamoorthy G, Khudyakov Y. Entropy of mitochondrial DNA circulating in blood is associated with hepatocellular carcinoma. BMC Medical Genomics 2019;12(Suppl 4).

9. Acknowledgements

To protect the privacy of the author, the acknowledgements have been omitted from this version of the thesis.

10. Declaration of own contribution

Except where stated otherwise by reference or acknowledgment, the work presented was generated by myself under the supervision of my advisors during my doctoral studies. All contributions from colleagues are explicitly referenced in the thesis. The material listed below was obtained in the context of collaborative research:

Figure 14: HBx-genotype A impairs mitochondrial associated signaling pathways

Collaboration partner:	Dr. Mirco Glitscher, Paul-Ehrlich-Institute, Langen, Germany
Contribution:	Bioinformatic analysis of significantly predicted kinases (Statistical analysis)
Own contribution:	Sample preparation and measurement, pathway enrichment analysis, data visualization

Figure 15: HBx protein of different genotypes indicates distinct regulatory effects in the kinome profile

Collaboration partner:	Dr. Mirco Glitscher, Paul-Ehrlich-Institute, Langen, Germany
Contribution:	Bioinformatic analysis of significantly predicted kinases (Statistical analysis), data visualization
Own contribution:	Sample preparation and measurement, data visualization (Mitochondria-specific kinase labeling)

Whenever a figure, table or text is identical to a previous publication, it is stated explicitly in the thesis that copyright permission and/or co-author agreement has been obtained.

The following parts of the thesis have been previously published:

- All figures in the result section are also part of the manuscript “The impact of HBx protein on mitochondrial dynamics and associated signaling pathways strongly depends on the Hepatitis B virus genotype“, which is currently in the submission process and therefore do not violate copyright guidelines.
- The figures 7 and 10 were previously published in [139]

Frankfurt / Main, _____ _____
(Date) (Signature)

11. Declaration of an oath

DECLARATION

I herewith declare that I have not previously participated in any doctoral examination procedure in a mathematics or natural science discipline.

Frankfurt / Main, _____ _____
(Date) (Signature)

AUTHOR'S DECLARATION

I herewith declare that I have produced my doctoral dissertation on the topic of

"Comparative characterization of Hepatitis B virus genotypes on mitochondrial dynamics and their relevance for host-associated signaling pathways"

independently and using only the tools indicated therein. In particular, all references borrowed from external sources are clearly acknowledged and identified.

I confirm that I have respected the principles of good scientific practice and have not made use of the services of any commercial agency in respect of my doctorate.

Frankfurt / Main, _____ _____
(Date) (Signature)

12. Publications

Peer-reviewed first author publications

The impact of HBx protein on mitochondrial dynamics and associated signaling pathways strongly depends on the Hepatitis B virus genotype

Schollmeier A, Basic M, Glitscher M, Hildt E; J Virol., 2024, Doi: 10.1128/jvi.00424-24

Relevance of HBx for Hepatitis B Virus-Associated Pathogenesis.

Schollmeier A, Glitscher M, Hildt E; Int J Mol Sci. 2023 Mar 4;24(5):4964.
Doi: 10.3390/ijms24054964

Peer-reviewed co-author publications

Guanylate-binding protein 1 acts as a pro-viral factor for the life cycle of hepatitis C virus

Bender D, Koulouri A, Wen X, Glitscher M, **Schollmeier A**, Fernandes da Costa L, Murra R, Carra G, Haberger V, Praefcke G, Hildt E. PLoS Pathog. 2024 Doi: 10.1371/journal.ppat.1011976

Presence of Intact Hepatitis B Virions in Exosomes

Wu Q, Glitscher M, Tonnemacher S, **Schollmeier A**, Raupach J, Zahn T, Eberle R, Krijnse-Locker J, Basic M, Hildt E. Cell Mol Gestroenterol Hepatol. 2023;15(1):237-259. Doi: 10.1016/j.jcmgh.2022.09.012

Identification of the interferon-inducible GTPase GBP1 as major restriction factor for the Hepatitis E virus.

Glitscher M, Himmelsbach K, Woytinek K, **Schollmeier A**, Johne R, Praefcke GJK, Hildt E. J Virol. 2021 Jan 20; JVI.01564-20. Doi: 10.1128/JVI.01564-20

Loss of HBeAg is not causative for impaired HBsAg release and antiproliferative/antioxidant cell regulation.

Basic M, Thiyagarajah K, Glitscher M, **Schollmeier A**, Wu Q, Görgülü E, Dietz J, Finkelmeier F, Trebicka J, Zeuzem S, Sarrazin C, Hildt E, Peiffer K.
<under submission>

Poster presentations

2022 31st Annual Meeting of the Society for Virology (Digital conference)

Genotype related impact of the Hepatitis B virus regulatory protein HBx on the radical oxygen regulating system of the host,
Schollmeier A, Basic M, Wu Q, Hildt E

2022 International HBV conference, Paris, France

Genotype related impact of the hepatitis B virus protein HBx on mitochondrial dynamics and the functional role in associated signaling pathways
Schollmeier A, Basic M, Wu Q, Hildt E

2023 32nd Annual Meeting of the Society for Virology, Ulm, Germany

Genotype related impact of the Hepatitis B virus regulatory protein HBx on the radical oxygen regulating system of the host
Schollmeier A, Basic M, Wu Q, Hildt E

13. Curriculum vitae

To protect the privacy of the author, the curriculum vitae has been omitted from this version of the thesis.